NTNU – Trondheim
Norwegian University of
Science and Technology

Upheaval Buckling of Offshore Pipelines

Shengsheng Fan

Marine Technology
Submission date: June 2013
Supervisor: Svein Sævik, IMT

Norwegian University of Science and Technology
Department of Marine Technology

NTNU
Norwegian University of Science and Technology
Department of Marine Technology

Master Thesis

Title:	**Delivered:**
Upheaval Buckling of Buried Pipelines	2012 06 10
	Availability: Open
Student: Shengsheng Fan	**Number of pages:** 110

Abstract

The main purpose of this thesis was to develop a MATLAB program based on Terndrup-Pedersen' analytical method for upheaval buckling analysis and verify the analytical model by comparing with FE analysis using software SIMLA. In addition, an elastic-plastic pipe model was built in SIMLA to investigate the plastic behavior of pipeline and its effect on the pipeline design.

All simulations of the analytical model and FE model are based on the use of MATLAB and SIMLA.A brief introduction to the program, which consists of the input data, solver and output data, is included. A brief description of methods applied in SIMLA and nonlinear finite element analysis is included. The thesis also contains a chapter describes the relevant concepts of upheaval buckling, like effective axial force, buckle force. A summary of needed data and procedure for the analytical method is given.

A group of cases with imperfection level δ_P varying from 0.1m to 0.6m and burial depth H varying from 0.4m to 1.6m has been defined and analyzed in both analytical model and FE model. Elastic-plastic material is also considered in the FE model to investigate the plastic behavior of the pipeline.

By comparing the results of analytical and elastic FE model, it is clearly verified the analytical model proposed by Terndrup-Pedersen will always give results that will be consistent with results of FE modeling in SIMLA. The MATLAB program developed is able to implement the analytical method and give very good results for design. However, it should be noted that the analytical model will always give conservative results compared with the results given by FE model.

The results clearly indicate the allowable operating temperature and buckle force will decrease significantly as the imperfection level increases, on the contrary the maximum bending moment will increase as the imperfection level increases. It is also evident to see the allowable operating temperature and buckle force will increase as the burial depth increase, while the maximum bending moment increase a little bit and is nearly a constant for given imperfection level.

It is also noted that the deviation of the analytical and FE results are dependent on the imperfection level for given soil conditions. The analytical model tends to give results close to FE model for large imperfection levels, say 0.3m or larger in the thesis, while the deviation may be larger for small imperfection level, say 0.2m or smaller. It is affected by the difference in the modeling of soil/pipe model in two models. The penetration of pipe into the seabed in the FE model may result a difference. In addition, it is found that the burial depth will have little effect on the deviation between the analytical and FE model.

Finally, it is also found the elastic-plastic properties of the pipe will affect the design temperature and buckle force to some extent. The results given by the elastic pipe model will always give conservative results for design. Therefore it is wise to take the elastic-plastic material properties into consideration.

Keyword:

Pipeline, Buried, upheaval buckling

Advisor:

Prof. Svein Sævik, Specilist. Tornes Knut and Helland Lars-Rune(JP KENNY)

Address: NTNU
Department of Marine Technology
N-7491 Trondheim

Location:
Marinteknisk Senter
O. Nielsens vei 10

Tel. +47 45170657

NTNU
Norwegian University of Science and Technology
Department of Marine Technology

Master Thesis

MASTER THESIS SPRING 2013

for

Stud. tech. Shengsheng Fan

Upheaval Buckling of Buried Pipelines

Vertikal knekning av nedgravde rørledninger

High temperature and pressure pipelines (HPHT) are subjected to global buckling due to the plane strain condition introduced by axial soil friction and/or subsea facilities. Global buckling is not a failure mode by itself rather a load response which can imply other failure modes such as local buckling, fracture, fatigue, etc. While lateral or horizontal buckling occurs for exposed pipelines, upheaval or vertical buckling occurs for buried or trenched pipelines. Due to the large transverse soil resistance of buried pipes, large bending moments may be introduced at the buckling apex leading to bending failure by either local buckling or fracture. It is therefore essential to avoid upheaval buckling of buried pipelines which is the topic of the thesis work defined below:

1) Definition of problem, including literature review on the background to upheaval buckling, related failure modes, basic concepts as the effective axial force and the mechanisms of pipeline expansion, pipe/soil interaction, methods of analysis with focus on the benefit of using analytical versus FE models (with special focus on the Terndrup Pedersen model).
2) In detail describe and formulate the Terndrup-Pedersen model in terms of inputs and related procedures
3) In cooperation with JPK define the procedure needed to create a useful screening/ design engineering tool for upheaval buckling.
4) Define the case scenarios needed in order to verify the procedure versus FE analysis.
5) Conclusions and recommendations for further work

The required input data will be provided by JPK.

The work scope may prove to be larger than initially anticipated. Subject to approval from the supervisors, topics may be deleted from the list above or reduced in extent.

In the thesis the candidate shall present his personal contribution to the resolution of problems within the scope of the thesis work

Theories and conclusions should be based on mathematical derivations and/or logic reasoning identifying the various steps in the deduction.

The candidate should utilise the existing possibilities for obtaining relevant literature.

Thesis format

The thesis should be organised in a rational manner to give a clear exposition of results, assessments, and conclusions. The text should be brief and to the point, with a clear language. Telegraphic language should be avoided.

The thesis shall contain the following elements: A text defining the scope, preface, list of contents, summary, main body of thesis, conclusions with recommendations for further work, list of symbols and acronyms, references and (optional) appendices. All figures, tables and equations shall be numerated.

The supervisors may require that the candidate, in an early stage of the work, presents a written plan for the completion of the work.

The original contribution of the candidate and material taken from other sources shall be clearly defined. Work from other sources shall be properly referenced using an acknowledged referencing system.

The report shall be submitted in two copies:

- Signed by the candidate
- The text defining the scope included
- In bound volume(s)
- Drawings and/or computer prints which cannot be bound should be organised in a separate folder.

Ownership

NTNU has according to the present rules the ownership of the thesis. Any use of the thesis has to be approved by NTNU (or external partner when this applies). The department has the right to use the thesis as if the work was carried out by a NTNU employee, if nothing else has been agreed in advance.

Thesis supervisors

Prof. Svein Sævik, NTNU

Specialist Engineer Tornes Knut and Helland Lars-Rune, JPKenny Norge (JPK)

Deadline: June 10 , 2013

Trondheim, January , 2013

Svein Sævik

Preface

The content of this thesis is based on the research conducted during the spring semester 2013 at the Department of Marine Technology at NTNU. The work is done as part of my Master degree in Marine Technology, with specialization in Marine Structures. Some of the contents in this thesis are taken from master project work I have done in the master project during the fall semester in 2012.

The main objective of the thesis was to describe and formulate the Terndrup-Pedersen's analytical model for upheaval buckling analysis in terms of inputs and related procedures. A specified program using MATLAB was developed to implement the method. In addition, FE modeling is conducted to verify the analytical model. The verification of the analytical model was done by FE modeling with the specified pipeline model software SIMLA from Marintek. What is more, the effect of imperfection amplitude, cover depth and material type were also investigated in those models. All the simulations for analytical models were based on MATLAB and all the simulations for the FE models are conducted in SIMLA.

Enclosed with this report is a zip file, which contains all the SIMLA input files for all simulations that have been conducted in this thesis. The poster for the master thesis is also included and a separate abstract is given in the zip file for printing.

Acknowledgement

Earning a master thesis is like writing a summary of the years as a student. It takes me a lot time to figure out the way and get onto the right track I wish to go. It is exciting to find something I am interested to work on as my final thesis and my future working area as well.

All the work in this thesis is done under the supervision of Professor Svein Sævik (Department of Marine Technology). I would like to express my deepest appreciation to him for his support and his discussion of my work during the last one year. His excellent work in pipeline analysis has greatly inspired me to devote myself to the research of pipeline.

I would also like to thank my co-supervisors and future colleagues, Tornes Knut and Helland Lars-Rune in JP Kenny, for their help and advice for my work. Their involvement in the thesis was essential for the development of the procedure of the thesis. I really appreciate the help from people in JP Kenny during the last semester.

I would also like to warmly thank my friends and some seniors at NTNU. Among these, I would like to mention Rui Zhang for his encouragement and help during the last six years, and Xiaopeng Wu for his help and guidance as I started my work on pipeline in SIMLA.

The content of this thesis is generated as my final thesis for the master degree in Marine Technology at NTNU. I would like to thank NTNU and Marintek for providing so many help, such as software, literature and services provided by them.

Content

Preface i

Acknowledgement ii

List of Figures I

List of Tables IV

List of Symbols V

Chapter 1 Introduction 1

1.1 Background and Motivation 1

1.2 Scope of Thesis 2

1.3 Structure of Thesis 3

Chapter 2 Relevant Concepts of Upheaval Buckling 5

2.1 Failure Modes of Upheaval Buckling 5

2.2 Derivation of Buckling Force 5

2.3 Discussion of Soil Resistance for Buried Pipelines 7

Chapter 3 Analysis Method of UHB without Initial Imperfection 8

3.1 Introduction 8

3.2 Analysis of Buckle Region 9

3.2.1 Linear Differential Equation 9

3.2.2 Effective Download 10

3.2.3 Deflection Equation 10

3.3 Analysis of Slip Length Region 10

3.4 Solutions 11

Chapter 4 Analysis Method of UHB with Initial Imperfection 13

4.1 Introduction 13

4.2 Assumptions of the Method 13

4.3 Foundation Imperfection 13

4.4 Pipeline Imperfection 14

4.5 Analysis of Buckle Region 14

4.5.1 Linear Differential Equation 14

4.5.2 Effective Download 15

4.5.3 Deflection equation 16

4.6 Analysis of Slip Length Region 17

4.7 Solutions 17

4.8 Calculation of Other Results 18
4.9 Summary of Date Required 18
4.9.1 Pipeline Properties 18
4.9.2 Steel Properties 18
4.9.3 Operating Parameters 19
4.9.4 Environmental Parameters 19
4.9.5 Backfill Material 19
4.9.6 Download 19
4.9.7 Pipe Imperfection 19
4.10 Summary of Solution Procedure 20
Chapter 5 Finite Element Methods for UHB analysis with SIMLA 21
5.1 Introduction 21
5.2 Theory Background 21
5.2.1 Basic of Finite Element Method 21
5.2.2 Non-linear effects 23
5.2.3 Lagrange Formulation 23
5.2.4 Incremental Stiffness Matrix 24
5.3 Command Cards Used 25
5.3.1 Input Commands 25
5.3.2 Output File 26
5.3.3 Post Process 26
Chapter 6 MATLAB Program for UHB analysis 27
6.1 Introduction 27
6.2 Input Data 27
6.2.1 Pipeline Properties 27
6.2.2 Steel Properties 27
6.2.3 Operating Parameters 28
6.2.4 Environmental Parameters 28
6.2.5 Pipe and Foundation Imperfection 28
6.2.6 Backfill Data 28
6.3 Solver Used 28
6.4 Output Data 29

Chapter 7 Definition of Cases 30
7.1 Introduction 30
7.2 Analytical Model 31
7.3 FE Model 32
7.3.1 Configuration of Pipeline and Foundation 32
7.3.2 Pipe Model 33
7.3.3 Boundary Conditions 35
7.3.4 Pipe/Seabed Model 35
7.3.5 Pipe/Burial Model 37
7.3.6 Load cases 39
Chapter 8 Results and Discussions 40
8.1 Introduction 40
8.2 Results of Analytical Model 42
8.2.1 Imperfection level $\delta p = 0.3m$ 43
8.2.2 Imperfection level $\delta p = 0.4m$ 45
8.3 Results of FE Model – Elastic Pipe 47
8.3.1 Imperfection level $\delta p = 0.3m$ 48
8.3.2 Imperfection level $\delta p = 0.4m$ 51
8.4 Results of FE Model – Elastic-plastic Pipe 53
8.4.1 Imperfection level $\delta p = 0.3m$ 54
8.4.2 Imperfection level $\delta p = 0.4m$ 57
8.5 Summary of Results 59
8.5.1 Results for Elastic Pipe $\delta p = 0.1m$ 60
8.5.2 Results for Elastic Pipe $\delta p = 0.2m$ 62
8.5.3 Results for Elastic Pipe $\delta p = 0.3m$ 64
8.5.4 Results for Elastic Pipe $\delta p = 0.4m$ 66
8.5.5 Results for Elastic Pipe $\delta p = 0.5m$ 68
8.5.6 Results for Elastic Pipe $\delta p = 0.6m$ 70
8.5.7 Results for Elastic-Plastic Pipe, $\delta p = 0.3m, 0.4m$ 72
8.6 Discussion of the Results 75
8.6.1 Comparison of Analytical and FE Results 75
8.6.2 Investigation on the Effect of Imperfection Level 79

8.6.3 Investigation on the Effect of Burial Depth 81
8.6.4 Investigation on the Effect of Material Type 82
Chapter 9 Conclusions and Recommendations for Future Work 83
9.1 Conclusions 83
9.2 Recommendations for Future Work 85
Reference 87
Appendix 89
Appendix I stress/strain relationship of the elastic to plastic material 89
Appendix II Screenshot of SIMLA model 90

List of Figures

Figure 1-1 Flowchart of the thesis 4

Figure 3-1 Force distribution along pipeline 8

Figure 4-1 Configuration of the model 14

Figure 4-2 Force distribution along pipeline 15

Figure 5-1 Modulus in SIMLA analysis 21

Figure 5-2 Reference configuration in SIMLA 24

Figure 7-1 Peak vertical stiffness versus cover depth 32

Figure 7-2 Configuration of FE model 33

Figure 7- 3 Configuration of FE model in SIMLA 33

Figure 7-4 stress/strain relationship of the steel material 35

Figure 7-5 Force factor in *x* direction 36

Figure 7-6 Force factor in *y* direction 36

Figure 7-7 Force/displacement relationship in *z* direction 37

Figure 7-8 Resistance from burial in *x* direction 38

Figure 7-9 Force/displacement in *y* direction 38

Figure 7-10 Resistance from burial in *z* direction 39

Figure 8-1 Allow temperature rise versus cover depth, $\delta p = 0.3m$ 43

Figure 8-2 Axial force versus cover depth, $\delta p = 0.3m$ 44

Figure 8-3 Max bending moment versus cover depth, $\delta p = 0.3m$ 44

Figure 8-4 Allow temperature rise versus cover depth, $\delta p = 0.4m$ 45

Figure 8-5 Axial force versus cover depth, $\delta p = 0.4m$ 46

Figure 8-6 Max bending moment versus cover depth, $\delta p = 0.4m$ 46

Figure 8-7 Difference of FE and analytical model 47

Figure 8-8 Displacement (z) versus time, $\delta p = 0.3m$, elastic 48

Figure 8-9 Temperature rise versus cover depth, $\delta p = 0.3m$, $\Delta = 2\text{cm}$ 49

Figure 8-10 Axial force versus cover depth, $\delta p = 0.3m$, $\Delta = 2\text{cm}$ 50
Figure 8-11 Max bending moment versus cover depth, $\delta p = 0.3m$, $\Delta = 2\text{cm}$ 50
Figure 8-12 Displacement (z) versus time,$\delta p = 0.4m$, elastic 51
Figure 8-13 Temperature rise versus cover depth,$\delta p = 0.4m$,$\Delta = 2\text{cm}$ 52
Figure 8-14 Axial force versus cover depth,$\delta p = 0.4m$,$\Delta = 2\text{cm}$ 52
Figure 8-15 Max bending moment versus cover depth,$\delta p = 0.4m$,$\Delta = 2\text{cm}$ 53
Figure 8-16 Displacement (z) versus time,$\delta p = 0.3m$, elastic-plastic 54
Figure 8-17 Temperature rise versus cover depth, $\delta p = 0.3m$, $\Delta = 2\text{cm}$ 55
Figure 8-18 Axial force versus cover depth,$\delta p = 0.3m$, $\Delta = 2\text{cm}$ 56
Figure 8-19 Max bending moment versus cover depth,$\delta p = 0.3m$, $\Delta = 2\text{cm}$ 56
Figure 8-20 Displacement (z) versus time,$\delta p = 0.4m$, elastic-plastic 57
Figure 8-21 Temperature rise versus cover depth,$\delta p = 0.3m$, $\Delta = 2\text{cm}$ 58
Figure 8-22 Axial force versus cover depth,$\delta p = 0.4m$, $\Delta = 2\text{cm}$ 58
Figure 8-23 Max bending moment versus cover depth,$\delta p = 0.4m$, $\Delta = 2\text{cm}$ 59
Figure 8-24 Temperature rise versus cover depth, $\delta p = 0.1m$ 61
Figure 8-25 Force versus cover depth, $\delta p = 0.1m$ 61
Figure 8-26 Max bending moment versus cover depth, $\delta p = 0.1m$ 61
Figure 8-27 Temperature rise versus cover depth, $\delta p = 0.2m$ 63
Figure 8-28 Force versus cover depth, $\delta p = 0.2m$ 63
Figure 8-29 Max bending moment versus cover depth, $\delta p = 0.2m$ 63
Figure 8-30 Temperature rise versus cover depth, $\delta p = 0.3m$ 65
Figure 8-31 Force versus cover depth, $\delta p = 0.3m$ 65
Figure 8-32 Max bending moment versus cover depth, $\delta p = 0.3m$ 65
Figure 8-33 Temperature rise versus cover depth, $\delta p = 0.4m$ 67
Figure 8-34 Force versus cover depth, $\delta p = 0.4m$ 67
Figure 8-35 Max bending moment versus cover depth, $\delta p = 0.4m$ 67
Figure 8-36 Temperature rise versus cover depth, $\delta p = 0.5m$ 69
Figure 8-37 Force versus cover depth, $\delta p = 0.5m$ 69
Figure 8-38 Max bending moment versus cover depth, $\delta p = 0.5m$ 69
Figure 8-39 Temperature rise versus cover depth, $\delta p = 0.6m$ 71
Figure 8-40 Force versus cover depth, $\delta p = 0.6m$ 71

Figure 8-41 Max bending moment versus cover depth, $\delta p = 0.6m$ 71
Figure 8-42 Comparison of temperature rise for different material, $\delta P = 0.3m$ 73
Figure 8-43 Comparison of force for different material, $\delta P = 0.3m$ 73
Figure 8-44 Comparison of max bending moment for different material, $\delta P = 0.3m$ 73
Figure 8-45 Comparison of temperature rise for different material, $\delta P = 0.4m$ 74
Figure 8-46 Comparison of force for different material, $\delta P = 0.4m$ 74
Figure 8-47 Comparison of max bending moment for different material, $\delta P = 0.4m$ 74
Figure 8-48 Deviation between FE and analytical results, $\delta p = 0.1m$ 76
Figure 8-49 Deviation between FE and analytical results, $\delta p = 0.2m$ 76
Figure 8-50 Deviation between FE and analytical results, $\delta p = 0.3m$ 77
Figure 8-51 Deviation between FE and analytical results, $\delta p = 0.4m$ 77
Figure 8-52 Deviation between FE and analytical results, $\delta p = 0.5m$ 78
Figure 8-53 Deviation between FE and analytical results, $\delta p = 0.6m$ 78
Figure 8-54 Deviation of temperature versus imperfection level 79
Figure 8-55 Deviation of force versus imperfection level 80
Figure 8-56 Deviation of max bending moment versus imperfection level 80
Figure 8-57 Deviation of temperature versus cover depth 81
Figure 8-58 Deviation of buckle force versus cover depth 81
Figure 8-59 Deviation of effective axial force versus cover depth 81
Figure 8-60 Deviation of max bending moment versus cover depth 81

List of Tables

Table 6-1 Pipeline properties 27
Table 6-2 Steel properties 27
Table 6-3 Operating parameters 28
Table 6-4 Environmental parameters 28
Table 6-5 Pipe and foundation imperfection 28
Table 6-6 Backfill data 28

Table 7-1 Summary of the case 30
Table 7-2 Input data for analytical model 31
Table 7-3 Imperfection wavelength versus imperfection level 31
Table 7-4 Peak vertical stiffness versus cover depth 32
Table 7-5 Pipe properties 34
Table 7-6 Elastic Material properties for SIMLA input 34

Table 8-1 Imperfection wavelength, $\delta p = 0.3m, 0.4m$ 42
Table 8-2 Analytical results for imperfection level $\delta p = 0.3m$ 43
Table 8-3 Analytical results for imperfection level $\delta p = 0.4m$ 45
Table 8-4 FE results for imperfection level $\delta p = 0.3m$, elastic 49
Table 8-5 FE results for imperfection level $\delta p = 0.4m$, elastic 51
Table 8-6 FE results for imperfection level $\delta p = 0.3m$, elastic-plastic 55
Table 8-7 FE results for imperfection level $\delta p = 0.4m$, elastic-plastic 57
Table 8-8 Summary of result for $\delta P = 0.1m$ 60
Table 8-9 Summary of result for $\delta P = 0.2m$ 62
Table 8-10 Summary of result for $\delta P = 0.3m$ 64
Table 8-11 Summary of result for $\delta P = 0.4m$ 66
Table 8-12 Summary of result for $\delta P = 0.5m$ 68
Table 8-13 Summary of result for $\delta P = 0.6m$ 70
Table 8- 14 Summary of result for $\delta P = 0.3$ and $0.4m$, elastic-plastic 72

List of Symbols

Parameter	Symbol	SI Unit
Foundation Imperfection Level	δ_f	m
Pipeline Imperfection Level	δ_p	m
Steel Pipe Outside Diameter	D_e	m
Steel Pipe Inside Diameter	D_i	m
Overall Outside Diameter Including Coatings	D_O	m
Mean Diameter	D_m	m
Steel Cross Section Area	A_s	m^2
Young's Modulus of Elasticity	E	N/m^2
Axial Force In Pipe Section	F	N
Axial Coefficient of Friction	$F_A = \mu_A$	-
Thermal Related Compressive Load	F_T	N
Acceleration Due to Gravity	g	g/s^2
Burial Depth to Center of Pipeline	H	m
Burial Depth to Top of Pipeline	H_C	m
Burial Depth Above Seabed	H_R	m
Trench Depth	H_T	m
Second Moment of Area Of Steel	I	m^4
Normal Stiffness of Foundation	K_N	N/m
Sliding Stiffness of Foundation	K_s	N/m
Half Buckle Wavelength	L	m
Foundation Imperfection Wavelength	L_0	m
Slip Length	L_S	m

Bending Moment	M	Nm
Maximum Bending Moment	M_{max}	N/m
Axial Compressive Load in Buckle	N	N
Axial Compressive Away from Buckle	N_0	N
Residual Lay Tension	N_{lay}	N
Internal Pressure in Pipeline	P_i	N/m^2
External Hydrostatic Pressure	$P_0 = \rho_w dg$	N/m^2
Total Download of Pipe and Soil	q	N/m
Equivalent Download at Pipe/Seabed Interface	q_b	N/m
Equivalent Download at Burial Pipe Interface	q_c	N/m
Pipe Dry Weight	q_d	N/m
Theoretical Download to Give Foundation Imperfection	q_f	N/m
Pipe Submerged Weight	q_{pipe}	N/m
Resistance to Uplift Of Soil Cover	q_s	N/m
Steel Pipe Wall Thickness	T	m
Ambient Sea Temperature	T_a	℃
Design Temperature	T_d	℃
Operating Temperature	T_p	℃
Axial Displacement	u=U	m
Axial Displacement at the Lift Of Point	U_{sb}	m
Maximum Buckle Amplitude	Y_{max}	m
Maximum Slope	Y'_{max}	-
Coefficient of Linear Thermal Expansion of Steel	$\alpha_s = 11.7 \times 10^{-6}$	1/℃
Seabed Friction Mobilisation Displacement	$U_m = 0.005$ for sand	m

Intermediate Calculated Variable	β	-
Intermediate Calculated Variable	γ	-
Submerged Weight of Burial Material Per Unit Volume	γ_c	kg/m^3
Coefficient of Axial Friction between Pipe and Seabed	μ_{ab}	-
Coefficient of Axial Friction between Burial And Pipe	μ_{ac}	-
Equivalent Friction Coefficient	μ_e	-
Poisson Ration for Steel Pipeline	$\nu = 0.3$	-
Pi	π	-
Density of Pipe Contents	ρ_p	kg/m^3
Density of Pipeline Steel	$\rho_s = 1025$	kg/m^3
Density of Soil Cover	ρ_{sc}	kg/m^3
Density of Seawater	$\rho_w = 1025$	kg/m^3
Axial Stress	σ_A	N/m^2
Bending Stress	σ_B	N/m^2
Von Mises Equivalent Stress	σ_e	N/m^2
Hoop Stress	σ_h	N/m^2
Trench Angle	Ψ_T	degree
Soil Cover Internal Friction Angle	ϕ_c	degree
Shear Stress	τ	N/m^2

Chapter 1 Introduction

1.1 Background and Motivation

Pipelines have been the main way of transporting oil and gas from offshore districts all over the world in the last decades. Pipelines are buried to avoid interference with other marine activities, like fishing activity. Pipeline operating at high temperature and pressure are subjected to global buckling due to the plane strain condition introduced by axial soil friction and or subsea facilities. While lateral or horizontal buckling occurs for exposed pipelines, upheaval or vertical buckling occurs for buried or trenched pipelines.

Palmer and Baldry [1] published the first paper on pipeline buckling in 1974. It is demonstrated that the constraint of expansion of a pipeline on account of raised internal pressure could induce buckling through a small-scale test. Then in 1981 and 1984, Hobbs [2-3] summarized basic models of buckling of pipeline. A major interest at that time was to study thermal induced buckling as some upheaval buckling (UHB) incidents occurred in the North Sea. Guijt, Nielsen N J R, Lyngberg B, and Pedersen T [4-5] pointed out several incidents caused by upheaval buckling of pipelines occurred around 1990. The failure of pipeline caused a significant of loss due to repairs and loss of production. Thermal induced buckling became a vital problem for oil and gas industry afterwards and a substantial study has been conducted in the past 30 years on upheaval buckling.

Analytical modeling of the upheaval buckling response of buried pipelines has progressed rapidly in the last decades [6-12]. It is initially progressed from the classical analysis method for vertical stability of railroad. Then it is further studied to pipeline with initial imperfections, pipeline with additional cover material with non-linearity and pipeline with large displacements. A significant number of studies have been conducted by Taylor and Gan, Boer, Friedman, Richards and Andronicou, Ju and Kyriakides, Pedersen and Jensen, Ballet and Hobbs [6-12], which mainly focus on the imperfection studies. The basic models presented by Hobbs [2-3] have been modified and refined with considering the pipeline imperfection and the elastic-plastic behavior of buckling pipelines in the past decades. Recently, numerical methods [15-17] have been applied to analyze the upheaval buckling of pipeline. All those progress contribute to improve the accuracy and consistency of upheaval buckling assessments.

This thesis deals with analytical methods for upheaval buckling, focus mainly on Terndrup-Pedersen's [18] model. A summary of the data needed to implement this method is presented, and a program based on the use of MATLAB has been developed for screening design stage. Cases with a specific pipeline with a mean diameter of 0.214m, thickness of 0.0142m and coating of 0.4m are defined and conducted using the program developed by the author. In addition, a similar FE model is built up in the special software for pipeline analysis, i.e. SIMLA from Marintek. The accuracy of the analytical model is investigated by comparing the results of the analytical model and FE model. The effects of the burial depth and imperfection amplitude are also investigated in this thesis. The elastic-plastic material is also considered in the FE model to investigate the plastic behavior of the pipeline. Based on the results, some useful actions may be used to avoid upheaval buckling are suggested.

1.2 Scope of Thesis

The analytical method for upheaval buckling analysis discussed in the thesis is based on the paper by Terndrup-Pedersen, which is published in 1989. Following the Hobb's method, some studies suggested that minimum - temperature criteria was insensitive to imperfections. A minimum-temperature criterion was suggested for analyzing subsea pipeline with initial imperfections. Pedersen's approach demonstrates if the pipeline with given initial imperfection is subjected to cyclic pressure and temperature load conditions, then Hobb's method can yield non-conservative result. Based on this conclusion, it was decided to develop a specific program to implement the analytical method and verify whether it will give conservative result or not by comparing with FE method.

In the analytical model, several simplified assumptions are introduced which may affect the accuracy of the method. For instance, the soil/pipe interaction is not taken into consideration. It just assumes an infinite stiff foundation and therefore no penetration will take place during the operation process, which is not conforming to reality. And the uplift resistance of the burial material is assumed to be a constant, which is only valid when the vertical displacement of the pipe is small. In addition, in the analytical model several degrees of freedom, like lateral and other rotational degrees of freedom are restricted, which may result in a conservative result. What is more, the analytical model is only valid for elastic material. All these assumptions lead to the limitation of the analytical model.

It is evident that the design parameters of given project is greatly dependent on the soil and burial conditions. Hence, in the FE model, some modifications are made to make the FE model closer to real industry. The pipe/soil interaction is modeled by introducing a contact interface which may give contact force in *x, y* and *z* direction. The pipe/burial interaction is modeled by introducing a contact element (spring), which has the same magnitude of resistance as the analytical model. The FE model also includes some cases which take the elastic-plastic material into consideration. However, there are still some limitations for the FE model. Some degrees of freedom in the FE model are fixed as well, to make it comparable with analytical model.

All the simulations for analytical model are based on the use of MATLAB and all the simulations for the FE model are based on the use of SIMLA. Several assumptions and simplifications have been introduced in the simulation models which may be explained in chapter 7 in detail.

1.3 Structure of Thesis

Chapter 2	Gives a brief introduction to the relevant concepts of upheaval buckling problem, like failure modes of upheaval buckling, buckling force, effective axial force, allowable operating temperature. A general introduction of the downward stiffness from burial soil is also included based on the recommended practice from DNV.
Chapter 3	Describes the analysis method for pipeline without initial imperfection, in terms of buckle region, slip region. Solution of the method is also given.
Chapter 4	Describes the analysis method for pipeline with initial imperfection with special based on Pedersen Terndrup's analytical model. A summary of the data need for this analytical model is presented and the procedures to implement this method are given.
Chapter 5	Gives a brief introduction of nonlinear finite element methods. The basic methods applied in SIMLA are of focus throughout the chapter. An introduction of the commands that has been used in UHB analysis in SIMLA is given.
Chapter 6	Gives a brief introduction of the MATLAB program to implement the analytical model, which includes three parts, input data, solver and output data. The pipeline and other properties are listed in this section.
Chapter 7	Defines cases needed to be conducted to verify the analytical model. A detail configuration of the analytical model and FE model is presented. It also describes how the model is built in detail, including pipe and steel properties, soil/pipe model, soil/burial model and load cases.
Chapter 8	Presents all the results for the simulations that have been done. It includes results for analytical model, FE mode with elastic material, and FE model with elastic-plastic material. A summary of all the cases conducted is given.
Chapter 9	Makes conclusions based on the results from previous chapters and recommendations for future work is made.

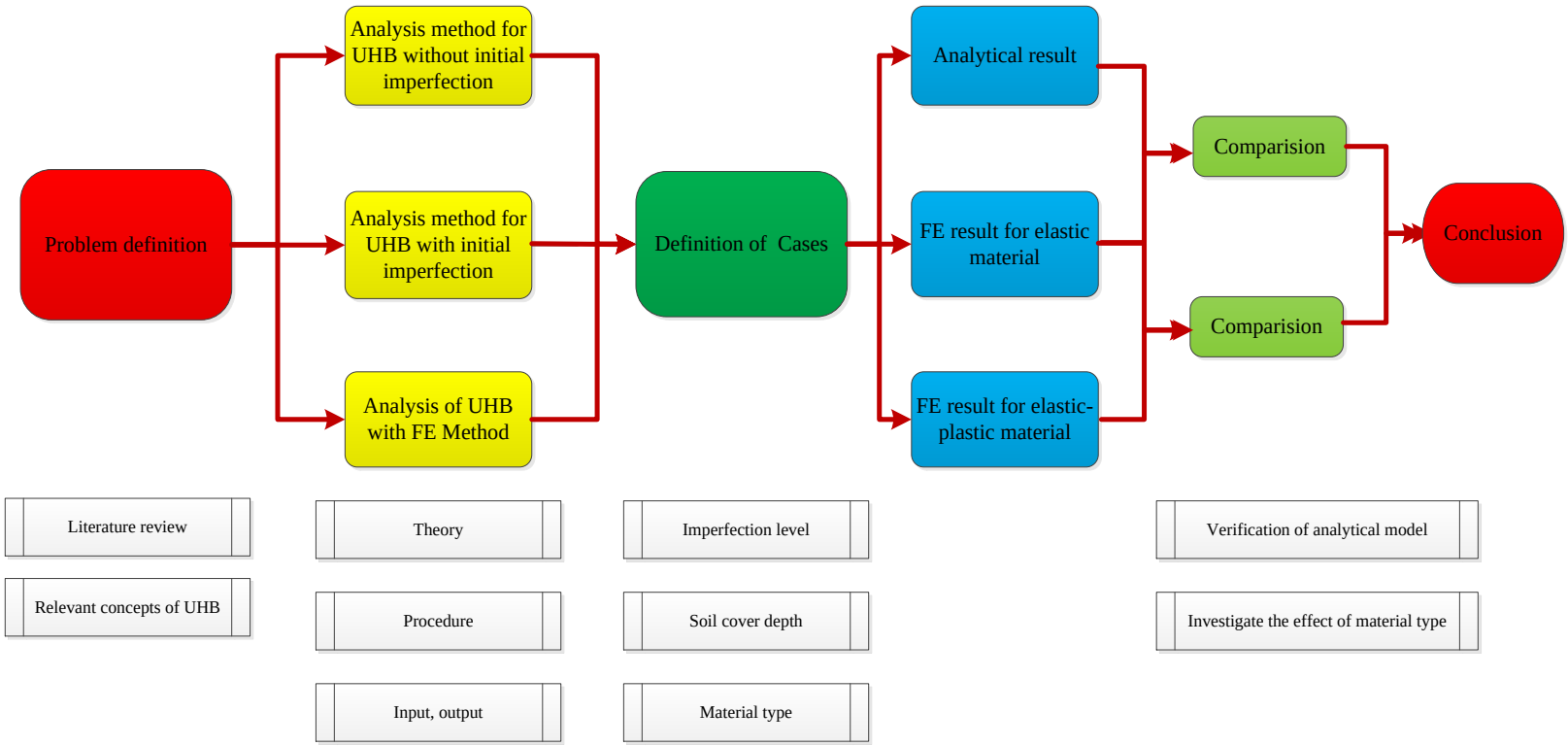

Figure 1-1 Flowchart of the thesis

Chapter 2 Relevant Concepts of Upheaval Buckling

2.1 Failure Modes of Upheaval Buckling

Global buckling of pipelines may be treated as the buckling of a bar (pipe) in compression. The global buckling may occur either downwards (free span), horizontally (lateral buckling on sea bed) or vertically (as upheaval buckling of buried pipelines or on a crest of exposed pipelines followed by a lateral turn-down). Local buckling is a gross deformation of the pipe cross section.

Global buckling is a response to compressive force generated by high temperature and high pressure (HP/HT), which will generally reduce the axial capacity of the pipeline. Pipelines exposed to high temperature and high pressure or pipeline with a low buckling capacity will be governed by global buckling. In DNV's RP-F110 [19], three global buckling scenarios resulted from HT/HP are introduced:

- Exposed pipelines on even seabed. Global buckling occurs in the horizontal plane, post buckling configuration may be allowed.
- Exposed pipelines in uneven seabed. Global buckling occurs first in the vertical plane (cause feed-in and uplift) and subsequently in the horizontal plane, or combined scenarios with scenario I, post buckling configuration may be allowed.
- Buried/covered pipelines, global buckling in the vertical plane, so called upheaval buckling.

Global buckling is a load response, not a failure mode. However, global buckling will imply some failure modes [20] such as:

- **Local buckling**, for pipeline subjected to combined pressure. Longitudinal force and bending, local buckling may occur. The failure mode may be yielding of the cross section or buckling on the compressive side of the pipe.
- **Fracture,** which is caused by tensile strain, generally includes brittle fracture and plastic collapse.
- **Fatigue,** pipeline components such as riser, unsupported free spans, welding should be assessed for fatigue. Potential cyclic loading fatigue damages, which may include vortex-induced-vibrations (VIV), wave induced hydrodynamic loads, cyclic pressure and thermal expansion loads.
- **Ratcheting,** ratcheting generally describes the accumulated plastic deformations under cyclic loads in pipelines that exposed to high temperature and high pressure.
- **Bursting,** it is governed by tensile hoop stress, which may occur in the tensile part of pipeline.

2.2 Derivation of Buckling Force

The effective axial force in the pipe wall is generally caused by the internal pressures and force caused by the temperature differential in the pipe wall, which is denoted as true force. The effective force over the entire pipe cross section can be calculated with the following procedure [20]:

Axial force

$$F_x = A_s E \varepsilon_x$$

Where:

$$A_s = \pi(D_e^2 - D_i^2)/4$$

$$\varepsilon_x = \alpha_S \Delta T + \frac{1}{E}(\sigma_x - \upsilon(\sigma_h + \sigma_r))$$

$$\Delta T = T_P - T_a$$

$E =$ Young's Modulus of Elasticity

$\varepsilon_x =$ Axial Strain

$\alpha_S =$ Linear coefficient of thermal expansion

$T_P =$ Average product temperature

$T_a =$ Ambient temperature

$\sigma_x =$ Axial stress

$\sigma_h =$ Hoop stress

$\sigma_r =$ Radial stress

The axial stress due to internal pressure with pipe ends is:

$$\sigma_x = \frac{P_i D_i^2 - P_o D_e^2}{D_e^2 - D_i^2}$$

Using the Lame stress distribution, the hoop and radial stresses are:

$$\sigma_h = \frac{P_i D_i^2 - P_o D_e^2 + \frac{D_i^2 D_e^2}{D^2}(P_i - P_o)}{D_e^2 - D_i^2}$$

$$\sigma_r = \frac{P_i D_i^2 - P_o D_e^2 - \frac{D_i^2 D_e^2}{D^2}(P_i - P_o)}{D_e^2 - D_i^2}$$

Where:

$D =$ Diameter at the point of interest

Therefore, substitute all the stresses component into the equation of axial force, the axial force can be written as:

$$F_x = \frac{\pi}{4} E \alpha_S (T_P - T_a)\left(D_e^2 - D_i^2\right) + \frac{\pi}{4}(1 - 2\nu)(P_i D_i^2 - P_0 D_e^2)$$

Therefore, the Buckling Force is the sum of the buckling force caused by temperature difference across the pipe wall and the buckling force caused by the pressure difference across the pipe wall, i.e. F_T andF_P.

$$F_x = F_T + F_P$$

Where:

$$F_T = \frac{\pi}{4} E \alpha_S (T_P - T_a)(D_e^2 - D_i^2)$$

$$F_P = \frac{\pi}{4} (1 - 2\nu)(P_i D_i^2 - P_0 D_e^2)$$

2.3 Discussion of Soil Resistance for Buried Pipelines

DNV has given recommendations regarding the uplift resistance modeling for burial pipelines as well as for the associated uncertainties for buried pipelines in RP-F110 [19]. It is recommended that the uncertainties in the resistance is significant and should be considered in design process. Descriptions of soil models for both cohesive (clay) and cohesion less (sand and rock) soil are given in the recommend practice from DNV.

The condition of the soil surrounding the pipeline is the most important aspect. It may also be influenced by the trenching methods. In addition, the clearance depth to intact soil conditions below the pipe in the trench will add to the uncertainties in respect to downward stiffness. Some specific calculation model where this effect is considered is proposed in the recommend practice. What's more, effects from additional gravel are also discussed, which is commonly used to increase the vertical stiffness.

More details about the calculation of downward stiffness may be found in DNV RP-F110. In this thesis, the downward stiffness of burial is based on the cohesion less soil model, using a simplified model, which is the same as in Pedersen's paper. The defining of downward stiffness in analytical model and FE is discussed further in Chapter 7.

Chapter 3 Analysis Method of UHB without Initial Imperfection

3.1 Introduction

The analysis of upheaval buckling can be generally considered in two regions as shown in Figure 3-1.

- Buckle region
- Slip region

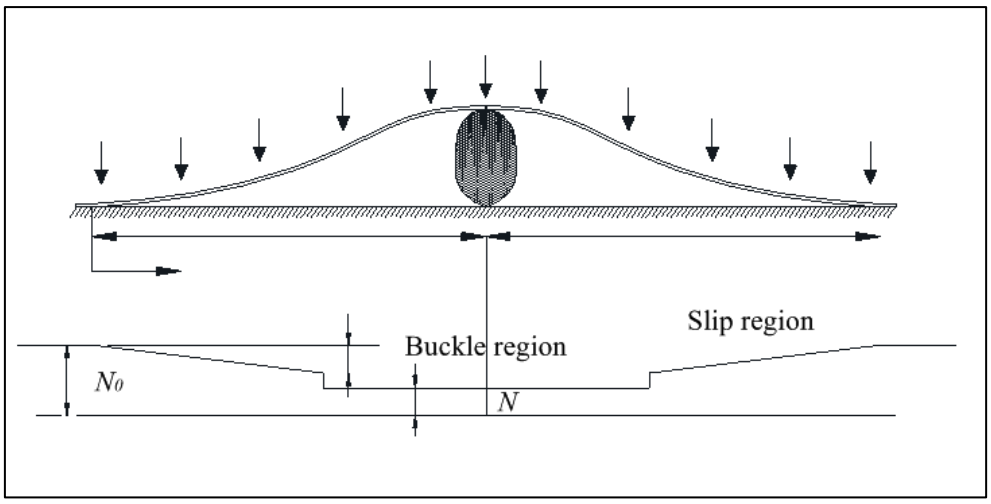

Figure 3-1 Force distribution along pipeline

For the buckle region, the increasing of displacements is caused by the temperature or pressured induced compressive force in the pipeline. The problem may be studied with a conventional beam bending theory. The location at which the upward displacement starts is of great interest for upheaval buckle analysis, i.e. the location of lift off position, which is dependent on the pipe properties and the soil/pipe friction relationship.

In order for the buckle region to develop further, the pipe material is 'fed' from the adjacent pipe lengths. The amount of 'feeding' is dependent on the magnitude of the friction force generated by the sliding with the slip length regions. At end of the slip length region, where the pipe is fully restrained (no axial movement), the temperature and pressure induced compressive force is given by the expansion defined in Section 2.2.

$$N_0 = F_T + F_p - N_{lay}$$

Where

$$F_T = \frac{\pi}{4} E \alpha_S (T_P - T_a)(D_e^2 - D_i^2)$$

$$F_P = \frac{\pi}{4}(1 - 2\nu)(P_i D_i^2 - P_0 D_e^2)$$

Where

F_T = Thermally induced compressive load

F_P = Pressure induced compressive load

E = Young's Modulus of Elasticity

α_S = Linear coefficient of thermal expansion

T_P = Average product temperature

T_a = Ambient temperature

D_e = Pipe outside diameter

D_i = Pipe inside diameter

ν = Poisson's ratio

P_i = Internal operating pressure

P_o = External hydrostatic pressure

N_{lay} = Residual lay tension

3.2 Analysis of Buckle Region

3.2.1 Linear Differential Equation

For a straight pipeline without any initial imperfection, the analysis procedure for the post-buckling behavior is based on the same method which has been used for analyzing the stability of railroad tracks.

The first step is to solve the linear differential equation for the deflected shape of the buckle part of the pipeline, i.e. the buckle region. This problem can be simply modeled as a straight beam column under uniform lateral load.

For a straight pipeline lying on an infinitely rigid seabed, which is an assumption aimed at making the problem linear, the linear differential equation describing the deflected shape of the buckle region may be written as:

$$\frac{d^4\omega}{dx^4} + n^2\frac{d^2\omega}{dx^2} + m = 0$$

Where:

$n^2 = N/EI$

$m = q/EI$

N = Axial load in the buckle region

q = Effective download due to self-weight and burial resistance in the buckle region

I = Second moment of area

ω = Vertical displacement

3.2.2 Effective Download

The effective download due to self-weight and burial resistance in the buckle region can be obtained from DNV RP-F110. In this thesis, the total effective download can be given as:

$$q = q_{pipe} + q_s$$

Where:

q_{pipe} = Pipe submerged weight

q_s = Uplift resistance of the burial material

Where:

$$q_s = \gamma_c(HD_o - \frac{\pi}{8}D_o^2 + H^2 tan\phi_c)g \text{ [18]}$$

$$q_{pipe} = m_0 g$$

Where:

D_o = Overall outside diameter including coatings

γ_c = Submerged weight of burial material per unit volume, 1000 kgm^3 in this paper

g = Acceleration Due to Gravity

H = Minimum height of the cover soil measure between the pipe center line and the sea floor

m_0 = Submerged mass per unit length of the pipeline

3.2.3 Deflection Equation

Obviously, we will see the bending moment at the lift off point is zero. In addition, it should be noted that the linear equation is valid when small slopes assumption is satisfied, otherwise, the result from this method may be not that good.

The boundary conditions may be written as follows:

$$\omega|_{x=\pm L} = \frac{d\omega}{dx}|_{x=\pm L} = \frac{d\omega}{dx}|_{x=0} = 0$$

We will easily see the slope and vertical deflection at the ends of the buckle region are zero. Based on this boundary condition, the deflection equation of the buckle region can be identified as:

$$\omega\frac{m}{n^4}\left[-\frac{\cos nx}{\cos nL} - \frac{n^2x^2}{2} + \frac{n^2L^2}{2} + 1\right]$$

This yields $tan\, nL = L$ or, as lowest root $nL = 4.4934$.

Then the next step is to compare the axial load N in the buckle region with the axial load N_0at points which is far from the buckle region. The axial compressive force distribution is shown in Figure 3-1.

3.3 Analysis of Slip Length Region

In order to achieve equilibrium between the axial force in the undisturbed pipeline and the axial force in the uplifted pipeline section, axial displacements and the associated friction forces should be considered.

As the buckle region develops, the length of the buckle region increases. The axial displacement at the lift off point can be written as:

$$U_{sb} = \frac{(N_0 - N)L}{A_s E} - \frac{1}{2}\int_0^L (\frac{d\omega}{dx})^2 dx$$

Similarly, based on the idealized dry friction model, the axial pull out of the section which is not lifted up from the foundation is:

$$U_{ss} = \frac{1}{2}\frac{(N_0 - N - \lambda qL)^2}{\lambda q A_s E}$$

Where:

q = Total effective download from soil cover weight and submerged pipe weight

$q = q_{pipe} + q_s$

λ = Equivalent friction coefficient

$\lambda = \frac{q_x}{q}$

3.4 Solutions

Based on the assumptions above and the compatibility of displacement, it requires that:

$$U_{ss} = U_{sb}$$

Namely,

$$\frac{(N_0 - N)L}{A_s E} - \frac{1}{2}\int_0^L \left(\frac{d\omega}{dx}\right)^2 dx = \frac{1}{2}\frac{(N_0 - N - \lambda qL)^2}{\lambda q A_s E}$$

Thus, we will see

$$N_0 = N + \left[\lambda q A_s E \int_0^L \left(\frac{d\omega}{dx}\right)^2 dx - (\lambda qL)^2\right]^{0.5}$$

The integral in the equation is calculated directly from integral of the deflection equation which has been identified in the above procedures.

We will obtain the following result from the steps above:

$$N = 20.19\frac{EI}{L^2}$$

$$N_0 = N + \frac{qL}{EI}[1.25.10^{-7}\lambda q A_s E L^5 - 0.25(\lambda EI)^2]^{0.5}$$

Where:

q = Total effective download from soil cover weight and submerged pipe weight

$q = q_{pipe} + q_s$

λ = Equivalent friction coefficient

$\lambda = \frac{q_x}{q}$

The maximum amplitude of the buckle region is:

$$\omega_{max} = 1.505.10^{-4}\frac{qL^4}{EI}$$

The maximum bending moment of the buckle region, which will occur at the center of the buckle region will be:

$$M_{max} = 0.017345qL^2$$

Length of the slip region:

$$L_s = \frac{(N_0 - N)}{\lambda q} - L$$

Chapter 4 Analysis Method of UHB with Initial Imperfection

4.1 Introduction

The design method adopted in this thesis taken from Terndrup-Pedersen's [18] analytical model, which is published in 1988. Most of the content in this chapter is summarized based on this paper. Following the Hobb's [3] method, some other studies suggested that minimum - temperature criteria was insensitive to imperfections. A minimum-temperature criterion was suggested for analyzing subsea pipeline with initial imperfections. Pedersen's approach demonstrates if the pipeline with given initial imperfection is subjected to cyclic pressure and temperature load conditions, then Hobb's method can yield non-conservative result.

4.2 Assumptions of the Method

The assumptions in Terndrup-Pedersen's approach are:

- Linear beam analysis;
- The foundation stiffness is infinite;
- The uplift resistance of the soil cover is a constant, which is proper only when the vertical displacement considered is small;
- The pipeline is completely elastic;
- The pipeline only undergoes small displacements;
- The pipeline and trench bottom may be imperfect;
- The imperfection profile for both pipeline and foundation is propped.

There are some other assumptions which are explained in the following theory part.

4.3 Foundation Imperfection

The choice of proper imperfection shape of the foundation is a difficult aspect for the analyzing of upheaval buckling. A number of numerical studies have already been conducted to assess the effects of pipeline or foundation imperfection on upheaval buckling.

In Pedersen's model, the prop shape is defined by the following equation:

$$\omega_f = \delta_f \left(\frac{x}{L_0}\right)^3 \left(4 - \frac{3x}{L_0}\right) \qquad 4\text{-}1$$

Where

$$\boldsymbol{L_0} = \left(\frac{72EI\delta_f}{q_f}\right)^{1/4} \qquad 4\text{-}2$$

Where:

δ_f = initial imperfection level

q_f = pipe submerged weight

This is the same as the deflection shape of an elastic pipeline with bending stiffness *EI* placed over a protruding object of height δ_f and loaded with a weight q_f per unit length, as shown in figure 4-1. In addition, it is assumed that the cavity below the propped pipe will be filled with soil, either through natural process or engineering backfill procedures. In practice, some soil may land on top of the pipe

during backfill process, and the process would reduce the imperfection wave length and possibly result in an asymmetric imperfection profile. However this possibility is neglected in Pedersen's model.

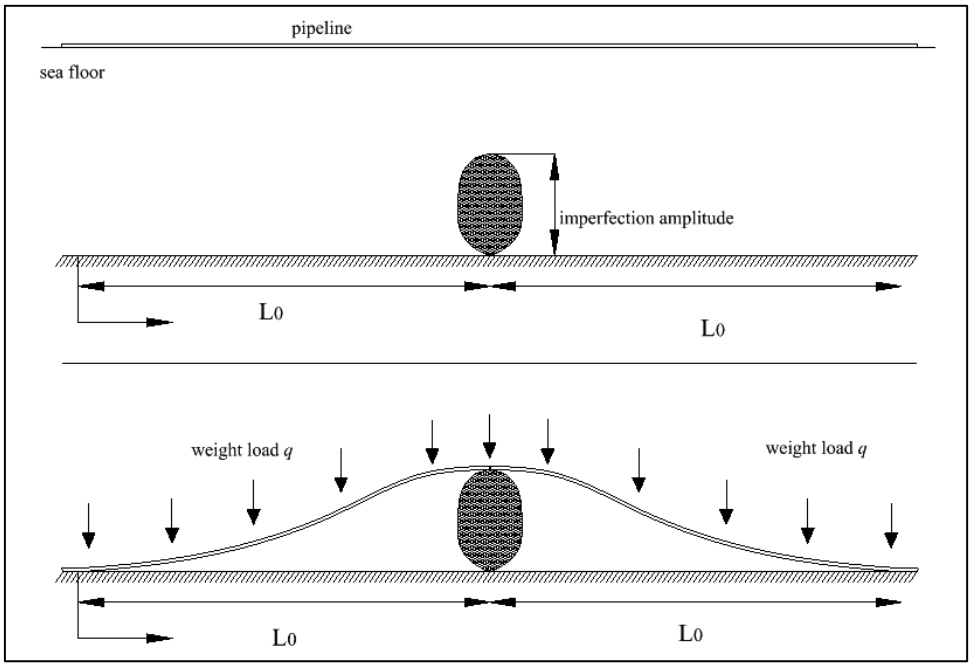

Figure 4-1 Configuration of the model

4.4 Pipeline Imperfection

In addition to the foundation imperfection, it is also easy to note that the pipeline itself may contain an initial out of straightness, which has the same wavelength as that of the foundation, i.e. $2L_0$, but with a different imperfection amplitude δ_p. Hence the stress free pipe imperfection shape is described as:

$$\omega_p = \delta_p \left(\frac{x}{L_0}\right)^3 \left(4 - \frac{3x}{L_0}\right) \qquad 4\text{-}3$$

The pipeline imperfection may be caused by plastic deformation or fabrication imperfection. The configuration of the pipeline and foundation is shown in Figure 4-1.

4.5 Analysis of Buckle Region

4.5.1 Linear Differential Equation

Assume a linear beam theory of the imperfection pipe uplifted in the *x*-*w* coordinate system, as shown in Figure 4-2, the vertical equilibrium differential equation can be given as:

$$EI\frac{d^4}{dx^4}(\omega - \omega_P) + N\frac{d^2\omega}{dx^2} + q = 0 \qquad 4\text{-}4$$

Here the parameter q is the total download due to the pipe submerged weight and burial resistance in the buckle region. Be noted that the analysis axis system is different from the imperfection specifications.

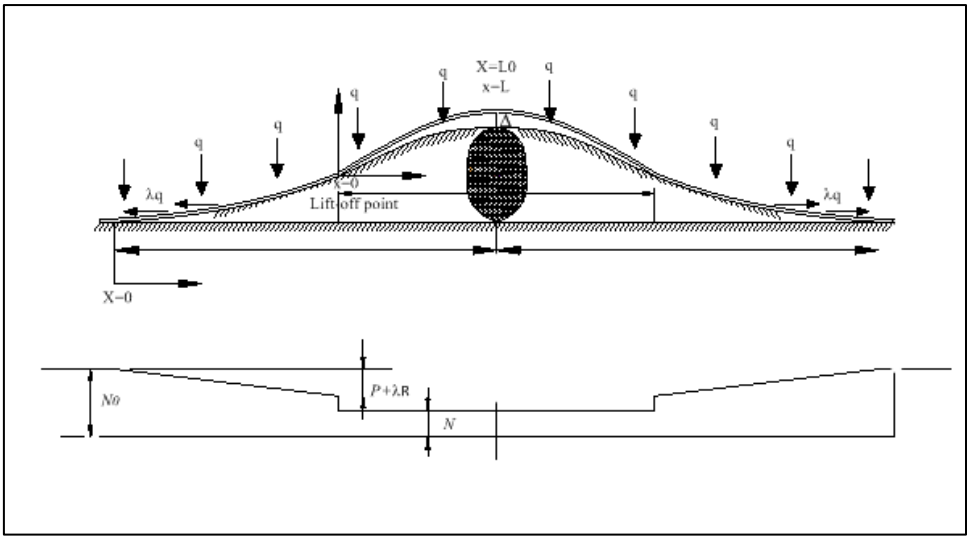

Figure 4-2 Force distribution along pipeline

The equation can be re-written as:

$$\frac{d^4\omega}{dx^4} + k^2\frac{d^2\omega}{dx^2} + (\frac{q}{EI} - \frac{d^4\omega_P}{dx^4}) = 0$$

It is easy to find $\frac{d^4\omega_P}{dx^4}$ may be shown to equal to $\frac{-q_p}{EI}$

$$\frac{d^4\omega_P}{dx^4} = \frac{-q_p}{EI}$$

It follows that:

$$\frac{\mathrm{d}^4\omega}{\mathrm{dx}^4} + \mathrm{k}^2\frac{\mathrm{d}^2\omega}{\mathrm{dx}^2} + \alpha = 0 \qquad 4\text{-}5$$

Where:

$$k^2 = \frac{N}{EI}$$

$$\alpha = \frac{q + q_p}{EI} = \frac{q}{EI} + \frac{72\delta_P}{L_0^4}$$

4.5.2 Effective Download

The effective load in this model can be identified with the same method stated in section 3.2.2. In Terndrup-Pedersen's paper, the total effective download can be given as:

$$q = q_{pipe} + q_s$$

Where:

$\mathrm{q_{pipe}}$ = Pipe submerged weight

$\mathrm{q_s}$ = Uplift resistance of the cover material

Where:

$$\mathrm{q_s} = \gamma_c(HD_o - \frac{\pi}{8}D_o^2 + H^2 tan\phi_c)g$$

$$q_{pipe} = m_0 g$$

Where:

D_o = Overall outside diameter including coatings

γ_c = Submerged weight of burial material per unit volume, 1000 kgm^3 in this paper

g = Acceleration Due to Gravity

H = Minimum height of the cover soil measure between the pipe center line and the sea floor

m_0 = Submerged mass per unit length of the pipeline

4.5.3 Deflection equation

The boundary condition for the equation indicates the pipeline should follow the initial foundation imperfection at the life off point. It is easy to note that the boundary conditions are dependent on the foundation shape and they can be expressed as:

$$\omega(0) = 0$$

$$\frac{\mathrm{d}\omega(0)}{dx} = \begin{cases} \frac{q_f}{6EI}(L_0 - L)^2 L \ , & L < L_0 \\ 0 \ , & L \geq L_0 \end{cases}$$

$$\frac{d^2\omega(0)}{dx^2} = \begin{cases} \frac{q_f}{6EI}(L_0 - L)(3L - L_0) \ , & L < L_0 \\ 0 \ , & L \geq L_0 \end{cases}$$

Boundary conditions express symmetry for$x = L$ are:

$$\frac{d\omega(L)}{dx} = 0$$

$$\frac{d^3\omega(L)}{dx^3} = \frac{-48\delta_P}{L_0^3}$$

The solution to Equation 4-5 may be written as:

$$\omega(x) = Acos(kx) + Bsin(kx) + \frac{1}{k^2}(-\frac{1}{2}\alpha x^2 + \beta x + \frac{\alpha}{k^2} + \gamma) \qquad 4\text{-}6$$

Where:

$$A = -(\frac{\alpha}{k^4} + \frac{\gamma}{k^2})$$

$$B = -\frac{\beta}{k^3} + \frac{\kappa}{k}$$

$$\gamma = \begin{cases} \frac{q_f}{6EI}(L_0 - L)(3L - L_0), & L < L_0 \\ 0 \ , & L \geq L_0 \end{cases}$$

$$\kappa = \begin{cases} \frac{q_f}{6EI}(L_0 - L)^2 L, & L < L_0 \\ 0 \ , & L \geq L_0 \end{cases}$$

The unknown quantity kL which determines the relationship between the buckle force N and uplift length L, is determined from the symmetry condition $d\omega(L)/dx = 0$ and is given by the solution of the transcendental Equation:

$$\left(\frac{\alpha}{k^3}+\frac{\gamma}{k}\right)\sin(kL)-\left(\frac{\beta}{k^2}-\kappa\right)\cos(kL)+\frac{1}{k^2}(-\alpha L+\beta)=0 \quad 4\text{-}7$$

The displacement profile of the buckle region can be solved based on Equations 4-6 for any given buckle wavelength.

4.6 Analysis of Slip Length Region

The analysis of slip length region can be conducted using the same method stated in section 3.3. To achieve equilibrium between the axial force in the undisturbed pipeline and the axial force in the uplifted pipeline section, axial displacements and the associated friction forces should be considered.

The length of the buckle region will increase as the buckle region develops. The axial displacement at the lift off point can be written as:

$$U_{sb}=\frac{(N_0-N)L}{A_sE}-\frac{1}{2}\int_0^L((\frac{d\omega}{dx})^2-\left(\frac{d\omega_f}{dx}\right)^2)dx$$

Similarly, based on the idealized dry friction model, the axial pull out of the section which is not lifted up from the foundation is:

$$U_{ss}=\frac{1}{2}\frac{(N_0-N-\lambda qL)^2}{\lambda qA_sE}$$

Providing that $N_0-N\geq\lambda qL$, here qL denotes the vertical reaction at the lift off point.

Where:

q = Total effective download from soil cover weight and submerged pipe weight

$q=q_{pipe}+q_s$

λ = Equivalent friction coefficient

$\lambda=\frac{q_x}{q}$

4.7 Solutions

The buckle force N for any given buckle length can be determined from the symmetry condition $d\omega(L)/dx = 0$ and is given by the solution of the transcendental equation:

$$\left(\frac{\alpha}{k^3}+\frac{\gamma}{k}\right)\sin(kL)-\left(\frac{\beta}{k^2}-\kappa\right)\cos(kL)+\frac{1}{k^2}(-\alpha L+\beta)=0$$

Based on the assumptions above and the compatibility of displacement, it requires that:

$$U_{ss}=U_{sb}$$

Namely,

$$\frac{(N_0-N)L}{A_sE}-\frac{1}{2}\int_0^L((\frac{d\omega}{dx})^2-\left(\frac{d\omega_f}{dx}\right)^2)dx=\frac{1}{2}\frac{(N_0-N-\lambda qL)^2}{\lambda qA_sE}$$

Thus, we will see

$$N_0 = N + \left[\lambda q A_s E \int_0^L ((\frac{d\omega}{dx})^2 - \left(\frac{d\omega_f}{dx}\right)^2)dx - (\lambda qL)^2\right]^{0.5} \qquad 4\text{-}8$$

Where the integrals in the equation can be calculated analytically using Equations as follows:

$$\int_0^L \left(\frac{d\omega}{dx}\right)^2 dx = \frac{kA^2}{2}(kL - \cos(kL)\sin(kL)) + \frac{kB^2}{2}(kL + \cos(kL)\sin(kL)) + \frac{1}{3}\frac{\alpha^2}{k^7}(kL)^3 + \frac{\beta^2}{k^5}(kL) - kABsin^2(kL) + \frac{2A\alpha}{k^3}\left(\sin(kL) - kLcos(kL)\right) - \frac{2A\beta}{k^2}\left(1 - cos(kL)\right) - \frac{2B\alpha}{k^3}(\cos(kL) + kLsin(kL) - 1) + \frac{2B\beta}{k^2}\sin(kL) - \frac{\alpha\beta}{k^6}(kL)^2 \qquad 4\text{-}8(a)$$

$$\int_0^L \left(\frac{d\omega_f}{dx}\right)^2 d = (\frac{q_f}{6EI})^2 \left[\frac{1}{5}L_0^2\left(L_0^5 - (L_0 - L)^5\right) + \frac{1}{7}(L_0^7 - (L_0 - L)^7) - \frac{1}{3}L_0(L_0^6 - (L_0 - L)^6)\right] \qquad 4\text{-}8(b)$$

Then allowable temperature rise may be calculated with equation:

$$N_0 = \frac{\pi}{4}E\alpha_S\left(D_e^2 - D_i^2\right)\Delta T + \frac{\pi}{4}(1 - 2\nu)(P_i D_i^2 - P_0 D_e^2) \qquad 4\text{-}9$$

4.8 Calculation of Other Results

After the buckle profile is identified, other items, like bending moment, axial stress can be calculated.

Bending moment:

$$\mathrm{M_{max}} = \mathrm{EI}\frac{\mathrm{d}^2\omega}{\mathrm{dx}^2}|_{\mathrm{x=L}}$$

$$M_{max} = EI\left[Ak^2\cos(kL) + Bk^2 sin(kL) + \frac{\alpha}{k^2}\right] \quad 4\text{-}10$$

Axial stress:

$$\sigma_A = \frac{N}{A_s}$$

Where

$$N = k^2 EI$$

4.9 Summary of Date Required

A summary of all the data needed for upheaval buckling analysis is given in this chapter.

4.9.1 Pipeline Properties

- Pipe Steel Mean Diameter [m], the mean diameter of pipe wall, without coatings;
- Pipe Wall Thickness [m],the pipe wall thickness of the steel pipe;
- Pipe Coating [m], out diameter of the concrete coating.

4.9.2 Steel Properties

- Thermal Expansion Coefficient [1/℃], typically 11.7 x 10-6 /K for carbon steel at ambient temperature;

- Young's Modulus [MPa], typically 2.07E5*MPa* for elastic material, which actually may be temperature dependent;
- Stress/strain relationship for elastic-plastic material;
- Poisson Ratio [-], typically 0.3 for steel at ambient temperature;
- Steel Density [kg/m^3], typically 7850 kg/m^3 for steel.

4.9.3 Operating Parameters

- Internal Pressure [bar], pressure of the pipeline contents at the buckle;
- Internal Temperature [℃], temperature of the pipeline contents at the buckle.

4.9.4 Environmental Parameters

- Seawater Density [kg/m^3]; ρ_w is $1025kg/m^3$;
- Water Depth [m]; in this thesis, water depth is *300m*;
- Ambient Temperature [℃], ambient seawater temperature external to the pipeline.

4.9.5 Backfill Material

- Internal Angle of Friction [degrees], the critical state angle of friction of the backfill soil. This is only appropriate for the cohesive less soil model. In this thesis, it is 20deg;
- Submerged soil density [kg/m^3], obtained from soil testing data;
- Burial depth[m], depth of cover from the top surface of the coated pipe to the seabed surface at the point above the seabed imperfection. This represents the cover height prior to any uplift of the pipeline;

4.9.6 Download

- User Defined Download, q_f [N/m]. It is affected by the status of the pipeline, i.e. empty, water filled or operating conditions. It may be adjusted in the analysis step in SIMLA.

4.9.7 Pipe Imperfection

- Initial Pipe Imperfection, δ_P [m]. It is the initial imperfection in the pipeline profile, e.g. through pipeline reeling/straightening or the manufacturing process.
- Initial Foundation Imperfection, δ_f [m]. It is the initial imperfection of the foundation caused by uneven seabed.

4.10 Summary of Solution Procedure

No.	Description	Equations
Step 1	Establish initial imperfection configuration for a given submerged weight and imperfection amplitude, the imperfection wave length can be calculated	4-1 4-2 4-3
Step 2	Calculate the buckle length L corresponding to the allowable maximum uplift $\Delta = 2cm$. Iterative method is used to find the critical buckle length.	4-6 4-7
Step 3	For the choose buckle length L in step 2, calculate the various parameters $\beta\ \gamma\ \alpha\ \kappa\ A\ \&\ B$	4-6
Step 4	Solve equation for kL and determine k	4-7
Step 5	Calculate the buckle force in buckle region N	4-5
Step 6	Calculate the displacement integrals	4-8(a) 4-8(b)
Step 7	Calculate the effective axial force N_0 away from buckle region	4-8
Step 8	Calculate the allowable temperature rise ΔT , compare with the design temperature	4-9
Step 9	Calculate other results, like maximum bending moment, maximum stress	4-10
Step 10	Vary the cover depth, or other parameters and repeat step 1-9	All

Chapter 5 Finite Element Methods for UHB analysis with SIMLA

5.1 Introduction

SIMLA is a special computer tool for analysis of offshore pipeline during design, installation and operation. Several modulus are involved in a typical SIMLA analysis, which may be seen Figure 5-1. FlexEdit is a text editor tailored for use with a variety of MARINTEK programs, including SIMLA. The input file for SIMLA analysis is written in FlexEdit, which you will see some example files in enclosed zip files. SIMPOST is a program that extracts results generated by SIMLA, and arranges it suitable for plotting. Results are saved on an ASCII file. MatrixPlot is a post processor used for plotting of results extracted by SIMPOST. SimVis is a 3D visualization program that shows the pipe and the surrounding environment. Xpost is a 3D visualization program. Compared with SimVis the visualization in this program is linked more closely to the numerical model.

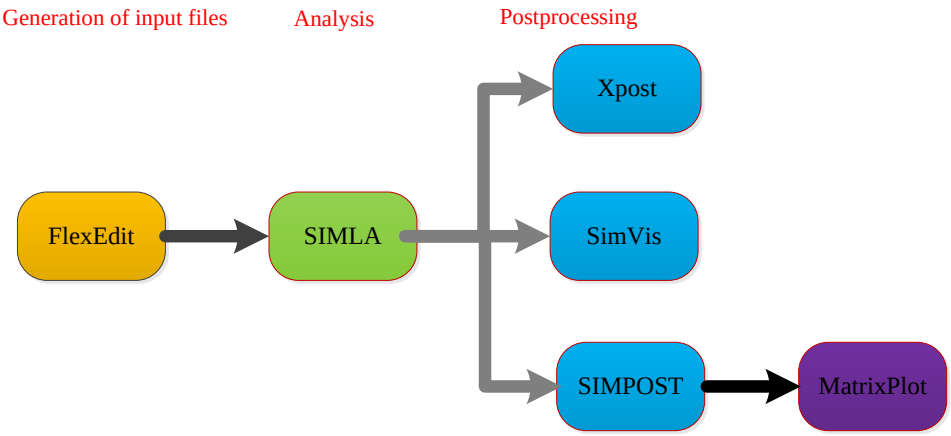

Figure 5-1 Modulus in SIMLA analysis

5.2 Theory Background

The content of this chapter consists of some general theory about advanced structure analysis and advanced dynamic analysis. Some basic theory of FEM is included here to illustrate the knowledge and method [21-25] enrolled in the use of SIMLA software, which is used to do the FE analysis part of the thesis.

5.2.1 Basic of Finite Element Method

The three basic principles for both linear and non-linear structure analysis are listed as follows:

- Compatibility
- Equilibrium
- Constitutive equations

Compatibility (expressed by stresses)

The compatibility requirement for a beam assures that adjacent cross-sections get the same deformation and that the material is continuous when it deforms. This is fulfilled by describing the displacements with continuous interpolation functions and ensuring that the strain is finite at the element boundaries. In SIMLA the pipe elements obey the Bernoulli-Euler deformation hypothesis which assumes that plane cross-sections perpendicular to the neutral axis will remain plane and perpendicular to the neutral axis in the deformed configuration, i.e. shear deformations are neglected. In SIMLA the Green strain definition is applied and the 2nd order longitudinal engineering strain term is neglected.

$$E_{xx} = u_{,x} - yv_{,xx} - zw_{,xx} + \frac{1}{2}(v_{,x}^2 + w_{,x}^2) + \theta_{,x}(yw_{,x} - zv_{,x}) + \frac{1}{2}\theta_{,x}^2(y^2 + z^2) \quad 5\text{-}1$$

The equation 5-1 is based on the Bernoulli-Euler compatibility requirement which is valid also in the elastic-plastic range. In 5-1 the neutral axis coincides with the *x*-axis, and *u, v* and *w* is respectively the axial, horizontal and vertical displacement. The torsional rotation of the neutral axis is denoted as θ. The compatibility requirement is taken into account by including 5-1 in the equilibrium formulation.

Kinematic Equilibrium (expressed by strains)

Equilibrium is expressed by means of the Principle of Virtual Displacements. This principle states that the work performed by the constant true internal stresses and the constant external forces is zero when the structure is exposed to a virtual displacement field which satisfies the boundary conditions. The principle is valid if the stresses and external forces represent an equilibrium state. In the formulation in SIMLA the volume forces are neglected while initial stresses are accounted for. The Principle of Virtual Displacements expressed by tensors for the static case can then be written as:

$$\int_{V_0} (S - S_0)\delta E dV - \int_{\partial V_0} t\delta u dS = 0 \quad 5\text{-}2$$

Here subscript *0* refers to the initial state. *S* is the 2nd Piola-Kirchoff stress tensor, *t* is the surface traction vector, δu is a virtual compatible displacement field and δE is the corresponding virtual Green strain tensor.

Stress Strain Relationship

To solve the problem, the stresses in elements should be related to the strains. This is done with a constitutive equation which for the elastic case is given by Hooke's law. The effect of internal and external pressure will result in a circumferential stress in a subsea pipeline. In the elastic-plastic case this stress must be included in the finite element formulation. Nonlinear problems are solved by incremental methods and therefore a flow rule which gives the plastic strain increments at every point in the load history must be found. Three features must be defined in order to calculate the plastic strain:

- An initial yield condition, which describes the state of stress for which plastic deformation first occurs. For a 2D problem, the 2-dimensional von Mises yield criterion can be write as:

$$f = \sqrt{\sigma_1^2 + \sigma_2^2 - \sigma_1\sigma_2 + 3\tau_{12}^2} - \sigma_Y = 0$$

- A hardening rule. It describes the modification of the yield condition due to strain hardening during plastic flow. In SIMLA, both kinematic and isotropic hardenings are included in the material model.
- A flow rule, which allows the determination of plastic strain increments at each point in the load history. The starting point in the derivation of the flow rule is to define the yield surface, f. In SIMLA the yield surface is assumed to depend on the2nd deviatoric stress invariant J_2, and a hardening parameter κ.

$$f(J_2, \kappa) = 0$$

$f < 0$: Elastic range

$f = 0$: Plastic range

$f > 0$: Inadmissible

More details about the derivation of the flow rule in SIMLA can be found in the Theory Manual of SIMLA by Svein Sævik [23].

5.2.2 Non-linear effects

For structure analysis, the following nonlinearities will be included:

- Material
- Geometry
- Boundary conditions

The material behaves nonlinearly when the stress exceeds the yield limit. Geometric nonlinearity will arise when the structure deforms such that the equilibrium equations must be expressed with respect to the deformed configuration. Nonlinear boundary conditions can for pipeline and trawl board interaction can be, for instance, contact problems in SIMLA.

5.2.3 Lagrange Formulation

Two commonly used methods, namely Updated Lagrange formulation and Total Lagrange formulation are used in finite element method for nonlinear geometrical problems in structural engineering. The difference between the methods is related to the reference configuration. In the total Lagrange method the incremental equations are formulated such that stresses and strains refer to a coordinate system which is fixed with respect to the initial element configuration. Contrary, the updated Lagrange method uses a curvilinear coordinate system which is fixed to the deformed body and continuously updated as the body deforms. The updated Lagrange formulation uses C_n as reference, while the total Lagrange formulation uses C_0 as reference, which is shown in Figure 5-2.

In SIMLA the formulation is based on a co-rotational reference. This method resembles on the updated Lagrange formulation since a Cartesian coordinate system is attached to the element and is continuously updated as the element deforms. The difference between a co-rotational formulation and an updated Lagrange formulation can be neglected for small strains. For a beam element the co-

rotated coordinate system is defined such that the longitudinal coordinate axis intersects the end nodes in the last known equilibrium configuration. When the coordinate system is defined in this manner, the rigid body motions will be separated from the relative element deformation. In Figure 5-2 the co-rotated formulation will have the ghost configuration C_{0n} as the reference [23].

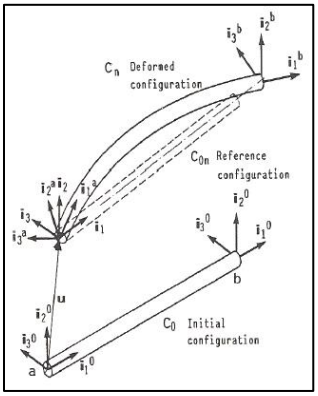

Figure 5-2 Reference configuration in SIMLA

5.2.4 Incremental Stiffness Matrix

Incremental methods are used to solve problems which are nonlinear in terms of material behavior or geometry. Therefore it is necessary to formulate an incremental stiffness matrix. The first step is to apply the Principle of Virtual Displacements in equation 5-3 on two configurations which are close to each other in terms of stresses and strains. Thereafter the integrated equilibrium equations are subtracted from each other. When 2nd order contributions are neglected the result can be expressed Here C^m is the elasticity tensor, S is the 2nd Piola-Kirchoff stress tensor, E is the Green strain tensor, δ is a virtual quantity and Δ denotes the increment between the two configurations.

$$\int_{V_{0n}} (C^m : \Delta E) : \delta E dV + \int_{V_{0n}} S : \delta \Delta E dV - \int_{\partial V_{0n}} \Delta t \times \delta u dS - \int t \times \delta u (\Delta dS) = 0 \qquad 5\text{-}3$$

The first term in equation 5-3 corresponds to the material stiffness matrix, the second term gives the initial stress stiffness matrix and the two last terms will result in an incremental load vector. A load correction stiffness matrix will appear if the loading depend on the motion of the element [23].

The incremental stiffness relation is found on matrix form when the strain measure from equation 5-1 is inserted into equation 5-3 together with the constitutive relation and the selected displacement interpolation functions. When the numerical integration has been executed the tangent stiffness matrix can be expressed as

$$K_T = K_M + K_\sigma$$

Here K_M is the material stiffness matrix and K_σ is the initial stress stiffness matrix on element level. The orientation of the co-rotated coordinate system will in general not coincide with the global coordinate system used for assembly of global matrices. Therefore it is necessary to transform both local displacements and local forces into the global coordinates. This can be expressed by means of transformation matrices as

$$K_T^{Global} = T^T K_T^{Local} T$$

In the co-rotated formulation the continuous updating of transformation matrices accounts for the nonlinear geometry which arises for large rotations [23]. The system equation is obtained by adding the transformed incremental load vectors and element tangent stiffness matrices into a global matrix system. For a static problem the system incremental relation can be expressed as

$$K_T \Delta r = \Delta R$$

Here Δr is the displacement increment and ΔR is the load increment. A static problem is solved stepwise by incrementing the load until a given load level is achieved. In addition equilibrium iterations are typically performed at each load step.

5.3 Command Cards Used

In this section, a summary of the Command Cards used in UHB analysis in SIMLA is presented. More details about the format of each command are given in the enclosed zip file, where all input files for SIMLA are included.

5.3.1 Input Commands

CONTROL: control parameters, which are defined in the analysis process.

TIMECO: time control data. With which the user can define the analysis as a function of time.

NOCOOR: nodal coordinates of model, with which, the user can specify the initial coordinates of the elements.

ELCON: element connectivity and properties. The elements in SIMLA are organized into element groups each having a specific name. Each group is further defined by a reference to element type and material type. By the ELCON command, the user defines the element group, references to element and material types as well as the element connectivity.

ELORIENT: orientation of elements, the ELORIENT command is used to define the initial orientation of the element coordinate systems.

COSURFPR: contact surface properties, the COSURFPR command allows the user to define the contact surface properties, relative to the curvilinear position along the contact surface (determined by *KP* points).

COSUPR: contact surface material properties, the COSUPR command defines the material properties along a route/line on *KP* basis.

CONTINT: contact interfaces, which is defined to optimize the contact search.

ELPROP: element properties, which is used to define the element properties. There are many different types of elements in SIMLA. It should be noted they have to be defined with different formats.

CLOAD: concentrated loads, it should be noted it is defined in global coordinated system.

PELOAD: external pressure and gravity loading

PILOAD: internal pressure load

SEALO: sea load specification, The SEALO command allows the user to define current loading that depends on the position relative to a predefined curvilinear path in the SIMLA coordinate system.

CURLOAD: current loading, the current loading is specified along a route using the curvilinear coordinate of the route as basis for interpolating an arbitrary number of current profiles.

WAVELO: regular and irregular wave loading

THIST: time histories, by the THIST command the user is allowed to describe the load histories related to the different loads specified.

BONCON: boundary Conditions, which can be defined as global or local boundary conditions

CONSTR: constrains, which allows the user to define constraints in the FE model.

MATERIAL: material properties, which can be used to define many different material types as needed.

EPCURVE : elastic-plastic material behavior with kinematic/isotropic hardening.

HYCURVE: hyper elastic (non-linear elastic) material behavior.

5.3.2 Output File

The results from SIMLA are written to several files:

Prefix.sof : The SIMLA Output File which prints out all model information.

Prefix.slf: The SIMLA Log File writes out analysis information such as number of iterations for each step, warnings and errors.

Prefix.raf: The SIMLA result database, this file contains model data, and all element and nodal results required to perform a restart of the analysis, visual representation of the results in XPOST, and post processing by SIMPOST.

Prefix.log: Used for visual representation in SimVis, contains nodal and element results require giving the results stated in the SIMLA input file. The prefix for the prefix.log file is given in the input file (HLA input card).

5.3.3 Post Process

This feature applies the modules SIMPOST and MatrixPlot. SIMPOST extracts the given data from the binary file prefix.raf, and prints out the wanted results on ASCII files with user defined prefixes and the file extension mpf.

Files used for post processing are:

Prefix.spi – The SIMPOST Input file. This file defines the prefix.raf file to be used as input and the prefix.mpf file to be used as output and which results to be plotted. Prefix.mpf is thus user defined.

Prefix.mpf – The MatrixPlot File, an ASCII file containing the results defined in prefix.spi.

Of course it is possible to do post process with user defined software after reading the data from the result file, here the author use MATLAB for instance.

Chapter 6 MATLAB Program for UHB analysis

6.1 Introduction

In this section, the main structure of the MATLAB program for Terndrup-Pedersen's analytical model is presented, which is consist of three parts, i.e. input, solver and output. It is not a generalized program that can deal with all the UHB problems, but it can handle the problem in this thesis by giving right input data.

As it is stated in earlier section, the analytical model has its limitations because of some assumption aiming at simplifying the model, like the soil stiffness is assumed to be infinite, and the pipeline imperfection is assumed the same as the foundation imperfection. However, it may still be used as a useful tool for upheaval buckling analysis at an early design stage.

The input data for this MATLAB program and its core iterative method are defined in section 6.1 and 6.2. The output to the author's concern is introduced in section 6.3.

6.2 Input Data

In this section, all the required data for the analytical model is summarized in the following subsections. The input data should contain the following parts: pipeline properties, steel properties, operating parameters, environmental parameters, pipe and foundation imperfection, backfill data and download from soil cover.

6.2.1 Pipeline Properties

Table 6-1 Pipeline properties

pipe mean diameter	D_m (m)	0.214
pipe wall thickness	t (m)	0.0142
Pipe Coating	D_o (m)	0.4

6.2.2 Steel Properties

Table 6-2 Steel properties

Thermal Expansion Coefficient	$\alpha_s(1/℃)$	11.7 x 10-6	
Young's Modulus	E(MPa)	Elastic material 2.07E5	Plastic material User define curve
Poisson Ratio	ν	0.3	
Steel Density	$\rho_{steel}(kg/m^3)$	7850	
Thermal conductivity	W/m℃	50	
Heat capacity	J/kg℃	800	

6.2.3 Operating Parameters

Table 6-3 Operating parameters

Operating Internal pressure	$P_I(Mpa)$	26.02
Operating External pressure	$P_o(Mpa)$	3.02
Allowable Temperature	δ_T [℃]	To be calculated

6.2.4 Environmental Parameters

Table 6-4 Environmental parameters

Sea water density	$\rho_s(kg/m^3)$	1025
Water depth	$h_{sea}(m)$	300
Ambient Temperature	$T_o(℃)$	0

6.2.5 Pipe and Foundation Imperfection

Table 6-5 Pipe and foundation imperfection

Foundation Imperfection	$\delta_f(m)$	0.1-0.6
Pipeline Imperfection	$\delta_p(m)$	0.1-0.6
Foundation Imperfection half Wavelength	$L_0(m)$	Calculated
Pipeline Imperfection half Wavelength	$L_0(m)$	Calculated

6.2.6 Backfill Data

Table 6-6 Backfill data

Internal Angle of Friction	$\phi_c(°)$	20
Submerged soil density	$\rho_{sc}(kg/m^3)$	1000
Burial depth	$H(m)$	0.4-1.6
User Defined Download	$q(kg/m)$	133

6.3 Solver Used

The most critical procedure for this method is to find the critical buckle length$L$, and afterwards, other parameters can be obtained by just solving an equation with an iterative method in MATLAB. Iterative method is used to find the buckle length L corresponding to the allowable maximum uplift$\Delta = 2cm$. MATLAB is able to solve the equation by several iterative methods. In the program, *fzero* is used to find the root of the equation concerned.

In MATLAB, *x = fzero (fun, x0)* is used to find a zero of fun near *x0*, if *x0* is a scalar, where fun is a function to be handles. The value x returned by *fzero* is near a point where fun changes sign, or *NaN* if the search fails. The search terminates when the search interval is expanded until an *Inf, NaN,* or complex value is found.

There are some limitations for *fzero* function. The *fzero* command finds a point where the function changes sign. If the function is continuous, this is a point where the function has a value near zero. If the function is not continuous, *fzero* may return values that are discontinuous points instead of zeros. Furthermore, the *fzero* command defines a *zero* as a point where the function crosses the *x*-axis. Points where the function touches, but does not cross, the *x*-axis are not valid zeros. For example, $y = x^2$ is a parabola that touches the *x*-axis at 0. Because the function never crosses the *x*-axis, however,

no zero is found. For functions with no valid zeros, *fzero* executes until *Inf, NaN,* or a complex value is detected.

The author also found that the root given by *fzero* is sensitive to the initial guess value *x0*. Hence, in the program, three different initial guess values which are in the range of 0-1 are given to make sure that *fzero* will give the smallest eigenvalue of the concerned equation.

6.4 Output Data

The program may give out the deflection equation of the pipeline for a maximum uplift of 2cm, with which many concerned parameters may be calculated.

- Half imperfection wavelength,L_0 is dependent on the imperfection levelδ_p, pipe submerged weight $q_p$and bending stiffness (*EI*) of the pipeline.
- Critical Buckle length *L*, corresponding to the maximum uplift defined.
- Buckle force in the buckle region, *N*.
- Effective axial force in the region away from the buckle region, $N_{0.}$
- Allowable temperature rise at give operating pressure, δ_T or ΔT.
- Maximum bending moment in the pipeline$M_{max,}$ which is dependent on shape of deflection equation.
- Axial stress, σ.

Obviously it is possible to give some other results like slip length after the deflection equation is identified. Here in this thesis, the main focus will be put on the axial force, maximum bending moment and allowable temperature rise.

Chapter 7 Definition of Cases

7.1 Introduction

In this chapter, the cases needed to be conducted are defined in detail in both analytical model and FE model. A group of imperfection level varying from 0.1m to 0.6m is to be studied in both Pedersen's analytical mode and FE model in software SIMLA. For each imperfection level, there may be different burial depth, which varies from 0.4m to 1.6m. The main focus will be put on the difference between the axial force in the buckle region and the effective axial force in the region away from the buckle region when the maximum uplift is 2 cm, i.e. vertical displacement at he left end of the pipeline is 2 cm. Allowable temperature rise may also be calculate for both analytical and FE model. Then a comparison study between the analytical result and FE result will be conducted to see whether the result given by the analytical model is acceptable or not.

In addition, elastic-plastic material behavior of pipe material is considered afterwards, which is not included in the research proposal. The pipe material has a great effect on its upheaval buckling behavior in fact. Hence, it is necessary to see what will be happen if elastic-plastic material is introduced. A comparison study of analytical result and FE result will be conducted. A summary of the cases conducted is given in Table 7-1.

Table 7-1 Summary of the case

Analytical model (6x7 cases)	
Elastic material(E=2.07E5MPa)	
Burial depth H(m)	Imperfection level δ_p (m)
0.4 -1.6	0.1 - 0.6
FE model (6x7 cases)	
Elastic material(E=2.07E5MPa)	
Burial depth H(m)	Imperfection level δ_p (m)
0.4 -1.6	0.1 - 0.6
FE model (2x7 cases)	
Elastic-plastic material(stress/strain curve)	
Burial depth H(m)	Imperfection level δ_p (m)
0.4 -1.6	0.3,0.4

7.2 Analytical Model

The analytical solution is based on the MATLAB program developed described in Chapter 6. The required data to be given as input for the program is listed in Table 7-2.

Table 7-2 Input data for analytical model

Item	**Magnitude**	**unit**
pipe mean diameter	0.214	m
pipe wall thickness	0.0142	m
pipe coating	0.4	m
Thermal Expansion Coefficient	11.7E6	$1/℃$
Young's Modulus	2.07E5	*[MPa]*
Poisson Ratio	0.3	-
Steel Density	7850	kg/m^3
Seawater Density	1025	kg/m^3
Internal Angle of Friction	20	°
Submerged soil density	1000	kg/m^3
Initial Pipe Imperfection	0.1-0.6	m
Initial Foundation Imperfection	0.1-0.6	m
Operating pressure difference ($P_i - P_o$)	230	bar
pipe submerged weight (γ_c)	133	kg/m
water depth (d)	300	m

The imperfection level will affect the magnitude of the imperfection wave length. The relationship between the imperfection level and the imperfection wavelength is stated in section 4.3 and 4.4. A summary of the relationship between the imperfection level and half imperfection wavelength is given in Table 7-3.

Table 7-3 Imperfection wavelength versus imperfection level

imperfection level δ_p, δ_f (m)	Half imperfection wavelength L_0(m)
0.1	15.8241
0.2	18.8182
0.3	20.8257
0.4	22.3787
0.5	23.6626
0.6	24.7661

The depth of the burial will affect the magnitude of the uplift resistance of the burial material. The uplift resistance will increase as the depth of soil cover increases, as shown in Figure 7-1. The relationship between the burial depth and the peak vertical stiffness is given in section 4.5.2. A summary of their relationships is given in Table 7-4.

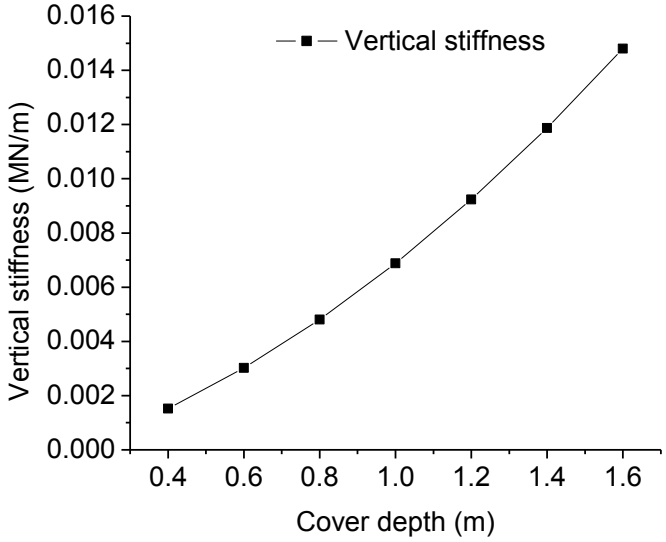

Figure 7-1 Peak vertical stiffness versus cover depth

Table 7-4 Peak vertical stiffness versus cover depth

Cover depth H [m]	**Peak vertical stiffness q_s [M.N/m]**
0.4	1.52E-03
0.6	3.02E-03
0.8	4.81E-03
1.0	6.88E-03
1.2	9.23E-03
1.4	1.19E-02
1.6	1.48E-02

7.3 FE Model

7.3.1 Configuration of Pipeline and Foundation

To verify the result from the analytical model, another model which is almost the same as the analytical model is built and analyzed in SIMLA. The pipeline and steel properties is exactly the same as the analytical model. However, it should be noted that the analytical model doesn't include the soil/pipe interaction, for that the foundation is assumed infinite stiff in analytical model. The configuration of the model in SIMLA is given in Figure 7-2 and 7-3. Due to symmetry, only half of the pipeline is to be modeled. To be noted, the pipeline and foundation imperfection half wavelength is dependent on the imperfection amplitude. Hence, imperfection wavelength should be updated based on Equation 4-2 for different imperfection amplitude. In addition, the download of the pipeline is a

constant in this model, which is fixed at 133*kg/m*, the same as the analytical model. The resistance of the soil cover is calculated based on the dimension of the pipe coating (0.4m used in analytical model).

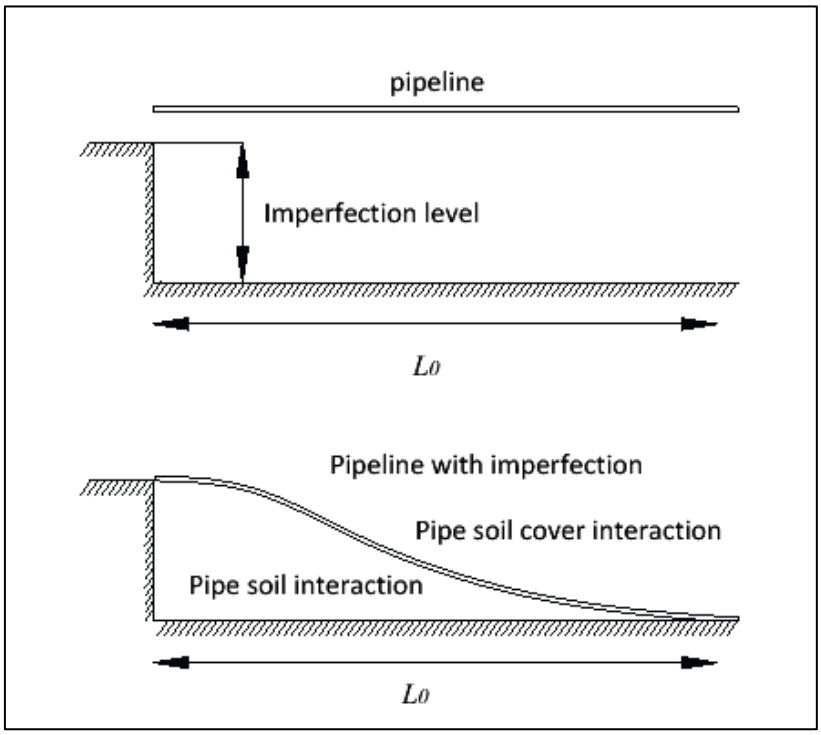

Figure 7-2 Configuration of FE model

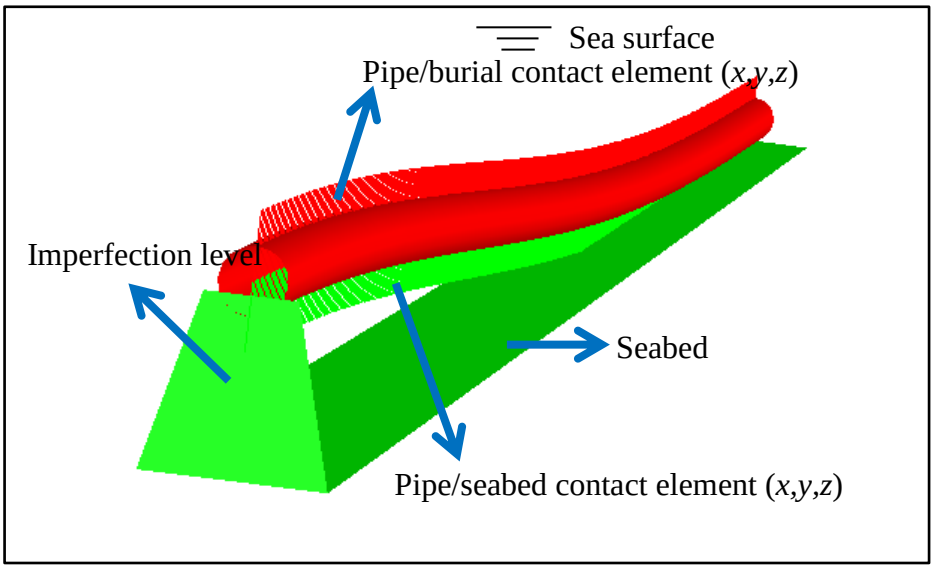

Figure 7- 3 Configuration of FE model in SIMLA

7.3.2 Pipe Model

The initial object of conducting FE analysis in this thesis is to verify the analytical method, where elastic material is assumed. Hence, to make sure that the FE model is similar to the analytical model,

an elastic steel material with a Young's modulus of *2.07E5MPa* is used in the FE model at an early stage. However, the behavior of elastic-plastic material is vital to the analysis of pipeline upheaval buckling. Therefore, additional work was done to study the effect of material on pipeline .upheaval buckling. The dimension of the pipeline in FE model is given in Table 7-5.

Table 7-5 Pipe properties

Item	**magnitude**	**unit**
Pipe external diameter (D_e)	0.2282	m
Pipe internal diameter D_i	0.1998	m
pipe wall thickness (t)	0.0142	m
Poisson Ratio (ν)	0.3	-
Thermal Expansion Coefficient (ν)	1.17E-05	$1/℃$
Thermal conductivity (α_s)	50	$W/m℃$
Heat capacity (dummy)	800	$J/kg℃$
Tension/torsion coupling parameter	0	-

In SIMLA, different element type is used for elastic material and elastic-plastic material. For elastic material, the pipe 31 element is to be used. The Young's modulus of elastic material will be a constant, and other properties like axial stiffness, bending stiffness may be identified. The input properties for pipe31 element are given in Table 7-6. For elastic-plastic material, the pipe33 element is to be used. The stress/strain relationship of the material is required to be given in the input file. It should be noted that pipe31 and pipe33 elements have different formats when defining it properties in SIMLA input file.

Table 7-6 Elastic Material properties for SIMLA input

Item	**magnitude**	**unit**
Axial stiffness (EA)	1976.1611	MN
Bending stiffness about y axis (EI)	11.3623	MNm^2
Bending stiffness about z axis (EI)	11.3623	MNm^2
Torsion stiffness (GI_P)	8.74E+00	MNm^2
Young's Modulus (E)	2.07E+05	MPa
Shear modulus (G)	7.96E+04	MPa
Submerged weight (m_0)	133	kg/m

The elastic-plastic material model used to represent the complete stress/strain relationship for the pipeline material is given in Figure 7-4, which includes nonlinear behavior. In the elastic range, the stress/strain relationship is governed by supplying the Young's modulus of the material. The plastic behavior of the material is defined by specifying numerically the complete plastic stress/strain curve for the steel, usually from test results.

To be noted, the Young's modulus of the used steel pipe will be temperature dependent, but in this thesis, this effect will be neglected. And the stress/strain curve used here is a typical steel material of pipe wall.

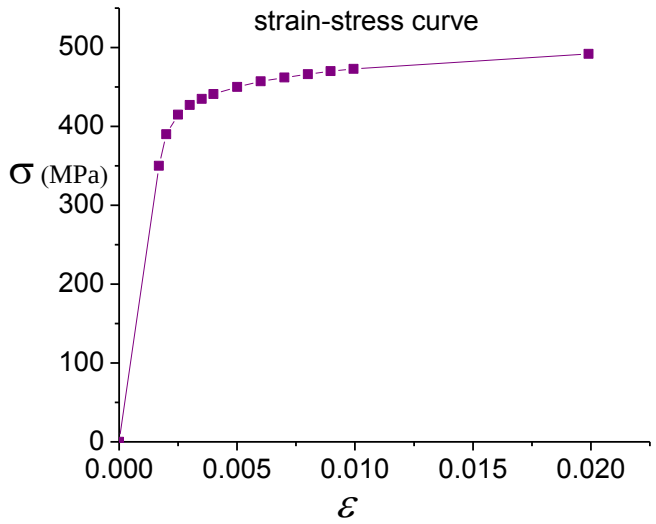

Figure 7-4 stress/strain relationship of the steel material

7.3.3 Boundary Conditions

Arbitrarily boundary conditions along the pipeline may be specified. In this thesis, only a section of the total pipeline length is to be modeled, half of the imperfection wavelength is modeled due to symmetry. It is reasonable for analyzer to simulate the stiffness of the rest of the pipeline with springs in the pipeline ends. In this thesis, the degree of freedoms in 1, 2 , 4 and 5 direction are fixed at the both ends of the pipeline and in addition the vertical displacement at the right end of pipeline is fixed, in SIMLA global coordinate system. The boundary conditions at two ends are the same as in the analytical model, which aims at investigating their differences.

7.3.4 Pipe/Seabed Model

The basis for the constructing the seabed model is data from measurements in the area where the pipeline is going to be installed. In this thesis, the seabed data is from some previous study the author has conducted.

In SIMLA, the seabed was modeled using CONT126 contact elements. The friction coefficients are scaled by a unit force factor. The force factors in the local *x* and *y* directions are given in Figure 7-5 and 7-6. The soil was modeled using an elastic-plastic material behavior (EPCURVE). The mobilization length is *0.005m* in the axial direction and *0.1m* in the lateral direction. The friction factor in *x* and *y* directions is 0.5 and 1. No torsional coupling is introduced in the soil model. In the vertical direction, the soil was modeled using linear elastic material behavior according to Figure 7-7. During laying process, the axial friction was turned off in SIMLA. This was done to obtain a more correct distribution of the axial forces in the pipeline. The axial friction was turned on before internal

pressure and thermal loads were applied. The force factor curves were scaled in the initial analysis to improve convergence.

The contact interface between pipe and seabed was activated in the initiation phase in both the local *y* and *z* directions, but friction in the axial direction was not activated until the operational phase (time>20.0 s).

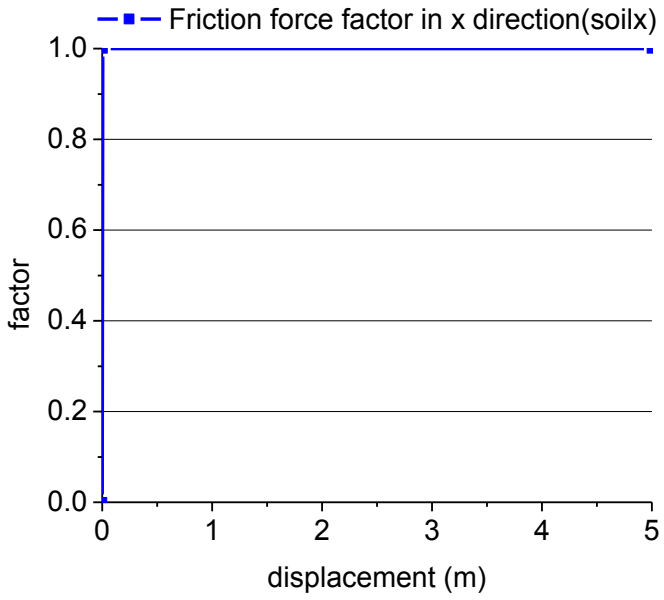

Figure 7-5 Force factor in *x* direction

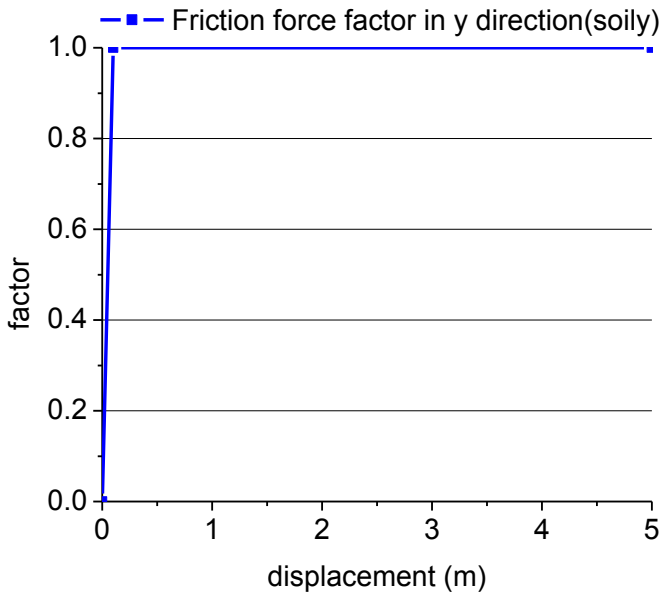

Figure 7-6 Force factor in *y* direction

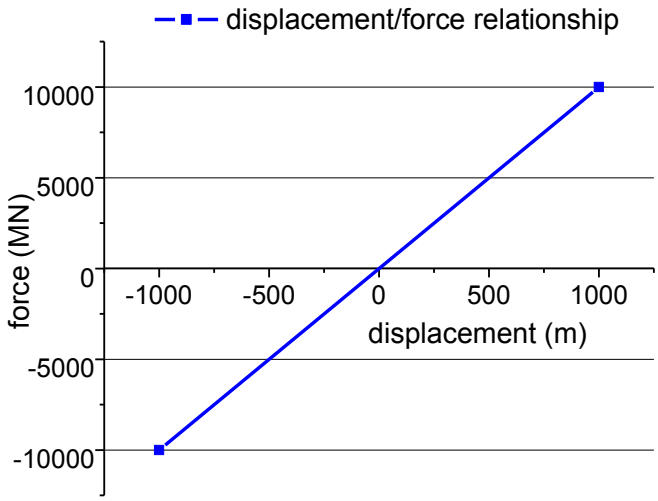

Figure 7-7 Force/displacement relationship in *z* direction

7.3.5 Pipe/Burial Model

The constructing of soil cover (burial) mode should base on data from measurements in the area where the pipeline is going to be installed as well, which is affected by the sand type and trench type, etc. In this thesis, the value of peak burial resistance is the same as the analytical model, in which cohesion less soil is used. However, it is slightly different from the analytical model, where a mobilization length is *0.005m* in the axial direction and *0.002m* in the vertical direction is introduced.

In SIMLA, the burial was modeled using CONT128 contact element, which is a spring element. It should be noted that the material curves for contact 128 element need to be defined using the HYCURVE or EPCURVE options and for both cases the curve is to be defined as a consecutive number of points defining displacement versus force per unit length. No torsional moment curve is introduced in the burial model. In the vertical direction, the soil was modeled using HYCURVE for nonlinear elastic description of the material according to Figure 7-10. In the horizontal direction, the soil was modeled by a HYCURVE model to represent pipe and soil interaction friction, with a friction factor of 0.5, which is the same as the analytical model, according to Figure 7-8. In the lateral direction, the soil was modeled using linear elastic material behavior according to Figure 7-9. During operating process, all the stiffness in three directions was activated. This was done by CONTINT command, by specifying the time when the stiffness is to be activated. In this thesis, the burial stiffness is activated just as the operating pressure is applied to the pipe elements. It should be noted here, the burial resistance is dependent on the burial depth, a larger burial depth will give a larger resistance.

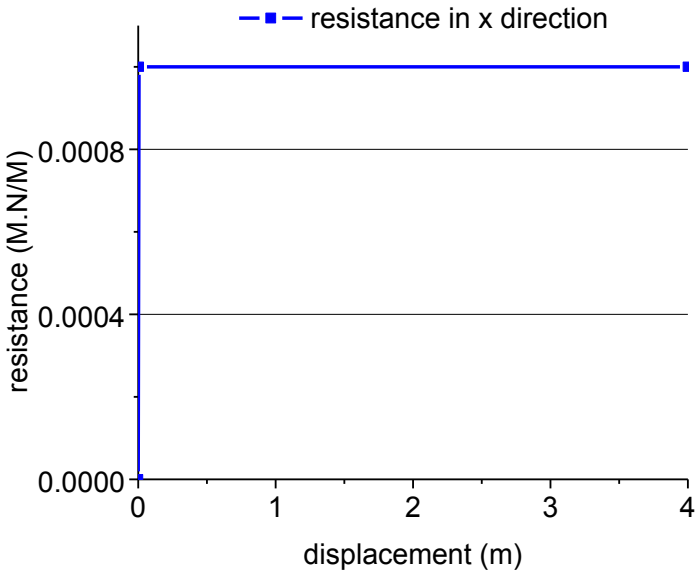

Figure 7-8 Resistance from burial in *x* direction

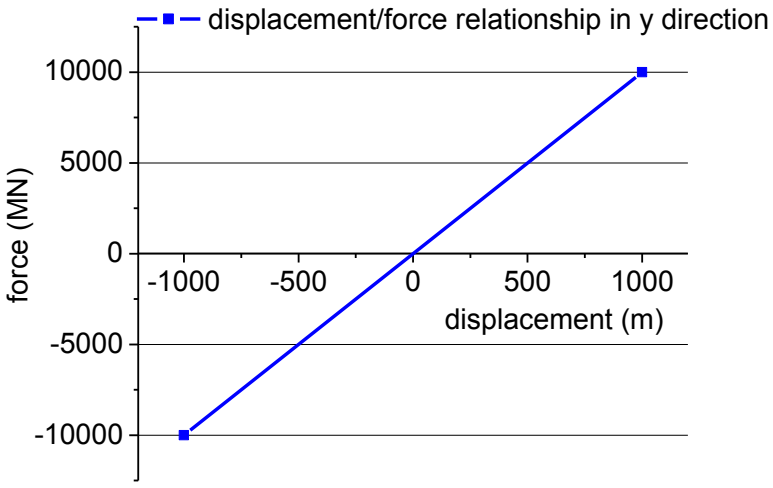

Figure 7-9 Force/displacement in *y* direction

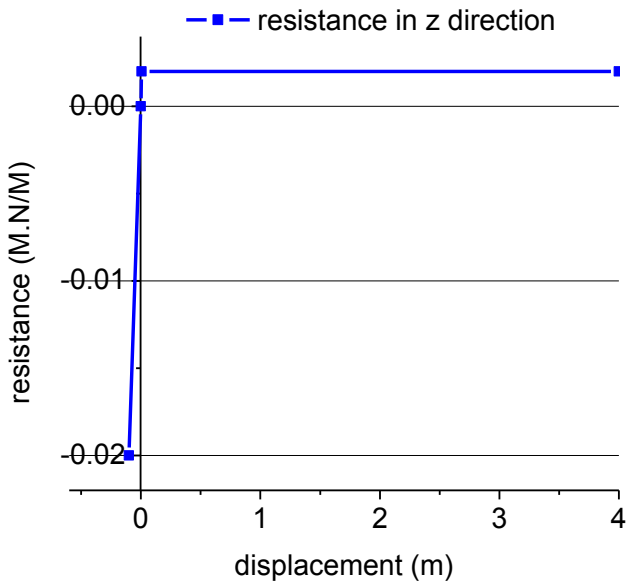

Figure 7-10 Resistance from burial in *z* direction

7.3.6 Load cases

Three load cases were applied sequentially in the SIMLA analysis.

- Initiation and hydrostatic loads (0<t<20). The pipe is installed in a trench resting on an imperfection with given imperfection height varying from *0.1m* to *0.6m* without pretension. When the straight pipe is bent into the imperfection configuration, stresses and strains will arise in the pipe. To achieve the correct buckling loads, it is important to take these effects into account. In SIMLA these effects can be simulated easily using the "AUTOSTART" procedure. This option will automatically deform the stress free, straight pipe to fit to the defined route. The initial analysis includes buoyancy effects and hydrostatic loads corresponding to a water depth of *300m*. Friction in the longitudinal direction is deactivated in this step.
- Internal pressure (20<t<25). The pipeline is exposed to the high pressure when it is filled with oil and gas. An automatic restart analysis was run to statically apply an internal pressure of *26.02 MPa*.
- Thermal load (25<t<45). In the final load case, the thermal expansion was taken into account. An operating temperature difference was applied in the pipe elements.

Chapter 8 Results and Discussions

8.1 Introduction

This section will give out the results from all the executed cases in the thesis and discussions of the results are given in this section.

Firstly, the results obtained from a semi-analytical, linearized model will be considered. The pipe material and geometric parameter are given in Chapter 7, i.e. pipe mean diameter *D*=0.214m, pipe wall thickness *t*=0.0142m, Young's modules *E*=2.07E5N/m^2 for elastic material model, Poisson ratio ν=0.3, and the linear thermal coefficient of expansion is$\bar{\alpha} = 11 \times 10^{-6}/℃$. The difference between the operating pressure in the internal part of pipe and the external pressure is$\Delta P = P_i - P_o = 230bar = 23MPa$. And in this simplified model, the burial resistance may be identified from DNV RP F-110, where in this thesis. A constant resistance from the pipe submerged weight and burial soil cover is assumed and may be calculated from:

$$q = q_{pipe} + q_{sc} = \rho_{sc}\left(HD_o + H^2 tan\phi_c - \frac{\pi}{8}D_o^2\right)g + q_{pipe}$$

Where

q_{pipe} : Pipe submerged weight

q_{sc} : Resistance from the soil cover

ρ_{sc} : Submerged soil density, $1000kg/m^3$

H : Cover depth

D_0: Out diameter of the pipe (coating), 0.4m used for both analytical FE model

ϕ_c : Internal friction angle, 20° is used here for both analytical and FE model

The friction factor between the pipe and the burial is assumed to be 0.5. The pipeline initial imperfection is assumed to be equal to be foundation and the pipeline will be stress free on the foundation imperfection.

With the assumption given above, the minimum temperature where the pipeline will start to lift up can be easily identified with Equation 4-7, it writes as follows:

$$\Delta T_{min} = \frac{qL_0^2}{12\bar{\alpha}EA_s\delta_f} - \frac{\Delta PD}{4Et\bar{\alpha}}(1-2\nu)$$

However, it may be easily found that, this limiting temperature where the pipe just starts to lift from the foundation is very low. For example, for the pipe given above with an imperfection level of 0.3m, and a cover height of 1.0m, the minimum lift up temperature for the pipeline will be about 9.1℃. And this lift up temperature only depends on the curvature of the apex of the initial imperfection. It will be very sensitive to the shape of prop imperfection. Therefore, Terndrup Pedersen proposed a certain allowable maximum finite uplift as a realistic criterion for the risk of gradual uplift. This new criterion reduces the influence from the local effects such as the curvature at some point along the pipeline. Furthermore, Pedersen suggested it is reasonable to assume a certain elasticity of the soil such that migration of sand into cavity below the pipe can take place only when a certain finite uplift occurs.

Hence, all the following results given are based on the design criterion proposed by Terndrup Pedersen. The main focus will be put on calculating the axial force, bending moment and allowable temperature rise for different burial depth, which may be used during an early design stage.

Section 8.2 includes part of results for analytical model. It will give out the axial force in the buckle region, effective axial force in the region away from buckle region and the maximum bending moment in the buckle region. The allowable operating temperature rise for the pipeline can be identified once the effective axial force in the pipeline is calculated. In the analytical model, the suggested acceptable maximum uplift is 2 cm. For given imperfection level, study on the effect of the burial depth will be conducted, by varying the burial depth, which will affect the magnitude of the uplift resistance of the burial. In addition, a study on the imperfection level is conducted to investigate its effect on the accuracy of the analytical model.

Section 8.3 includes part of results for FE model, where only elastic material is considered. It also gives out axial force in the buckle region, effective axial force in the region away from buckle region, the maximum bending moment in the buckle region and temperature rise when maximum uplift of the pipeline reaches 2 cm. Hence it will be comparable to the analytical result.

Section 8.4 includes results for FE model, where elastic-plastic material is considered. It is an additional part of content which is not listed in the research proposal. It is conducted to investigate the effect of the material properties on the result. A comparison study between the elastic material model and elastic-plastic model is made.

To be noted, only part of the analytical and FE results are included in section 8.2-8.4. Section 8.5 will give out a summary of all the result from all the cases that had been conducted during the thesis work.

8.2 Results of Analytical Model

In this section, the analytical results for elastic pipe with imperfection level $\delta_p = 0.3m$ and $\delta_p = 0.4m$ are included. The foundation imperfection half wavelength for initial imperfection $\delta_p = 0.3m$ is 20.8m, and for $\delta_p = 0.4m$ is 22.4m, as given in Table 8-1.

Table 8-1 Imperfection wavelength, $\delta_p = 0.3m, 0.4m$

Item	magnitude	magnitude	Unit
foundation imperfection level (δ_f)	0.3	0.4	M
pipeline imperfection level (δ_p)			M
foundation imperfection half wavelength (L_0)	20.8257	22.3787	M
pipeline imperfection half wavelength (L_0)			M

The initial configuration of the pipeline is found just by laying the pipeline on the seabed with its submerged weight for given prop imperfection level. The operating pressure is 26MPa and it was kept as a constant operating pressure. The allowable effective axial force and allowable operating temperature rise is calculated numerically for given allowable maximum uplift. The foundation is assumed to be infinite stiff in the vertical direction and no friction from the soil. The burial is modeled as a uniform distributed download and a friction force with a friction factor of 0.5 in the horizontal direction. It should be noted that the model of soil/pipe interaction makes the analytical and FE model different, and therefore may cause a larger difference of the result.

A summary of the axial force and maximum bending moment and corresponding allowable temperature rise will be given in Table 8-2 and 8-3, which also gives out how they vary as the burial depth increases. To be noted, those values are calculated corresponding to an allowable maximum uplift of Δ=2cm.

As it is shown in Figure 8-1 and 8-4, the allowable temperature rise for given imperfection level will significantly increase as the burial depth increases. It can also be seen from Figure 8-2 and 8-5 that the buckle force and allowable axial force will increase as the burial depth increases. It is evident to see the maximum bending moment will increase a little bit as the burial depth increase, as it is shown in Figure 8-3 and 8-6. It may be explained by the fact that the deflection shape of the pipe will give a larger curvature when the burial depth is larger. . In this analytical model, the maximum bending moment of the will only dependent on the second deviation of the deflection shape function of the buckle pipe. The maximum bending moment varies due to the change of burial depth, which will affect the magnitude of the critical buckle length corresponding to the design criterion, i.e. Δ=2cm. The actual deflection shape function of the buckle pipe is dependent on the buckle length, as it was shown in section 4.8. It is also evident to see that there is an obvious difference between the axial force in the buckle region and axial force away from buckle region as given in Figure 8-2 and 8-5, which may be explained by the friction force and "feed in" effect of pipeline.

For imperfection level$\delta_p = 0.3m$ and burial depth H=0.4m, the allowable temperature rise for the pipe is 17.98℃, the buckle force is 0.6995MN, while for burial depth H=1.0m, the allowable temperature rise will be about 60℃, which is much larger than the temperature the pipe starts to lift up as given in section 8.1 (9.1℃) and the buckle force is about 1.6439MN. The maximum bending moment for H=0.4m is about 0.1127M.Nm and it is 0.1231M.Nm for H=1.0m.

For imperfection level$\delta_p = 0.4m$ and burial depth H=0.4m, the allowable temperature rise for the pipe is 13.4℃, the buckle force is 0.5889MN, while for burial depth H=1.0m, the allowable temperature rise will be about 50℃ and the buckle force is about 1.4070MN. The maximum bending moment for H=0.4m is about 0.1264M.Nm and it is 0.1362M.Nm for H=1.0m.

8.2.1 Imperfection level $\delta_p = 0.3m$

Table 8-2 Analytical results for imperfection level $\delta_p = 0.3$m

Cover Depth	**Allowable Temperature Difference**	**Axial Force in Buckle Region**	**Axial Force away from Buckle Region**	**Max Bending Moment**
H [m]	**δ_T [℃]**	**N [MN]**	**N_0 [MN]**	**M_{max}[M.Nm]**
0.4	17.98	0.6995	0.7466	0.1127
0.6	30.6	0.9817	1.0384	0.1162
0.8	44.61	1.2969	1.3624	0.1197
1.0	59.97	1.6439	1.7176	0.1231
1.2	76.63	2.0213	2.1027	0.1266
1.4	94.52	2.4277	2.5163	0.1302
1.6	113.59	2.8620	2.9573	0.1338

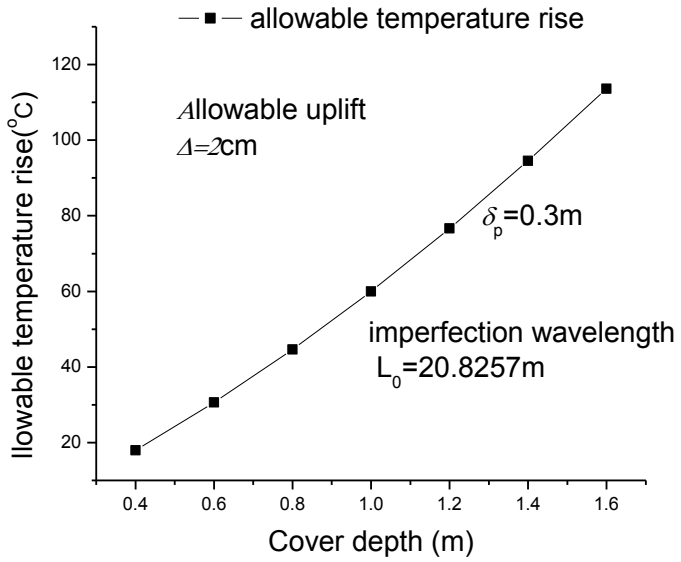

Figure 8-1 Allow temperature rise versus cover depth, $\delta_p = 0.3m$

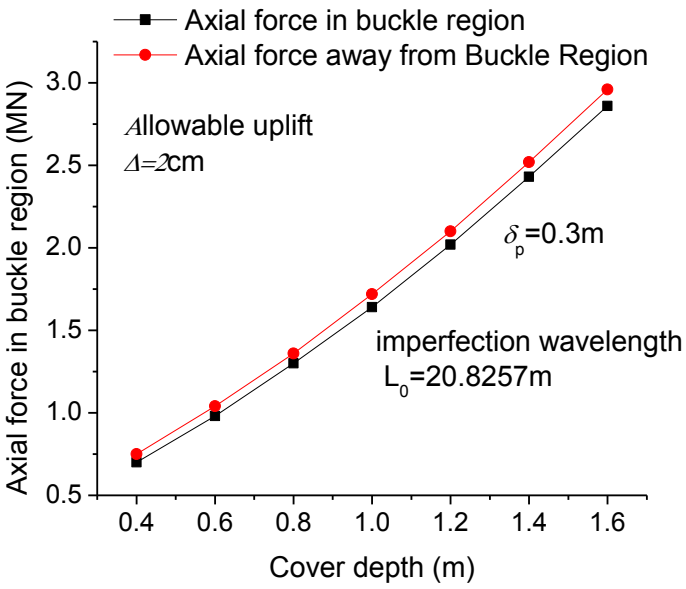

Figure 8-2 Axial force versus cover depth, $\delta_p = 0.3m$

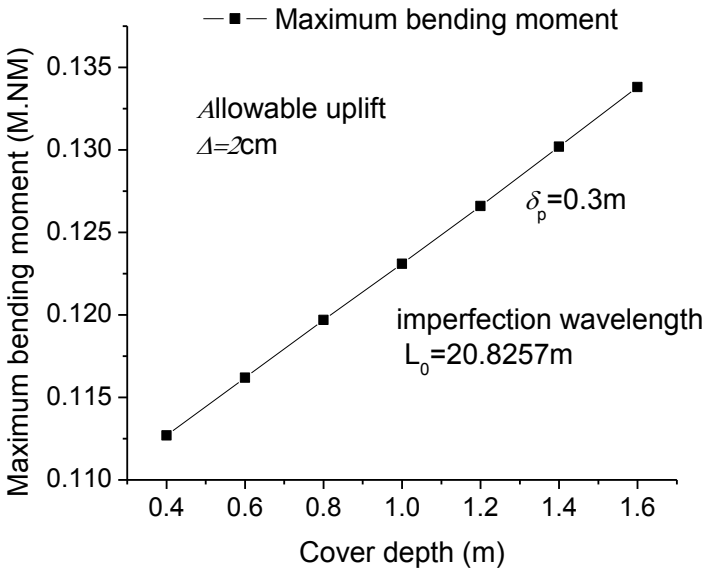

Figure 8-3 Max bending moment versus cover depth, $\delta_p = 0.3m$

8.2.2 Imperfection level $\delta_p = 0.4m$

Table 8-3 Analytical results for imperfection level $\delta_p = 0.4$m

Cover Depth	Allowable Temperature Difference	Axial Force in Buckle Region	Axial Force away from Buckle Region	Max Bending Moment
H [m]	δ_T [℃]	N [MN]	N_0 [MN]	M_{max}[M.Nm]
0.4	13.4	0.5889	0.6407	0.1264
0.6	24.36	0.8319	0.8942	0.1297
0.8	36.59	1.1050	1.1770	0.1329
1.0	50.05	1.4070	1.4882	0.1362
1.2	64.69	1.7369	1.8266	0.1394
1.4	80.46	2.0936	2.1912	0.1427
1.6	97.33	2.4762	2.5813	0.1461

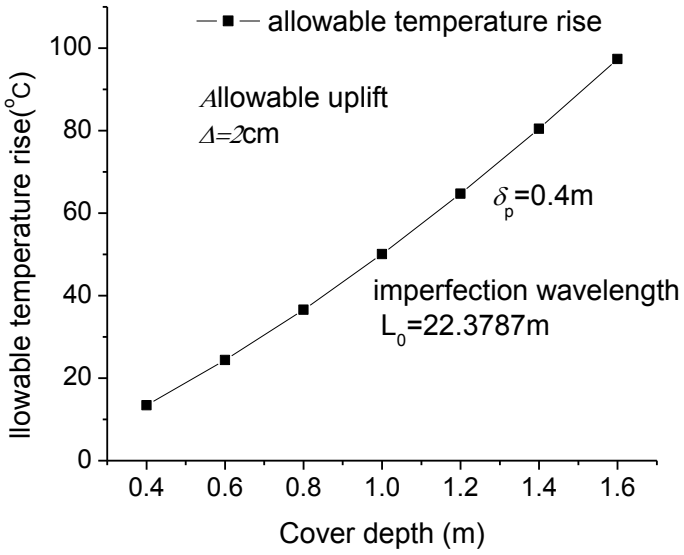

Figure 8-4 Allow temperature rise versus cover depth, $\delta_p = 0.4m$

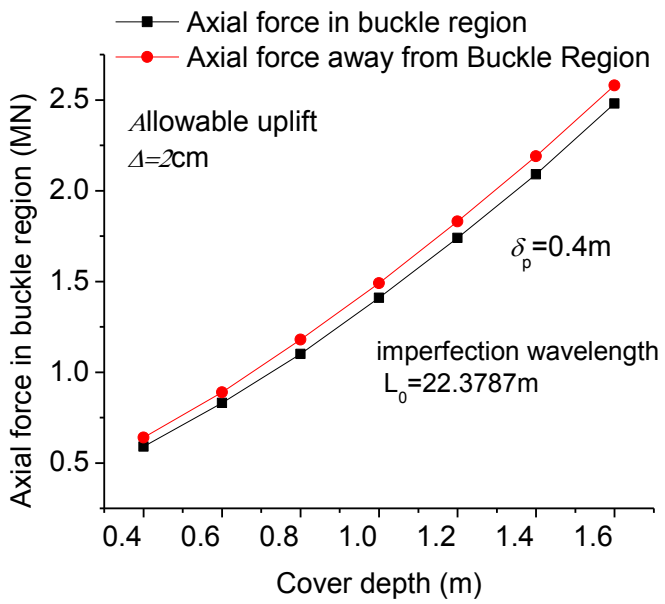

Figure 8-5 Axial force versus cover depth, $\delta_p = 0.4m$

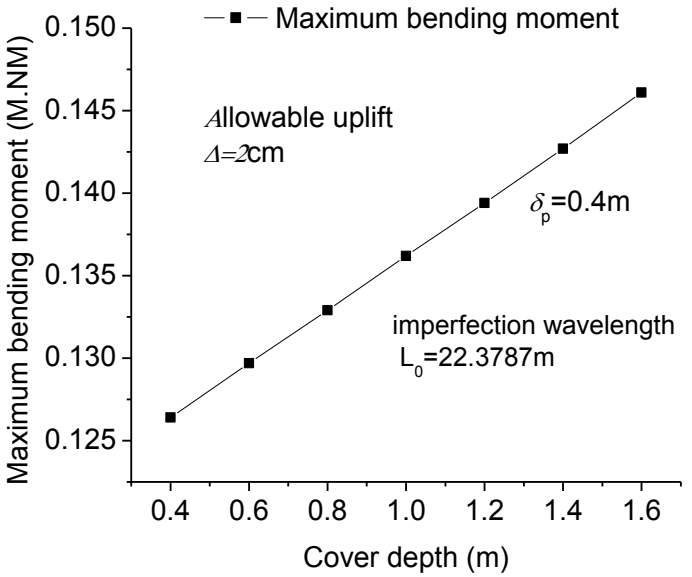

Figure 8-6 Max bending moment versus cover depth, $\delta_p = 0.4m$

8.3 Results of FE Model – Elastic Pipe

In this section, the FE results for elastic pipe with imperfection level $\delta_p = 0.3m$ and $\delta_p = 0.4m$ are included.

The foundation imperfection half wavelength for given imperfection level is the same as the analytical model as in Table 8-1. In the FE model, the pipeline is initially laid on the sea bed with its submerged weight to find its imperfection configuration automatically in 20 seconds. Then an operating pressure of 26MPa is applied in 5 seconds and it was kept as a constant operating pressure. The operating temperature is applied gradually in 20s. The boundary condition is the applied as described in section 7.3.3. The soil/pipe interaction is modeled with contact 126 element and the pipe/burial is modeled with a spring element, denoted as contact 128 in SIMLA. As it is stated before, the modeling of soil/pipe will result in a difference of analytical and FE model, which may be the reason for the difference in results.

A summary of the axial force and maximum bending moment and corresponding allowable temperature rise will be given in Table 8-4 and 8-5, which also gives out how they vary as the burial depth increases. To be noted, the value of interest is taken from a state where the maximum uplift reaches 2cm at the left hand side of the FE model. The time history of the uplift at the left side of the pipe is given in Figure 8-8 and 8-12.

As it is shown in Figure 8-9 – Figure 8-11 and Figure 8-13 – Figure 8-15, the allowable temperature rise, buckle force, effective axial force and maximum bending moment will has some similar trends to that of analytical model. However, you will see that the magnitude of those allowable temperature rise and buckle force given by the FE model are larger than that of analytical model, namely, the analytical model will give conservative results during design process. At the same time, it is found that the FE model will give a smaller maximum bending moment compared with the analytical model, which may be explained by the difference of soil/pipe interaction. As it is stated earlier, the foundation is assumed to be infinite stiff in the analytical model, while there is a penetration into the soil when the soil/pipe is modeled in the FE model, as it is shown in Figure 8-7. Therefore, it may result in a too stiff bending of the pipe in the analytical model and yield to a larger bending moment.

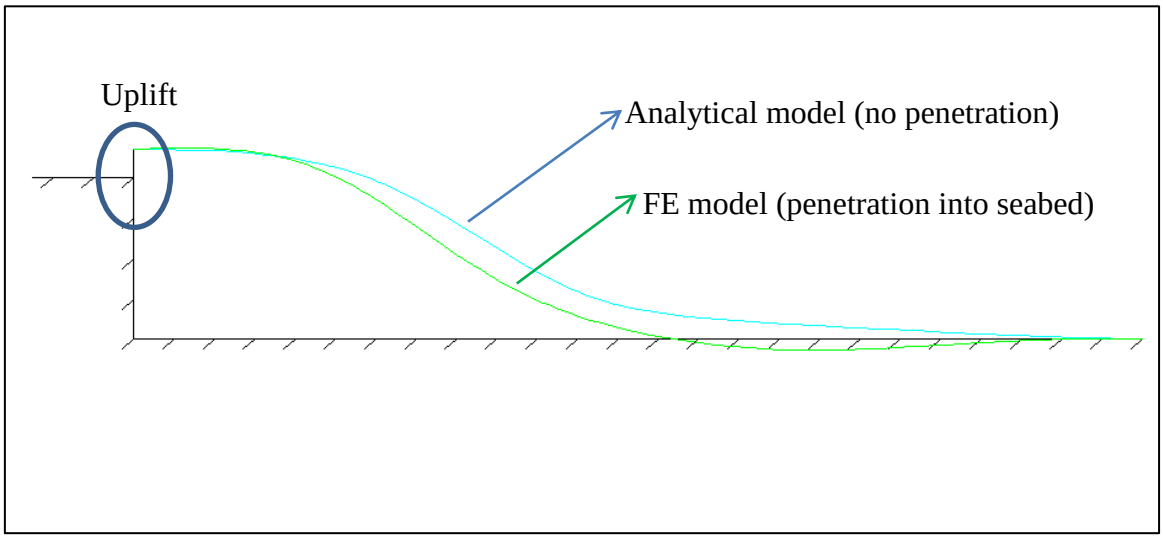

Figure 8-7 Difference of FE and analytical model

For imperfection level$\delta_p = 0.3m$ and burial depth H=0.4m, the allowable temperature rise for the pipe is 21.23℃, the buckle force is 0.7671MN; for burial depth H=1.0m, the allowable temperature rise will be about 69.43℃, and the buckle force is about 1.8822MN. It is evident that those values are slightly larger than the values given by the analytical model. The maximum bending moment for H=0.4m is about 0.0937M.Nm and it is 0.1065M.Nm for H=1.0m, and it is easy to see that they are slightly smaller compared with the results given in by the analytical model.

For imperfection level$\delta_p = 0.4m$ and burial depth H=0.4m, the allowable temperature rise for the pipe is 14.40℃, the buckle force is 0.6089MN; for burial depth H=1.0m, the allowable temperature rise will be about 55.89℃, and the buckle force is about 1.5664MN. It is also noted that those values are slightly larger than the values given by the analytical model. The maximum bending moment for H=0.4m is about 0.1078M.Nm and it is 0.1201M.Nm for H=1.0m, and it is also found that they are slightly smaller compared with the results given in by the analytical model.

Based on the discussions and comparisons above, it is concluded that the analytical model will give results that are consistent with FE model in SIMLA. However, it is also verified that the analytical model always give conservative results in terms of allowable operating temperature and allowable axial force and buckle force. The relative deviation of those parameters concerned between the analytical model and FE model is somehow not that larger for imperfection level $\delta_p = 0.3m$ and$\delta_p = 0.4m$. More discussions about the relative deviation will be given in section 8.6 for different imperfection level.

8.3.1 Imperfection level $\delta_p = 0.3m$

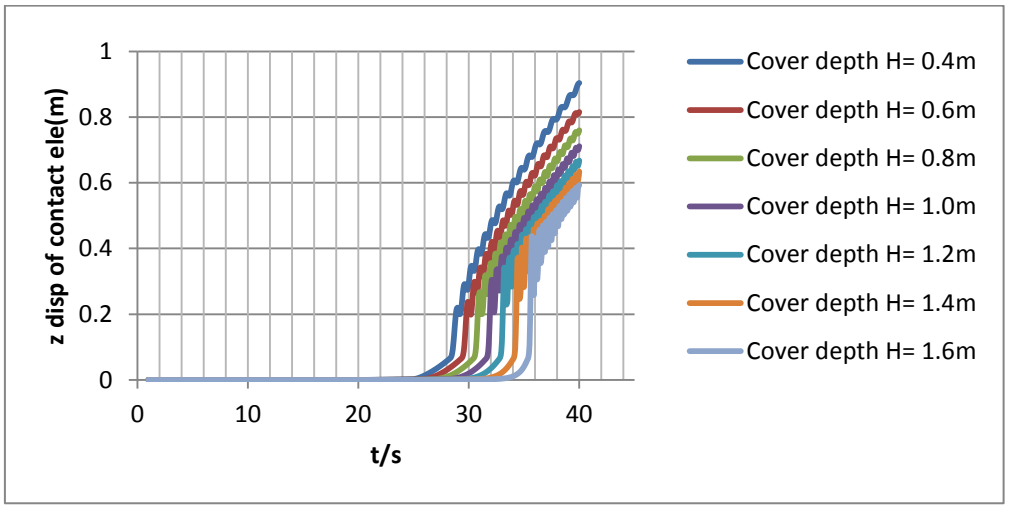

Figure 8-8 Displacement (z) versus time,$\delta_p = 0.3m$, elastic

Table 8-4 FE results for imperfection level$\delta_p = 0.3m$, elastic

Cover Depth	**Temperature Difference when $\Delta = 2$cm**	**Axial Force in Buckle Region when $\Delta = 2$cm**	**Axial Force away from Buckle Region when $\Delta = 2$cm**	**Max Bending Moment when $\Delta = 2$cm**
H [m]	**δ_T [℃]**	**N [MN]**	**N_0 [MN]**	**M_{max}[M.Nm]**
0.4	21.23	0.7671	0.7678	0.0937
0.6	35.98	1.1078	1.1089	0.0984
0.8	52.05	1.4787	1.4803	0.1025
1.0	69.43	1.8801	1.8822	0.1065
1.2	88.14	2.3120	2.3147	0.1104
1.4	108.16	2.7742	2.7776	0.1145
1.6	129.48	3.2664	3.2707	0.1191

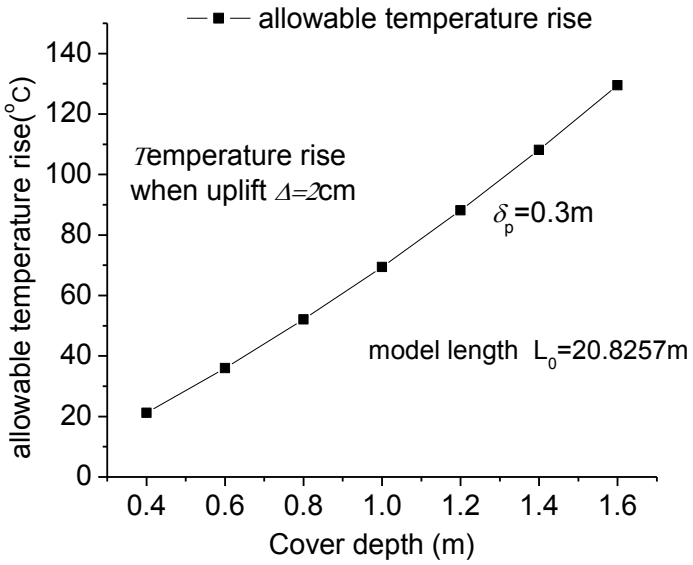

Figure 8-9 Temperature rise versus cover depth, $\delta_p = 0.3m$, $\Delta = 2$cm

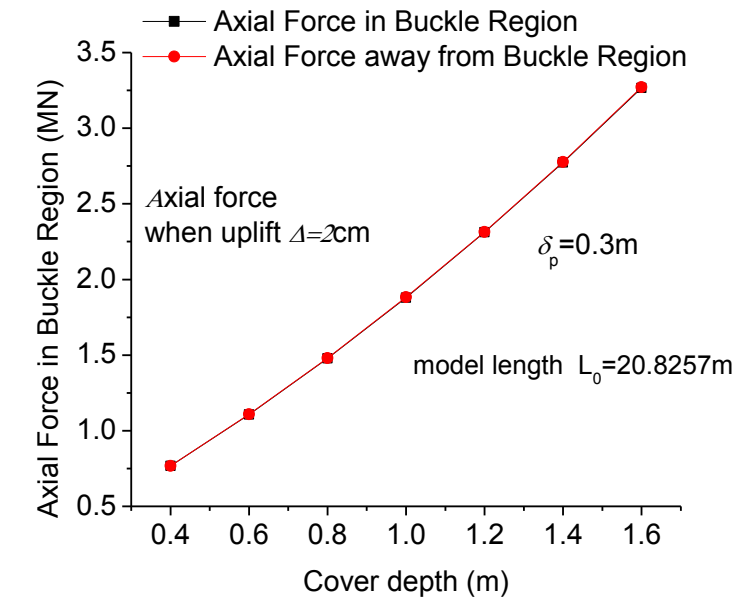

Figure 8-10 Axial force versus cover depth, $\delta_p = 0.3m$, $\Delta = 2\text{cm}$

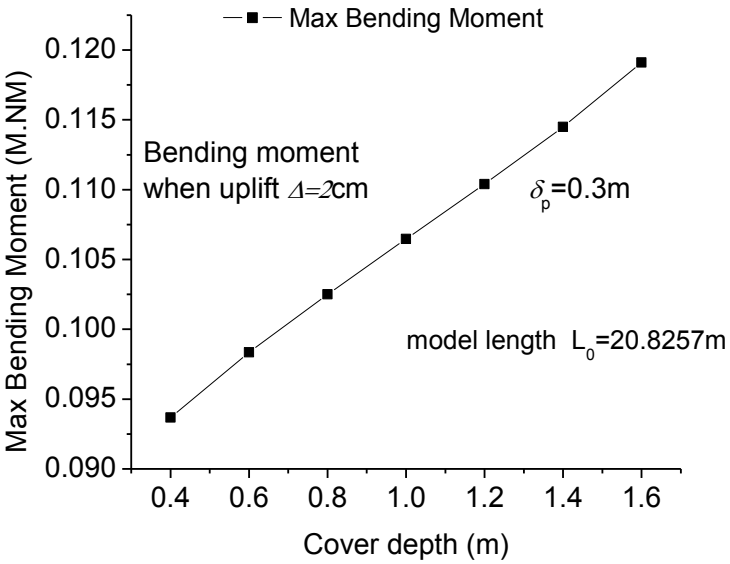

Figure 8-11 Max bending moment versus cover depth, $\delta_p = 0.3m$, $\Delta = 2\text{cm}$

8.3.2 Imperfection level $\delta_p = 0.4m$

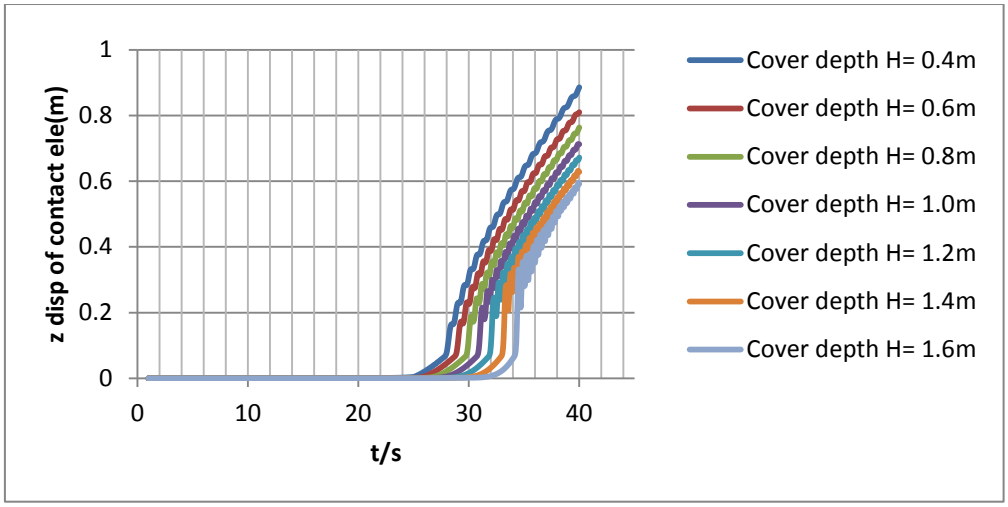

Figure 8-12 Displacement (z) versus time,$\delta_p = 0.4m$, elastic

Table 8-5 FE results for imperfection level$\delta_p = 0.4m$, elastic

Cover Depth	**Temperature Difference when $\Delta = 2$cm**	**Axial Force in Buckle Region when $\Delta = 2$cm**	**Axial Force away from Buckle Region when $\Delta = 2$cm**	**Max Bending Moment when $\Delta = 2$cm**
H [m]	**δ_T [℃]**	**N [MN]**	**N_0 [MN]**	**M_{max}[M.Nm]**
0.4	14.40	0.6089	0.6098	0.1078
0.6	26.57	0.8898	0.8912	0.1120
0.8	41.15	1.2263	1.2284	0.1164
1.0	55.89	1.5664	1.5692	0.1201
1.2	71.94	1.9367	1.9403	0.1237
1.4	88.13	2.3106	2.3146	0.1258
1.6	106.79	2.7411	2.7461	0.1297

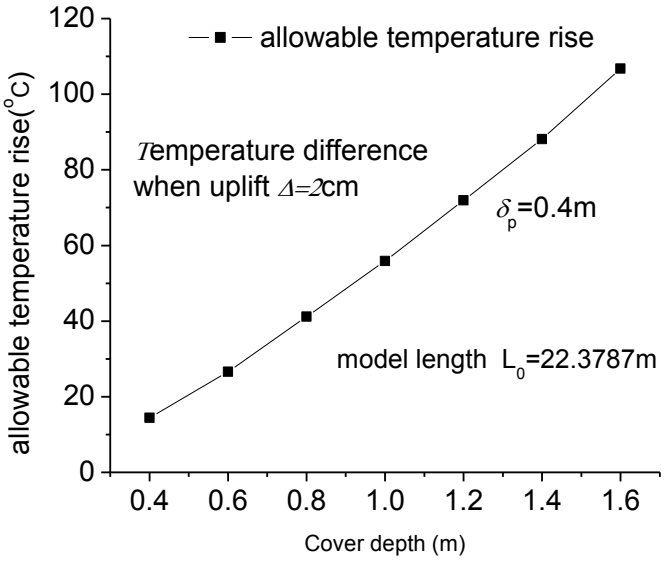

Figure 8-13 Temperature rise versus cover depth,$\delta_p = 0.4m$,$\Delta = 2$cm

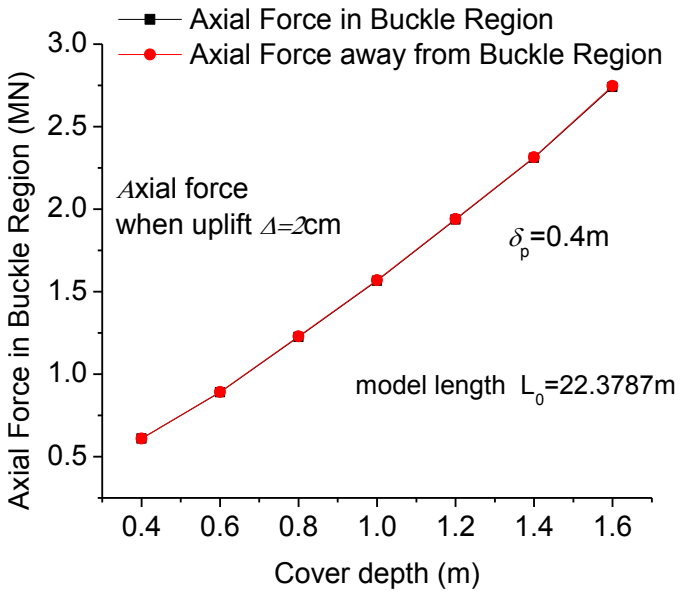

Figure 8-14 Axial force versus cover depth,$\delta_p = 0.4m$,$\Delta = 2$cm

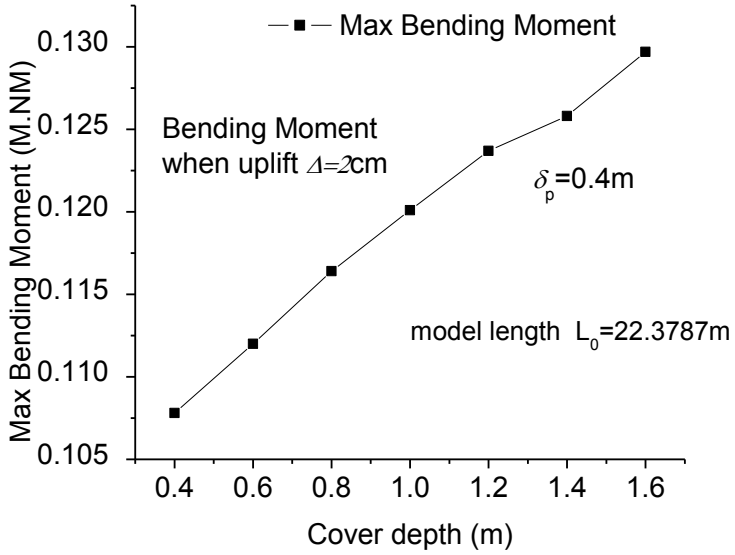

Figure 8-15 Max bending moment versus cover depth,$\delta_p = 0.4m$,$\Delta = 2\text{cm}$

8.4 Results of FE Model – Elastic-plastic Pipe

In this section, the results for elastic-plastic pipe will be included. The model configuration here is exactly the same as elastic model, other parameters such as pipe and steel properties are the same as elastic model. The only difference is the material type. The stress/strain curve is given in section 7.3.2 and the stress/strain relationship is given as appendix I. Load cases in this model is the same as elastic pipe model.

A summary of the axial force and maximum bending moment and corresponding allowable temperature rise will be given in Table 8-6 and 8-7, which also gives out how they vary as the burial depth increases. The value of interest is taken from a state where the maximum uplift reaches 2cm at the left hand side of the FE model. The time history of the uplift at the left side of the pipe is given in Figure 8-16 and 8-20.

As it is shown in Figure 8-17 – Figure 8-19 and Figure 8-21 – Figure 8-23, the allowable temperature rise, buckle force, effective axial force and maximum bending moment will has some similar trends to that of elastic pipe given in section 8.3. However, you will see that the magnitude of those allowable temperature rise, buckle force and maximum bending moment given by the elastic-plastic model are smaller than that of elastic model, namely, the elastic model will give non-conservative results during design process. Hence, to make sure that the design will be a safe one, it is necessary to consider the elastic-plastic behavior of the pipe. In addition, it is shown that the maximum bending moment in the pipeline is not strict monotone increasing as the burial depth increases for elastic-plastic model, which may be explained by elastic-plastic regime and fully plastic regime.

For imperfection level$\delta_p = 0.3m$ and burial depth H=0.4m, the allowable temperature rise for the pipe is 19.98℃, the buckle force is 0.7383MN and the maximum bending moment in the pipeline is 0.0920M.MNm; for burial depth H=1.0m, the allowable temperature rise will be about 66.72℃, the buckle force is about 1.8173MN and the maximum bending moment in the pipeline is 0.1027M.MNm. It is evident that those values are slightly smaller than the values given by the elastic model.

For imperfection level$\delta_p = 0.4m$ and burial depth H=0.4m, the allowable temperature rise for the pipe is 14.33℃, the buckle force is 0.6074MN and the maximum bending moment in the pipeline is 0.1061M.MNm; for burial depth H=1.0m, the allowable temperature rise will be about 54.46℃, the buckle force is about 1.5331MN and the maximum bending moment in the pipeline is 0.1170M.MNm. It is also noted that those values are slightly smaller than the values given by the elastic model.

The relative deviation between the elastic and elastic-plastic model may be explained by plastic buckling. Plastic buckling will generally occur slightly before the theoretical buckling strength of a structure, due to plasticity of the material. When the compressive load is near buckling, the structure will bow significantly and approach yield. The stress-strain behavior of materials is not strictly linear even below yield, and the modulus of elasticity decreases as stress increases, with more rapid change near yield. This lower rigidity reduces the buckling strength of the structure and causes premature buckling.

8.4.1 Imperfection level $\delta_p = 0.3m$

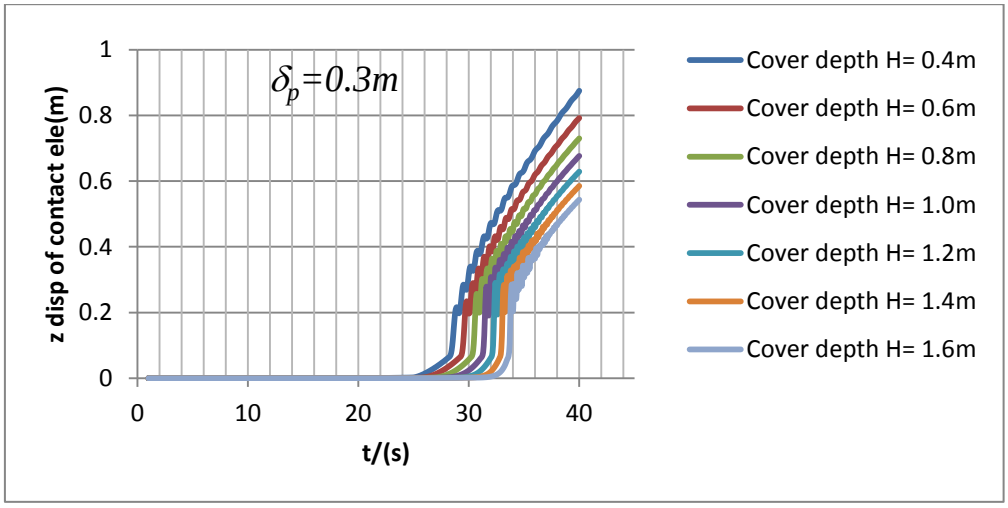

Figure 8-16 Displacement (z) versus time,$\delta_p = 0.3m$, elastic-plastic

Table 8-6 FE results for imperfection level$\delta_p = 0.3m$, elastic-plastic

Cover Depth	**Temperature Difference when $\Delta = 2$cm**	**Axial Force in Buckle Region when $\Delta = 2$cm**	**Axial Force away from Buckle Region when $\Delta = 2$cm**	**Max Bending Moment when $\Delta = 2$cm**
H [m]	**δ_T [℃]**	**N [MN]**	**N_0 [MN]**	**M_{max}[M.Nm]**
0.4	19.98	0.7383	0.7390	0.0920
0.6	34.72	1.0787	1.0797	0.0965
0.8	50.74	1.4486	1.4501	0.1005
1.0	66.72	1.8173	1.8196	0.1027
1.2	82.34	2.1764	2.1807	0.1025
1.4	95.27	2.4728	2.4796	0.0980
1.6	106.48	2.7275	2.7388	0.0911

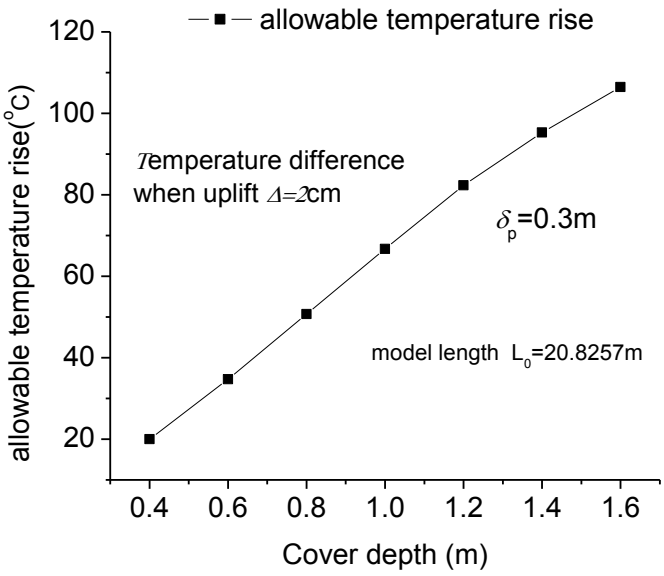

Figure 8-17 Temperature rise versus cover depth, $\delta_p = 0.3m$, $\Delta = 2$cm

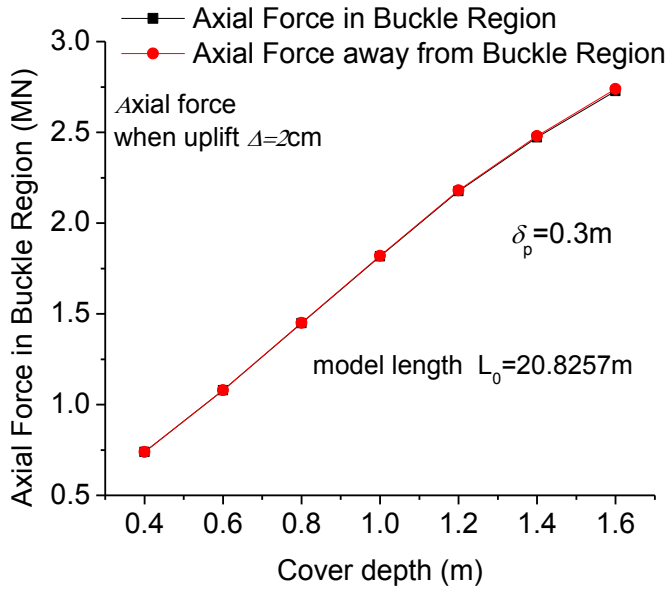

Figure 8-18 Axial force versus cover depth,$\delta_p = 0.3m$, $\Delta = 2$cm

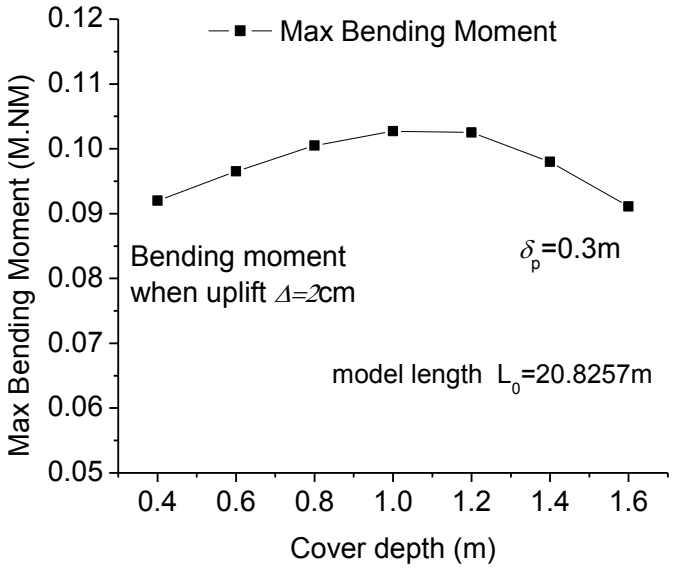

Figure 8-19 Max bending moment versus cover depth,$\delta_p = 0.3m$, $\Delta = 2$cm

8.4.2 Imperfection level $\delta_p = 0.4m$

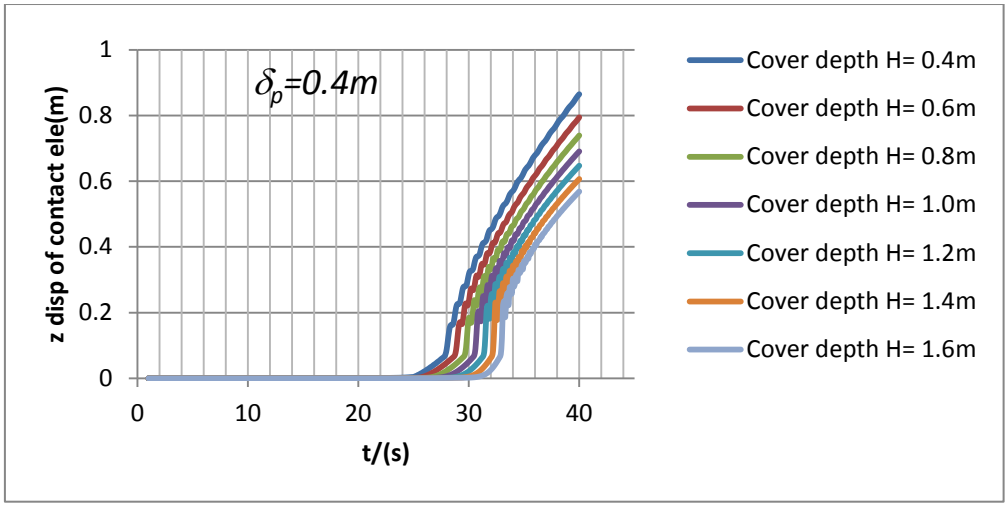

Figure 8-20 Displacement (z) versus time,$\delta_p = 0.4m$, elastic-plastic

Table 8-7 FE results for imperfection level$\delta_p = 0.4m$, elastic-plastic

Cover Depth	**Temperature Difference when $\Delta = 2$cm**	**Axial Force in Buckle Region when $\Delta = 2$cm**	**Axial Force away from Buckle Region when $\Delta = 2$cm**	**Max Bending Moment when $\Delta = 2$cm**
H [m]	**δ_T [℃]**	**N [MN]**	**N_0 [MN]**	**M_{max}[M.Nm]**
0.4	14.33	0.6074	0.6083	0.1061
0.6	26.48	0.8878	0.8892	0.1104
0.8	39.88	1.1969	1.1990	0.1141
1.0	54.46	1.5331	1.5361	0.1170
1.2	67.78	1.8397	1.8440	0.1167
1.4	80.81	2.1385	2.1454	0.1140
1.6	92.43	2.4031	2.4140	0.1086

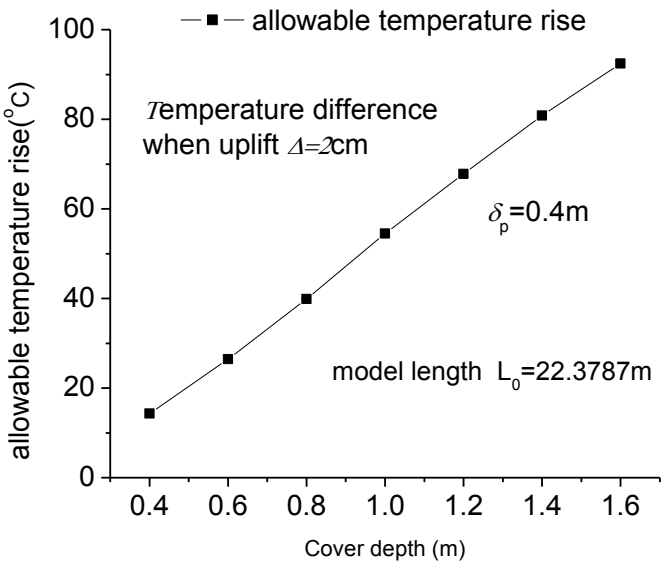

Figure 8-21 Temperature rise versus cover depth,$\delta_p = 0.3m$, $\Delta = 2\text{cm}$

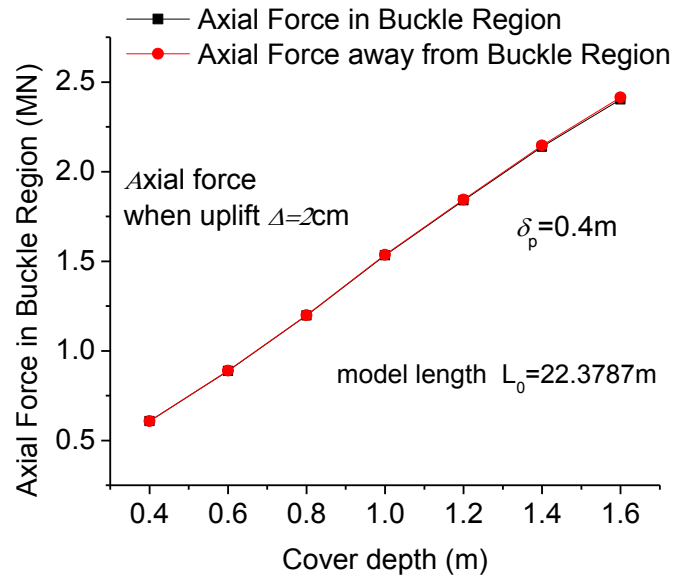

Figure 8-22 Axial force versus cover depth,$\delta_p = 0.4m$, $\Delta = 2\text{cm}$

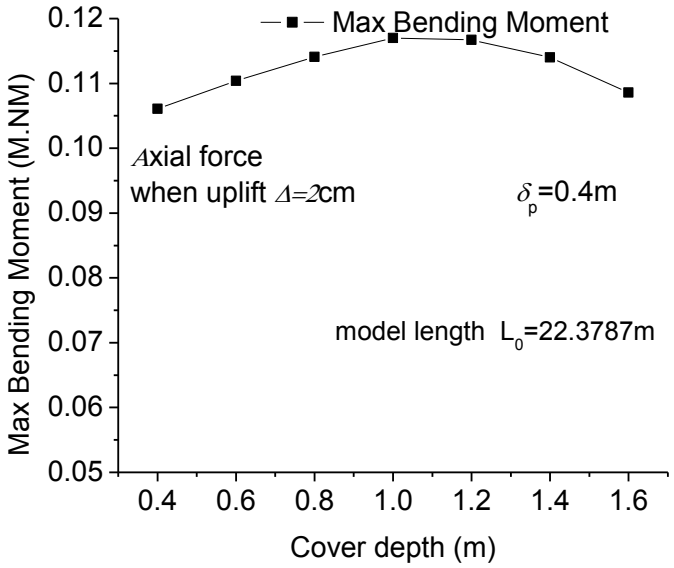

Figure 8-23 Max bending moment versus cover depth,$\delta_p = 0.4m$, $\Delta = 2$cm

8.5 Summary of Results

Only part of the results is presented in section 8.2-8.4. More cases study has been conducted during the thesis work. Summary of all the results is given in this section, which covers 42 cases for analytical model, 42 cases for Elastic Model and 14 cases for Elastic-plastic Model. For each imperfection level, the allowable temperature rise, axial force in the buckle region and away from buckle region and maximum bending moment are given corresponding to an allowable maximum uplift of Δ=2cm. Similarly, the same parameters are given corresponding to a maximum uplift of 2 cm at the left end of the FE model. In addition, an elastic-plastic model is built up to consider the plastic behavior of the pipe, including 14 more cases. All these results are given in section 8.5 and discussion of all these results are presented in section 8.6.

8.5.1 Results for Elastic Pipe $\delta_p = 0.1m$

The results for imperfection level $\delta_P = 0.1$m are included in this section. The length of the model is 15.8241m. As it is shown in Figure 8-24 – Figure 8-26, the allowable operating temperature, buckle force and maximum bending moment given by the analytical model are significantly smaller than those of FE model. For instance, for cover depth H=0.4m, the allowable temperature is about 44.06℃ according to analytical results, while it will be about 67.50℃ according to the FE results. The difference between the two models will increase as the burial depth increases. It may be explained by the difference of the pipe/soil model in two models. The magnitude of the penetration (about 0.013m), which is greatly dependent on the soil resistance defined in the soil/pipe model in the FE model, is relatively a bit too large compared with an imperfection level of 0.1m. The penetration of pipe into seabed in the FE model will affect the result to a large extent for the FE model. Therefore it is reasonable the FE model will give larger results in those terms concerned.

Table 8-8 Summary of result for $\delta_P = 0.1$m

No.1	**Imperfection level $\delta_P = \delta_f = 0.1$m**			
Analytical Results				
Cover Depth	Allowable Temperature Difference	Axial Force in Buckle Region	Axial Force away from Buckle Region	Max Bending Moment
H [m]	δ_T [℃]	N [MN]	N_0 [MN]	M_{max}[M.Nm]
0.4	44.06	1.3168	1.3496	0.0771
0.6	64.88	1.7913	1.8309	0.0815
0.8	87.47	2.3076	2.3534	0.0859
1.0	111.73	2.8627	2.9143	0.0904
1.2	137.53	3.4538	3.5108	0.0950
1.4	164.76	4.0784	4.1403	0.0997
1.6	193.29	4.7334	4.8000	0.1045
SIMLA Results (Elastic Material)				
Cover Depth	Temperature Difference when $\Delta = 2$cm	Axial Force in Buckle Region when $\Delta = 2$cm	Axial Force away from Buckle Region when $\Delta = 2$cm	Max Bending Moment when $\Delta = 2$cm
H [m]	δ_T [℃]	N [MN]	N_0 [MN]	M_{max}[M.Nm]
0.4	67.50	1.8373	1.8375	0.0543
0.6	98.13	2.5456	2.5459	0.0606
0.8	128.87	3.2561	3.2565	0.0645
1.0	162.22	4.0270	4.0275	0.0692
1.2	198.25	4.8600	4.8607	0.0731
1.4	237.28	5.7622	5.7632	0.0804
1.6	274.12	6.6522	6.6524	0.0865

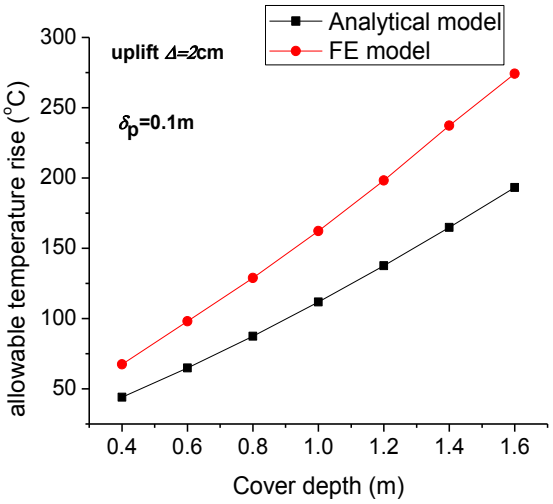

Figure 8-24 Temperature rise versus cover depth, $\delta_p = 0.1m$

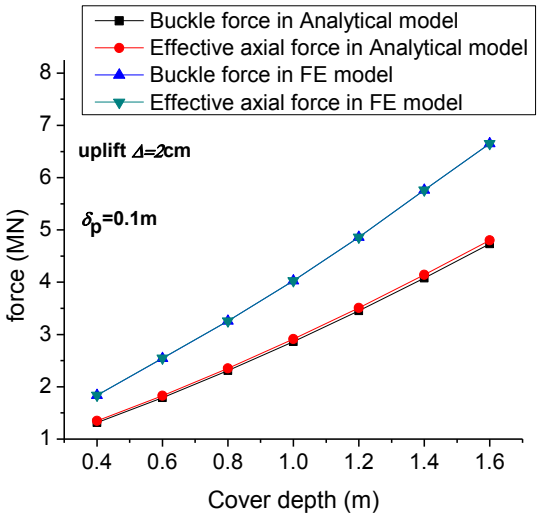

Figure 8-25 Force versus cover depth, $\delta_p = 0.1m$

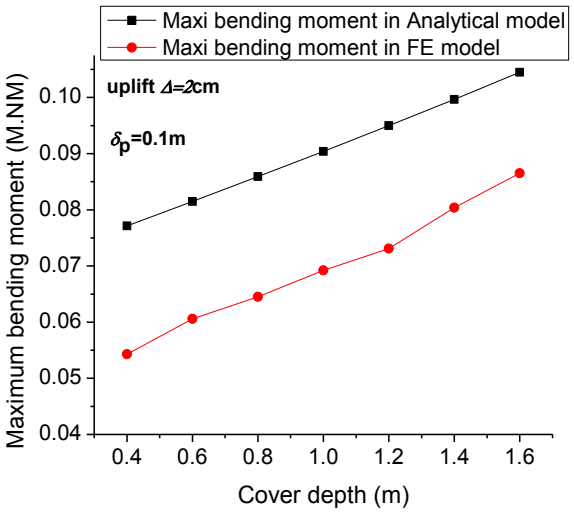

Figure 8-26 Max bending moment versus cover depth, $\delta_p = 0.1m$

8.5.2 Results for Elastic Pipe $\delta_p = 0.2m$

The results for imperfection level $\delta_P = 0.2$m are included in this section. The length of the model is 18.8182m. As it is shown in Figure 8-27 – Figure 8-29, the allowable operating temperature, buckle force and maximum bending moment given by the analytical model are smaller than those of FE model. For instance, for cover depth H=0.4m, the allowable temperature is about 25.90℃ according to analytical results, while it will be about 32.31℃ according to the FE results. The difference between the two models will also increase as the burial depth increases, but it is not that large as that of imperfection level$\delta_P = 0.1m$. It may still be explained by the difference of the pipe/soil model in two models. The magnitude of the penetration (about 0.013m), which is greatly dependent on the soil resistance defined in the soil/pipe model in the FE model, is relatively not as much large compared with an imperfection level of 0.2m. The penetration of pipe into seabed in the FE model will not affect the result to a very large extent for the FE model. It is shown in Figure 8-27 – Figure 8-29, the FE model will give results close to but larger than the analytical model.

Table 8-9 Summary of result for $\delta_P = 0.2$m

No.2	**Imperfection level $\delta_P = \delta_f = 0.2$m**			
Analytical Results				
Cover Depth	Allowable Temperature Difference	Axial Force in Buckle Region	Axial Force away from Buckle Region	Max Bending Moment
H [m]	δ_T [℃]	N [MN]	N_0 [MN]	M_{max}[M.Nm]
0.4	25.90	0.8887	0.9299	0.0969
0.6	41.21	1.2343	1.2838	0.1006
0.8	58.09	1.6169	1.6741	0.1044
1.0	76.49	2.0349	2.0993	0.1082
1.2	96.30	2.4862	2.5574	0.1121
1.4	117.46	2.9693	3.0467	0.1160
1.6	139.90	3.4823	3.5655	0.1201
SIMLA Results (Elastic Material)				
Cover Depth	Temperature Difference when $\Delta = 2$cm	Axial Force in Buckle Region when $\Delta = 2$cm	Axial Force away from Buckle Region when $\Delta = 2$cm	Max Bending Moment when $\Delta = 2$cm
H [m]	δ_T [℃]	N [MN]	N_0 [MN]	M_{max}[M.Nm]
0.4	32.31	1.0235	1.0239	0.0764
0.6	51.05	1.4567	1.4574	0.0811
0.8	72.35	1.9487	1.9497	0.0862
1.0	93.76	2.4434	2.4447	0.0900
1.2	117.69	2.9962	2.9981	0.0957
1.4	141.78	3.5528	3.5550	0.0990
1.6	167.25	4.1416	4.1439	0.1004

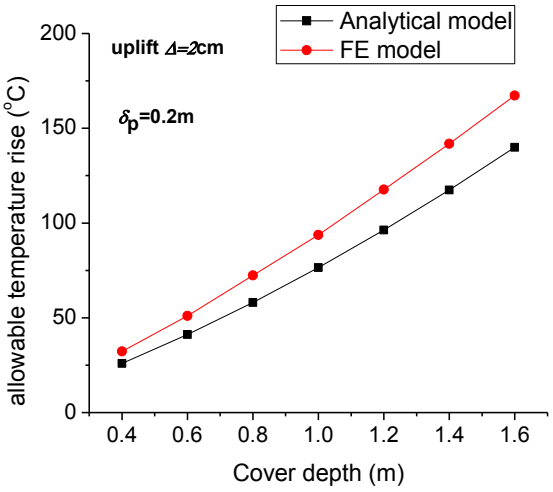

Figure 8-27 Temperature rise versus cover depth, $\delta_p = 0.2m$

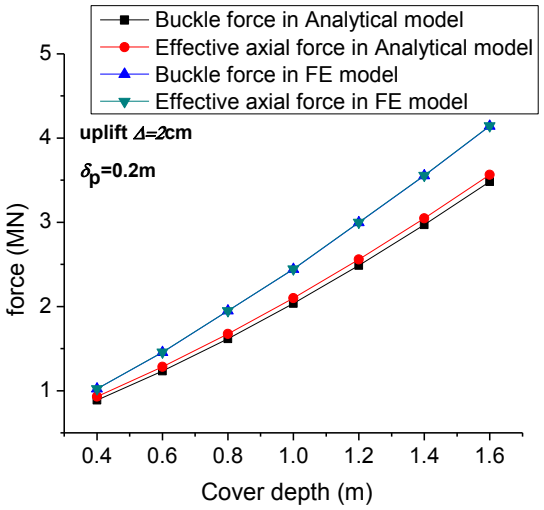

Figure 8-28 Force versus cover depth, $\delta_p = 0.2m$

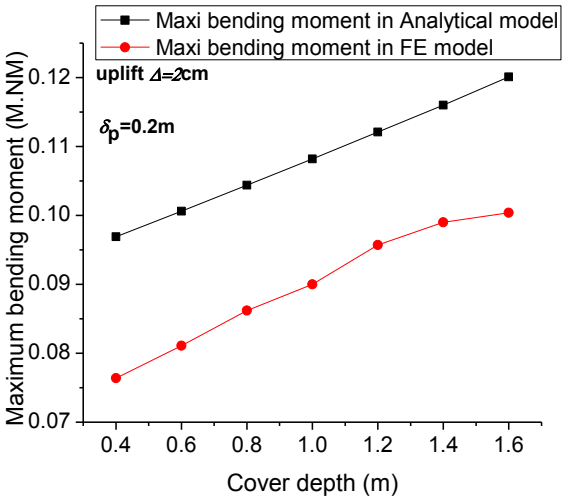

Figure 8-29 Max bending moment versus cover depth, $\delta_p = 0.2m$

8.5.3 Results for Elastic Pipe $\delta_p = 0.3m$

The results for imperfection level $\delta_P = 0.3$m are included in this section. The length of the model is 20.8257m. As it is shown in Figure 8-30 – Figure 8-32, the allowable operating temperature, buckle force and maximum bending moment given by the analytical model are slightly smaller than those of FE model. For instance, for cover depth H=0.4m, the allowable temperature is about 17.98℃ according to analytical results, while it will be about 21.23℃ according to the FE results. The difference between the two models will also increase as the burial depth increases, but it is not that large as that of imperfection level$\delta_P = 0.1 - 0.2m$. The magnitude of the penetration (about 0.013m), which is greatly dependent on the soil resistance defined in the soil/pipe model in the FE model, is relatively small compared with an imperfection level of 0.3m. The penetration of pipe into seabed in the FE model will not affect the result that much, i.e. the FE model becomes closer to the analytical model for large imperfections.

Table 8-10 Summary of result for $\delta_P = 0.3$m

No.3	**Imperfection level $\delta_P = \delta_f = 0.3$m**			
Analytical Results				
Cover Depth	Allowable Temperature Difference	Axial Force in Buckle Region	Axial Force away from Buckle Region	Max Bending Moment
H [m]	δ_T [℃]	N [MN]	N_0 [MN]	M_{max}[M.Nm]
0.4	17.98	0.6995	0.7466	0.1127
0.6	30.60	0.9817	1.0384	0.1162
0.8	44.61	1.2969	1.3624	0.1197
1.0	59.97	1.6439	1.7176	0.1231
1.2	76.63	2.0213	2.1027	0.1266
1.4	94.52	2.4277	2.5163	0.1302
1.6	113.59	2.8620	2.9573	0.1338
SIMLA Results (Elastic Material)				
Cover Depth	Temperature Difference when $\Delta = 2$cm	Axial Force in Buckle Region when $\Delta = 2$cm	Axial Force away from Buckle Region when $\Delta = 2$cm	Max Bending Moment when $\Delta = 2$cm
H [m]	δ_T [℃]	N [MN]	N_0 [MN]	M_{max}[M.Nm]
0.4	21.23	0.7671	0.7678	0.0937
0.6	35.98	1.1078	1.1089	0.0984
0.8	52.05	1.4787	1.4803	0.1025
1.0	69.43	1.8801	1.8822	0.1065
1.2	88.14	2.3120	2.3147	0.1104
1.4	108.16	2.7742	2.7776	0.1145
1.6	129.48	3.2664	3.2707	0.1191

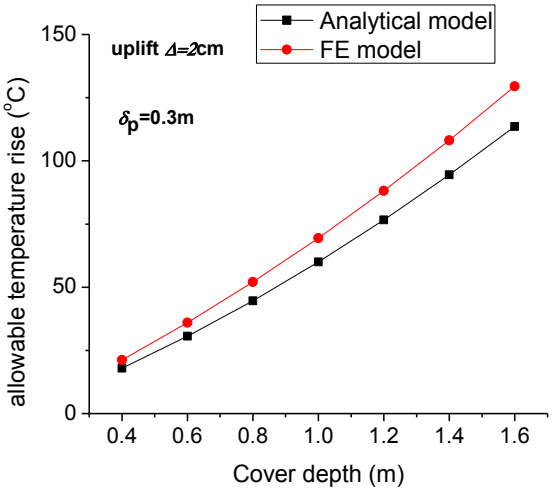

Figure 8-30 Temperature rise versus cover depth, $\delta_p = 0.3m$

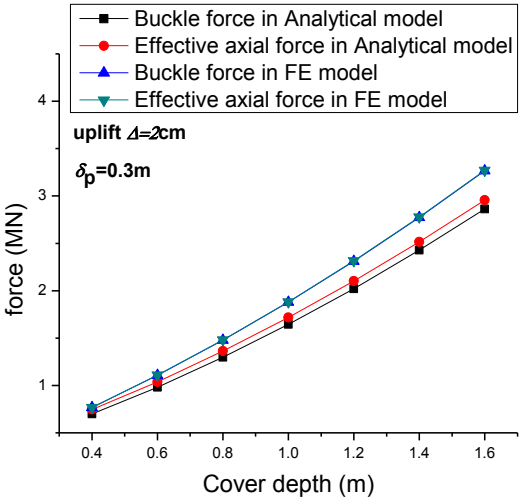

Figure 8-31 Force versus cover depth, $\delta_p = 0.3m$

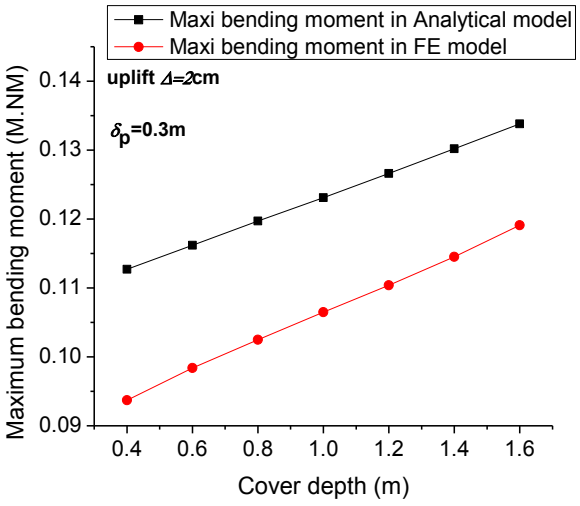

Figure 8-32 Max bending moment versus cover depth, $\delta_p = 0.3m$

8.5.4 Results for Elastic Pipe $\delta_p = 0.4m$

The results for imperfection level $\delta_P = 0.4$m are included in this section. The length of the model is 22.3787m. As it is shown in Figure 8-33 – Figure 8-35, the allowable operating temperature, buckle force and maximum bending moment given by the analytical model are very closer to but still a bit larger than those of FE model. For instance, for cover depth H=0.4m, the allowable temperature is about 13.40℃ according to analytical results, while it will be about 14.40℃ according to the FE results. The difference between the two models will also increase as the burial depth increases, but it is quite small compared with that of imperfection level $\delta_P = 0.1 - 0.3m$. The magnitude of the penetration is small compared with an imperfection level of 0.4m and the FE model becomes closer to the analytical model for large imperfections.

Table 8-11 Summary of result for $\delta_P = 0.4$m

No.4	**Imperfection level $\delta_P = \delta_f = 0.4$m**			
Analytical Results				
Cover Depth	Allowable Temperature Difference	Axial Force in Buckle Region	Axial Force away from Buckle Region	Max Bending Moment
H [m]	δ_T [℃]	N [MN]	N_0 [MN]	M_{max}[M.Nm]
0.4	13.40	0.5889	0.6407	0.1264
0.6	24.36	0.8319	0.8942	0.1297
0.8	36.59	1.1050	1.1770	0.1329
1.0	50.05	1.4070	1.4882	0.1362
1.2	64.69	1.7369	1.8266	0.1394
1.4	80.46	2.0936	2.1912	0.1427
1.6	97.33	2.4762	2.5813	0.1461
SIMLA Results (Elastic Material)				
Cover Depth	Temperature Difference when $\Delta = 2$cm	Axial Force in Buckle Region when $\Delta = 2$cm	Axial Force away from Buckle Region when $\Delta = 2$cm	Max Bending Moment when $\Delta = 2$cm
H [m]	δ_T [℃]	N [MN]	N_0 [MN]	M_{max}[M.Nm]
0.4	14.40	0.6089	0.6098	0.1078
0.6	26.57	0.8898	0.8912	0.1120
0.8	41.15	1.2263	1.2284	0.1164
1.0	55.89	1.5664	1.5692	0.1201
1.2	71.94	1.9367	1.9403	0.1237
1.4	88.13	2.3106	2.3146	0.1258
1.6	106.79	2.7411	2.7461	0.1297

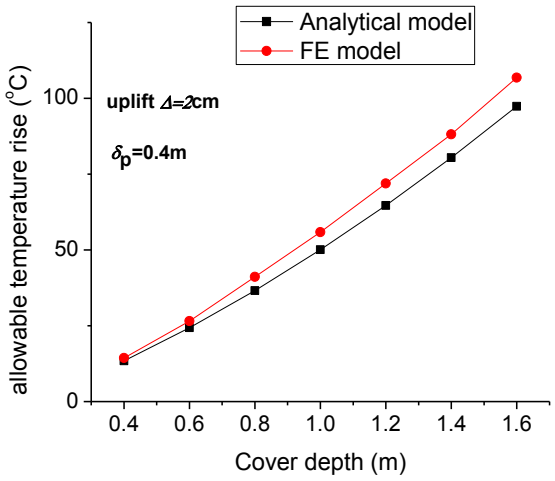

Figure 8-33 Temperature rise versus cover depth, $\delta_p = 0.4m$

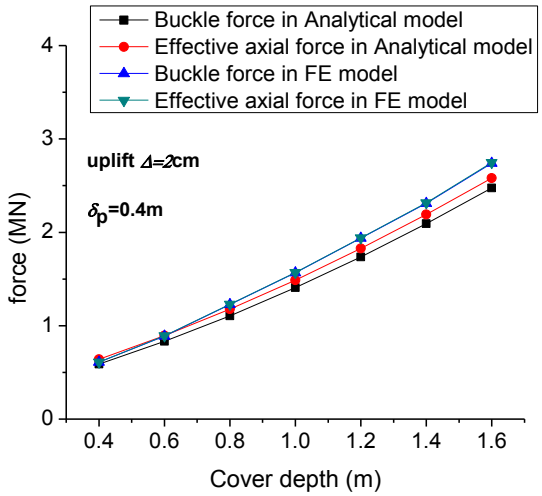

Figure 8-34 Force versus cover depth, $\delta_p = 0.4m$

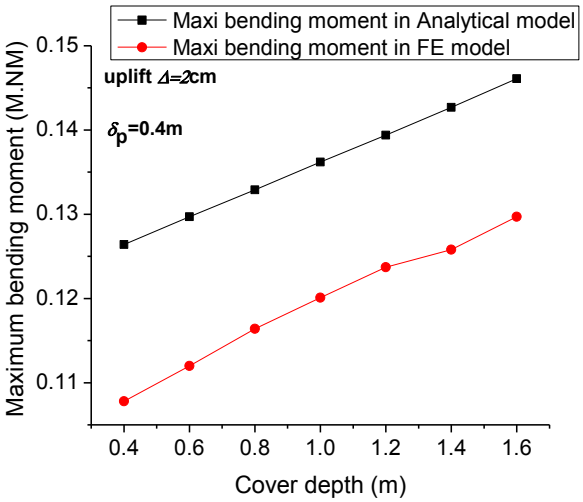

Figure 8-35 Max bending moment versus cover depth, $\delta_p = 0.4m$

8.5.5 Results for Elastic Pipe $\delta_p = 0.5m$

The results for imperfection level $\delta_P = 0.5$m are included in this section. The length of the model is 23.6626m. As it is shown in Figure 8-36 – Figure 8-38, the allowable operating temperature, buckle force and maximum bending moment given by the analytical model are very closer to but still a bit larger than those of FE model. For instance, for cover depth H=0.4m, the allowable temperature is about 10.37℃ according to analytical results, while it will be about 11.34℃ according to the FE results. The difference between the two models will also increase as the burial depth increases, but it is quite small. The magnitude of the penetration is very small compared with an imperfection level of 0.5m and the FE model is much closer to the analytical model for large imperfections.

Table 8-12 Summary of result for $\delta_P = 0.5$m

No.5	**Imperfection level $\delta_P = \delta_f = 0.5$m**			
Analytical Results				
Cover Depth	Allowable Temperature Difference	Axial Force in Buckle Region	Axial Force away from Buckle Region	Max Bending Moment
H [m]	δ_T [℃]	N [MN]	N_0 [MN]	M_{max}[M.Nm]
0.4	10.37	0.5149	0.5707	0.1386
0.6	20.20	0.7309	0.7979	0.1417
0.8	31.19	0.9745	1.0520	0.1448
1.0	43.30	1.2448	1.3321	0.1479
1.2	56.51	1.5409	1.6374	0.1510
1.4	70.78	1.8621	1.9673	0.1541
1.6	86.07	2.2075	2.3209	0.1573
SIMLA Results (Elastic Material)				
Cover Depth	Temperature Difference when $\Delta = 2$cm	Axial Force in Buckle Region when $\Delta = 2$cm	Axial Force away from Buckle Region when $\Delta = 2$cm	Max Bending Moment when $\Delta = 2$cm
H [m]	δ_T [℃]	N [MN]	N_0 [MN]	M_{max}[M.Nm]
0.4	11.34	0.5379	0.5391	0.1204
0.6	22.20	0.7884	0.7902	0.1249
0.8	34.28	1.0669	1.0695	0.1288
1.0	47.64	1.3748	1.3784	0.1326
1.2	61.16	1.6867	1.6910	0.1354
1.4	77.10	2.0539	2.0596	0.1396
1.6	93.20	2.4250	2.4318	0.1427

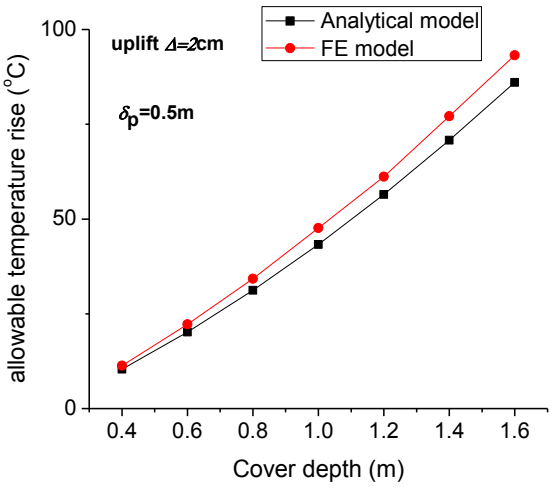

Figure 8-36 Temperature rise versus cover depth, $\delta_p = 0.5m$

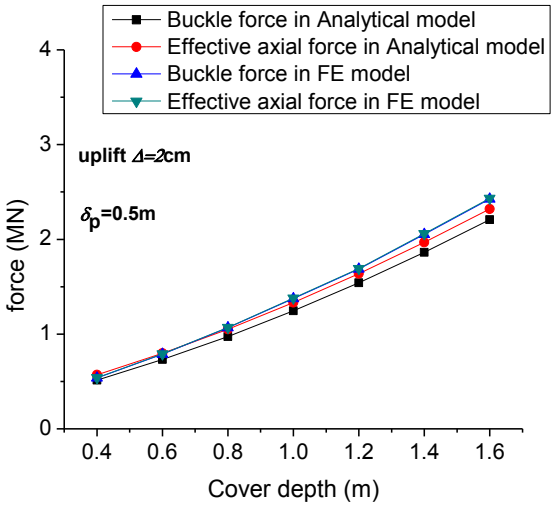

Figure 8-37 Force versus cover depth, $\delta_p = 0.5m$

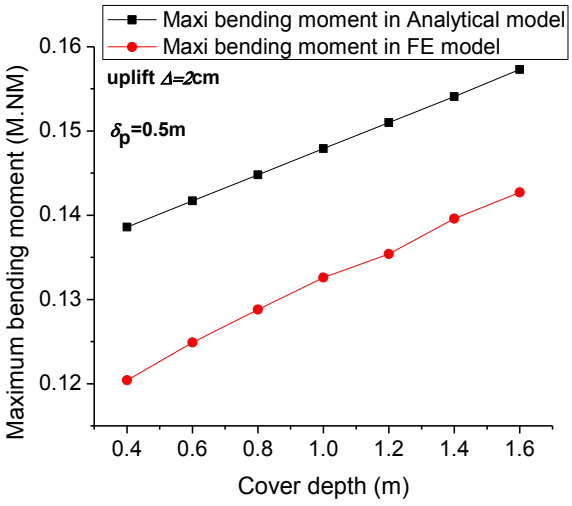

Figure 8-38 Max bending moment versus cover depth, $\delta_p = 0.5m$

8.5.6 Results for Elastic Pipe $\delta_p = 0.6m$

The results for imperfection level $\delta_P = 0.5$m are included in this section. The length of the model is 24.7661m. As it is shown in Figure 8-39 – Figure 8-41, the allowable operating temperature, buckle force and maximum bending moment given by the analytical model are very closer to but still a bit larger than those of FE model. For instance, for cover depth H=0.4m, the allowable temperature is about 8.20℃ according to analytical results, while it will be about 8.55℃ according to the FE results. The difference between the two models will also increase as the burial depth increases, but it is quite small. The magnitude of the penetration is very small compared with an imperfection level of 0.6m and the FE model is much closer to the analytical model for large imperfections.

Table 8-13 Summary of result for $\delta_P = 0.6$m

No.6	**Imperfection level $\delta_P = \delta_f = 0.6$m**			
Analytical Results				
Cover Depth	Allowable Temperature Difference	Axial Force in Buckle Region	Axial Force away from Buckle Region	Max Bending Moment
H [m]	δ_T [℃]	N [MN]	N_0 [MN]	M_{max}[M.Nm]
0.4	8.20	0.4612	0.5205	0.1497
0.6	17.19	0.6572	0.7284	0.1527
0.8	27.26	0.8787	0.9611	0.1557
1.0	38.37	1.1252	1.2181	0.1587
1.2	50.50	1.3959	1.4986	0.1617
1.4	63.62	1.6901	1.8020	0.1647
1.6	77.71	2.0071	2.1277	0.1677
SIMLA Results (Elastic Material)				
Cover Depth	Temperature Difference when $\Delta = 2$cm	Axial Force in Buckle Region when $\Delta = 2$cm	Axial Force away from Buckle Region when $\Delta = 2$cm	Max Bending Moment when $\Delta = 2$cm
H [m]	δ_T [℃]	N [MN]	N_0 [MN]	M_{max}[M.Nm]
0.4	8.55	0.4732	0.4745	0.1318
0.6	18.12	0.6937	0.6958	0.1361
0.8	28.89	0.9419	0.9449	0.1397
1.0	40.93	1.2192	1.2233	0.1439
1.2	53.13	1.5005	1.5053	0.1457
1.4	67.73	1.8364	1.8429	0.1497
1.6	82.48	2.1763	2.1839	0.1527

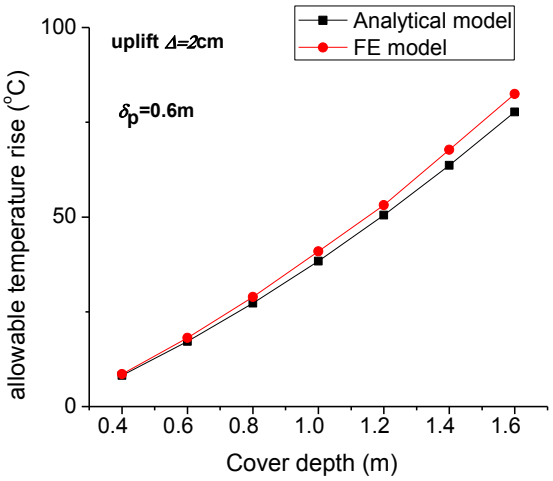

Figure 8-39 Temperature rise versus cover depth, $\delta_p = 0.6m$

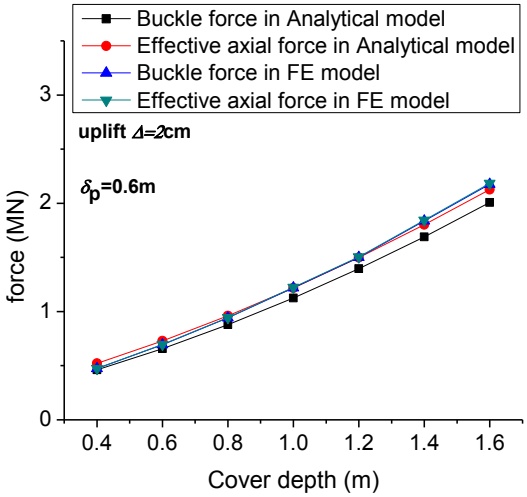

Figure 8-40 Force versus cover depth, $\delta_p = 0.6m$

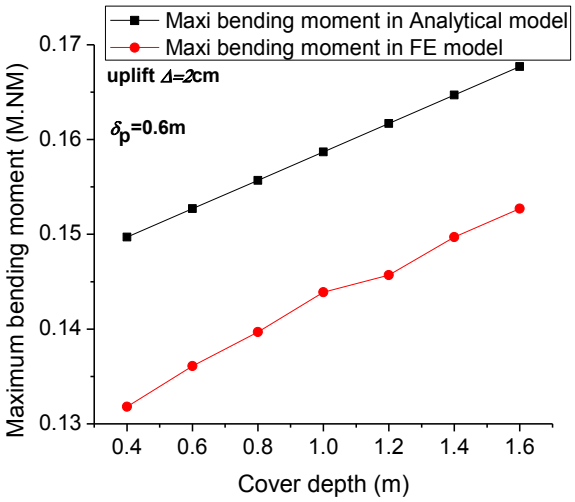

Figure 8-41 Max bending moment versus cover depth, $\delta_p = 0.6m$

8.5.7 Results for Elastic-Plastic Pipe, $\delta_p = 0.3m, 0.4m$

The results for elastic-plastic pipe with imperfection of 0.3m and 0.4m are included in this section. As it is shown in Figure 8-42 – Figure 8-47, it is evident that the allowable operating temperature, buckle force and maximum bending moment given by the elastic-plastic model is smaller than those of elastic model. As it is explained earlier, the difference between the elastic and elastic-plastic model may be explained by plastic buckling, which generally occur slightly before the theoretical buckling strength of a structure, due to plasticity of the material. When the compressive load is near buckling, the structure will bow significantly and approach yield. The stress-strain behavior of materials is not strictly linear even below yield, and the modulus of elasticity decreases as stress increases, with more rapid change near yield. This lower rigidity reduces the buckling strength of the structure and causes premature buckling.

Table 8- 14 Summary of result for$\delta_P = 0.3$ and 0.4m, elastic-plastic

No.7	**Imperfection level $\delta_P = \delta_f = 0.3m$**			
SIMLA Results (Elastic-plastic Material)				
Cover Depth	Temperature Difference when $\Delta = 2cm$	Axial Force in Buckle Region when $\Delta = 2cm$	Axial Force away from Buckle Region when $\Delta = 2cm$	Max Bending Moment when $\Delta = 2cm$
H [m]	δ_T [℃]	N [MN]	N_0 [MN]	M_{max}[M.Nm]
0.4	19.98	0.7383	0.7390	0.0920
0.6	34.72	1.0787	1.0797	0.0965
0.8	50.74	1.4486	1.4501	0.1005
1.0	66.72	1.8173	1.8196	0.1027
1.2	82.34	2.1764	2.1807	0.1025
1.4	95.27	2.4728	2.4796	0.0980
1.6	106.48	2.7275	2.7388	0.0911
SIMLA Results (Elastic-plastic Material)				
Cover Depth	Temperature Difference when $\Delta = 2cm$	Axial Force in Buckle Region when $\Delta = 2cm$	Axial Force away from Buckle Region when $\Delta = 2cm$	Max Bending Moment when $\Delta = 2cm$
H [m]	δ_T [℃]	N [MN]	N_0 [MN]	M_{max}[M.Nm]
0.4	14.33	0.6074	0.6083	0.1061
0.6	26.48	0.8878	0.8892	0.1104
0.8	39.88	1.1969	1.1990	0.1141
1.0	54.46	1.5331	1.5361	0.1170
1.2	67.78	1.8397	1.8440	0.1167
1.4	80.81	2.1385	2.1454	0.1140
1.6	92.43	2.4031	2.4140	0.1086

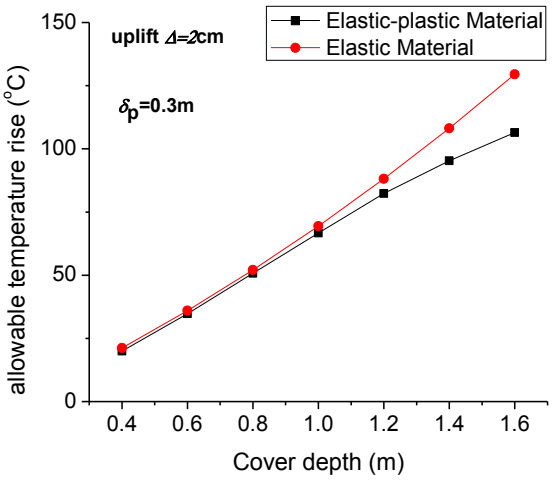

Figure 8-42 Comparison of temperature rise for different material, $\delta_P = 0.3m$

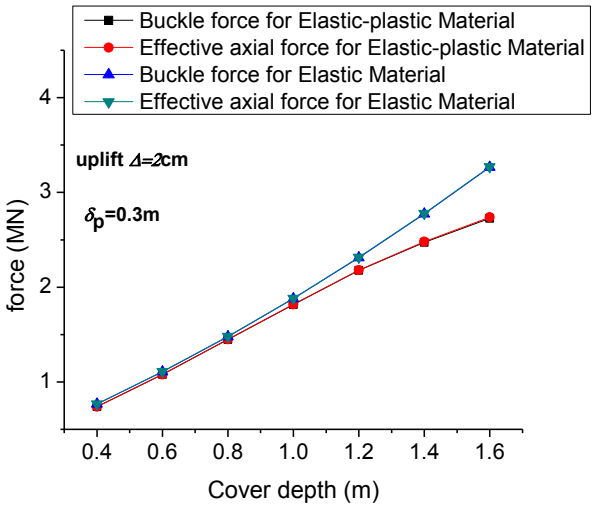

Figure 8-43 Comparison of force for different material, $\delta_P = 0.3m$

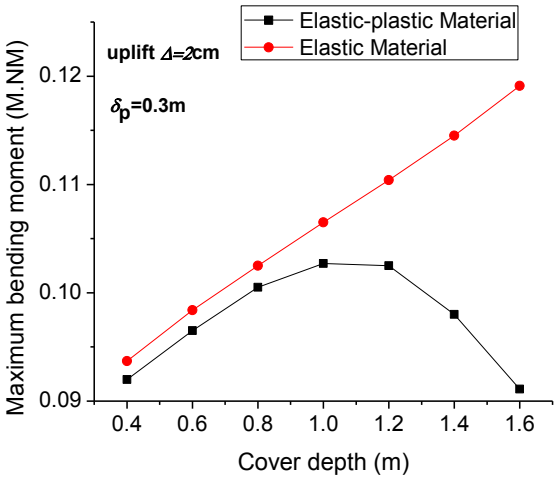

Figure 8-44 Comparison of max bending moment for different material, $\delta_P = 0.3m$

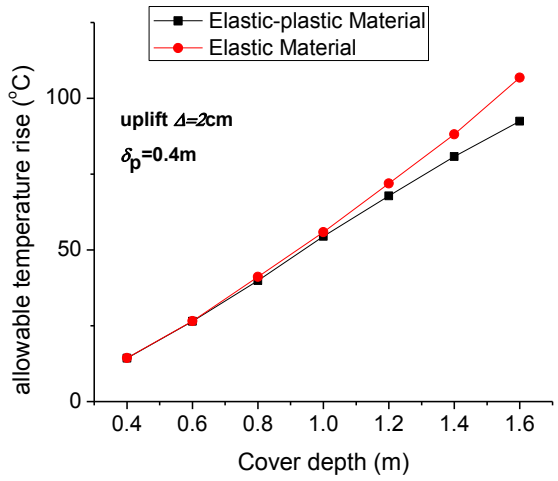

Figure 8-45 Comparison of temperature rise for different material, $\delta_P = 0.4m$

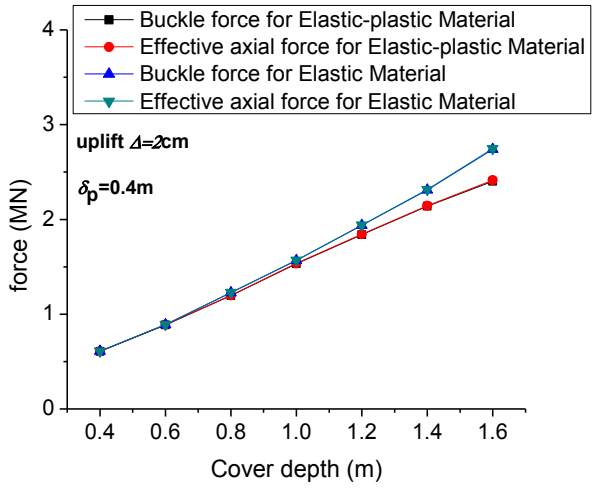

Figure 8-46 Comparison of force for different material, $\delta_P = 0.4m$

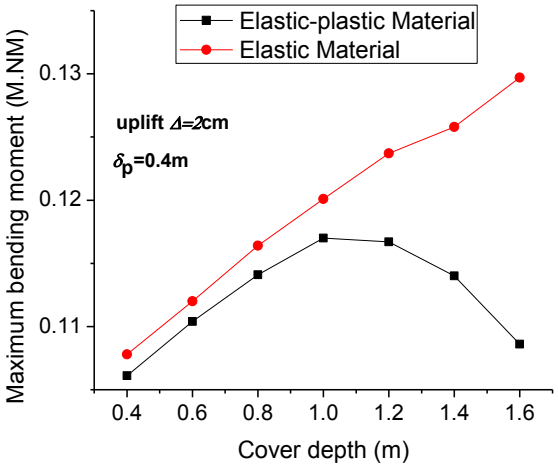

Figure 8-47 Comparison of max bending moment for different material, $\delta_P = 0.4m$

8.6 Discussion of the Results

A detail discussion of all the results from the conducted cases will be made in this section. Firstly, a comparison of the analytical and FE results is made to inspect and verify the analytical model is applicable or not. Secondly, an investigation on the effect of imperfection level and burial depth on the accuracy of the analytical model is made. Finally, the elastic-plastic behavior of the pipe is considered in the FE model.

8.6.1 Comparison of Analytical and FE Results

A group of cases with imperfection level δ_P varying from 0.1m to 0.6m has been defined and analyzed in both analytical model and FE model. In addition, a group of burial depth H varying from 0.4m to 1.6m has been studied for each imperfection level. For each case with given imperfection level and burial depth, the magnitude of allowable operating temperature, buckle force in the buckle region, effective axial force away from buckle region and maximum bending moment given by the analytical can FE method are compared to inspect and verify the analytical model. The relative deviation between the analytical results and FE results is therefore identified. In this thesis, the relative deviation is defined as follows:

Relative deviation of operating temperature rises:

$$\varepsilon_T = (\Delta T_{FE} - \Delta T_{Analytical})/\Delta T_{FE}$$

Relative deviation of buckle force (axial force in buckle region):

$$\varepsilon_N = (N_{FE} - N_{Analytical})/N_{FE}$$

Relative deviation of effective axial force (axial force away from buckle region):

$$\varepsilon_{N_0} = (N_{0_{FE}} - N_{0_{Analytical}})/N_{0_{FE}}$$

Relative deviation of maximum bending moment:

$$\varepsilon_{M_{max}} = (M_{max_{FE}} - M_{max_{Analytical}})/M_{max_{FE}}$$

The subscript *FE* and *Analytical* here represents where the results are taken from, FE or analytical method.

The relative deviation of each term for every imperfection level is presented in Figure 8-48 – 8-53, it is verified that the results given by the analytical model are close to the result given by FE model, especially for larger imperfection levels. For small imperfection level, the deviation of buckle force and temperature rise may be a little large, say about 30% for$\delta_P = 0.1m$. The deviation will become small as the imperfection level increase. The analytical model will give very good results compared with the FE model for larger imperfection level, say 10% for$\delta_P = 0.3m$. As it is explained earlier in section 8.3, this may be explained by the soil/pipe model difference of two models and the penetration effect of pipe in FE model. However, it is fair to conclude that the analytical model is a very good method with good accuracy for screening design process. For small imperfection levels, say smaller than 0.2m, it is reasonable to use a scale factor, which is larger than 1.0 for the results given by analytical model. For large imperfection level, say 0.3m, the analytical model will give quite good design parameters.

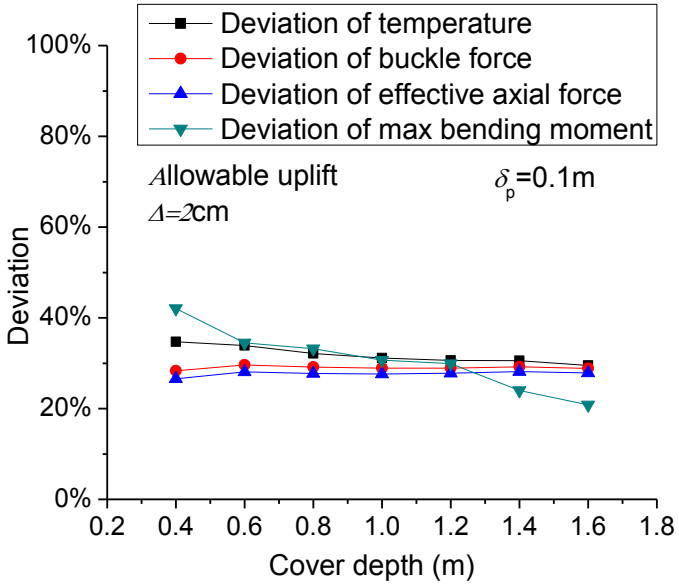

Figure 8-48 Deviation between FE and analytical results, $\delta_p = 0.1m$

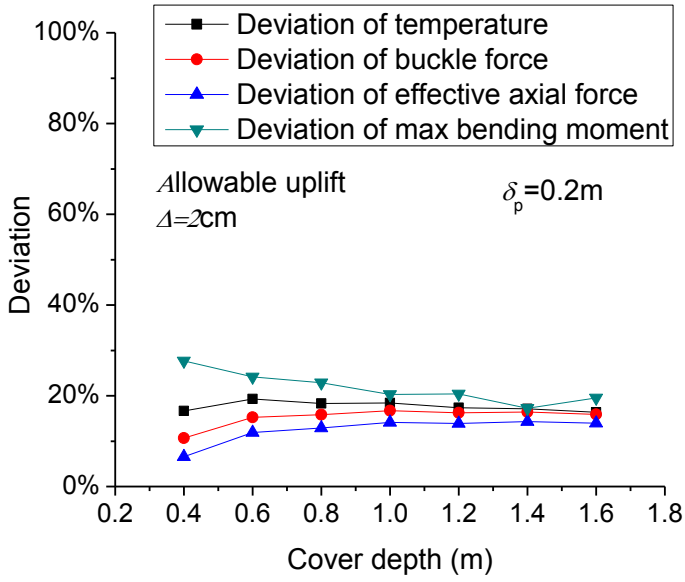

Figure 8-49 Deviation between FE and analytical results, $\delta_p = 0.2m$

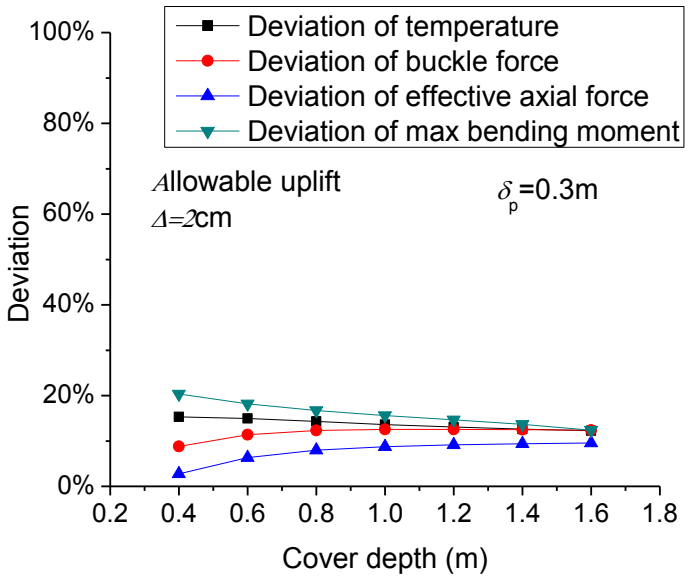

Figure 8-50 Deviation between FE and analytical results, $\delta_p = 0.3m$

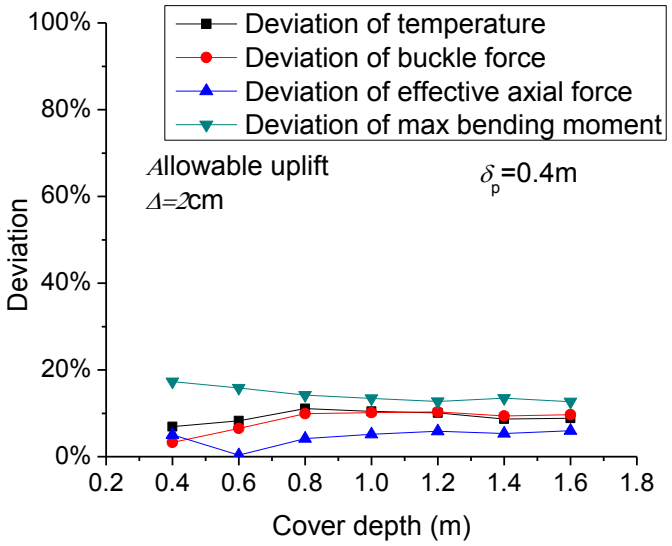

Figure 8-51 Deviation between FE and analytical results, $\delta_p = 0.4m$

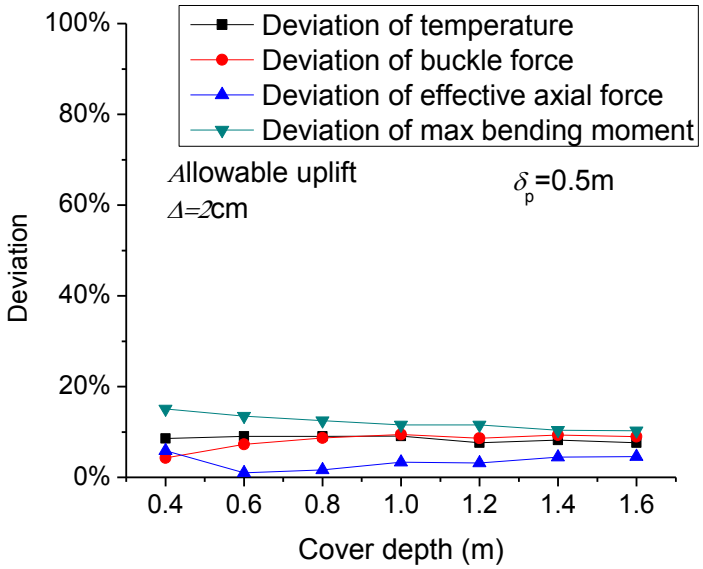

Figure 8-52 Deviation between FE and analytical results, $\delta_p = 0.5m$

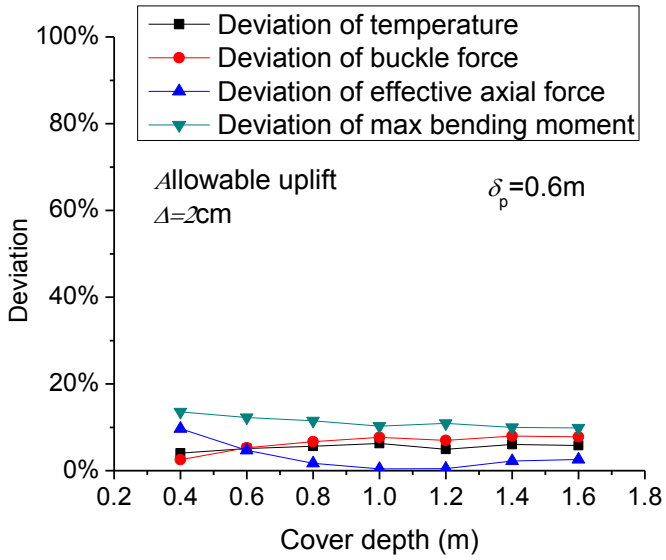

Figure 8-53 Deviation between FE and analytical results, $\delta_p = 0.6m$

8.6.2 Investigation on the Effect of Imperfection Level

It is noted that the deviation between the analytical results and the FE results are affected by the magnitude of the imperfection level, as stated in last section. The analytical model tends to give results close to the FE model as the imperfection level increase. Take H=0.4m, 1.0m and 1.6m as examples, as it is shown in Figure 8-54 – Figure 8-56, the deviation of allowable operating temperature given by analytical and FE model is about 30% when the imperfection level is 0.1m, while the deviation is about 5% when the imperfection is 0.6m. The magnitude of the deviation decreases significantly as the imperfection level increases. The deviation of axial force and bending moment will have the same trends as well, i.e. the magnitude of relative deviation will decrease as the imperfection level increase.

It may be explained by the fact that as the imperfection level increases, the ratio between the allowable maximum uplift Δ=2cm and imperfection level will decrease. For example, for an imperfection level of 0.1m, the ratio Δ/δ_p is about 20%, while for an imperfection level of 0.6m, the ratioΔ/δ_p is about 3%. And magnitude of the penetration into the seabed, about 0.013m will have a larger influence on the deviation for smaller imperfection level. The effect from the difference of soil/pipe model in the analytical and FE model will be largely reduced when the imperfection level is relative larger, the penetration effect will not affect the deviation to such large extent.

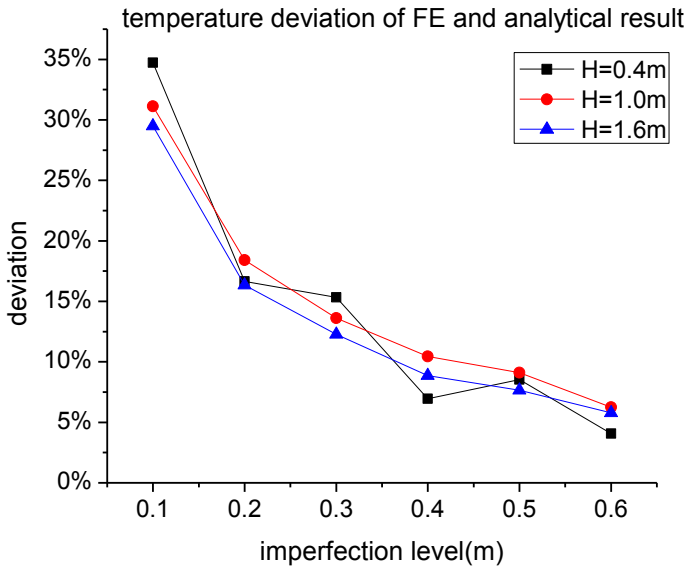

Figure 8-54 Deviation of temperature versus imperfection level

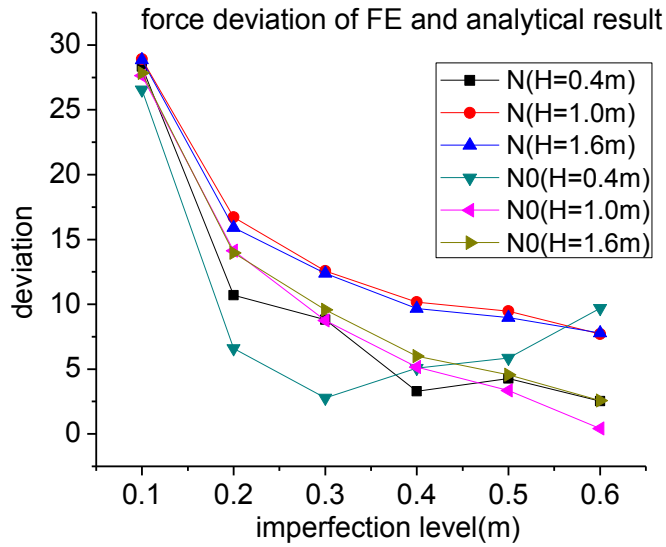

Figure 8-55 Deviation of force versus imperfection level

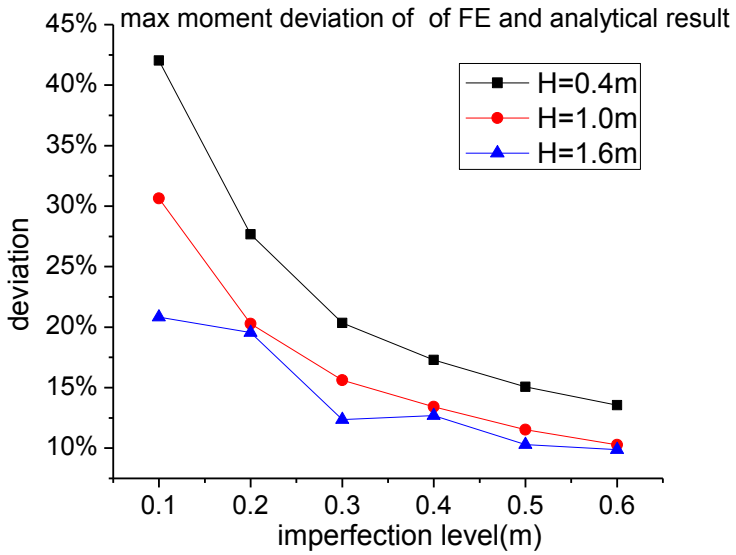

Figure 8-56 Deviation of max bending moment versus imperfection level

8.6.3 Investigation on the Effect of Burial Depth

It is aimed at investigating whether the change of burial depth will affect the magnitude of deviation between analytical and FE results in this section. As it is shown in Figure 8-57 – 8-60, it is noted that the burial depth will not influence the accuracy of the analytical model that much. For given imperfection level, the magnitude of the deviation in allowable operating temperature, buckle force and effective axial force away from buckle region tend to be constants as the burial depth increases. However, it is noted that the magnitude of the deviation in maximum bending moment will decrease as the burial depth increases, i.e. the analytical model tend to give results closer to FE model for larger cover depth.

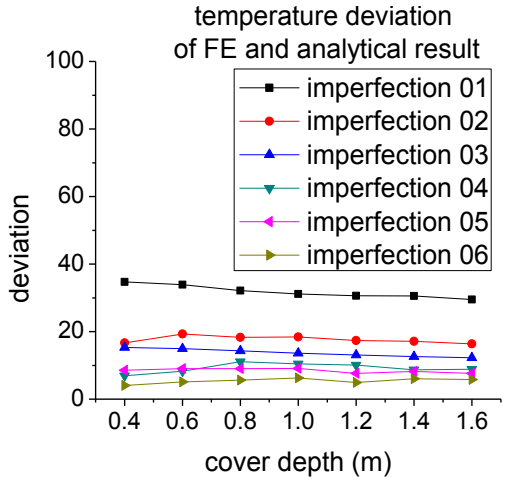

Figure 8-57 Deviation of temperature versus cover depth

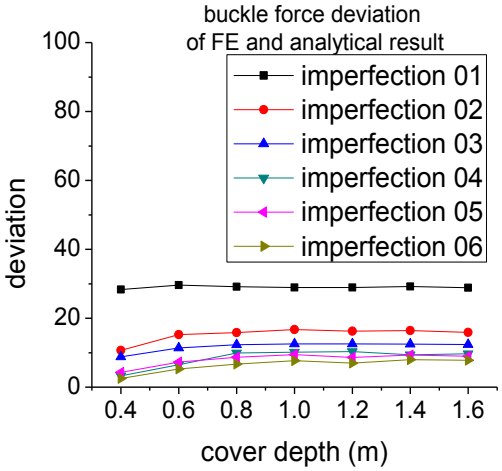

Figure 8-58 Deviation of buckle force versus cover depth

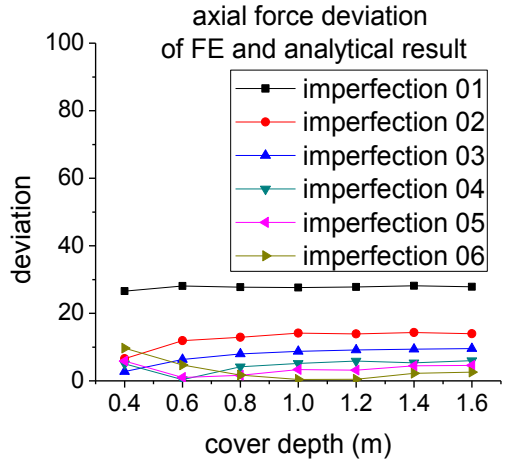

Figure 8-59 Deviation of effective axial force versus cover depth

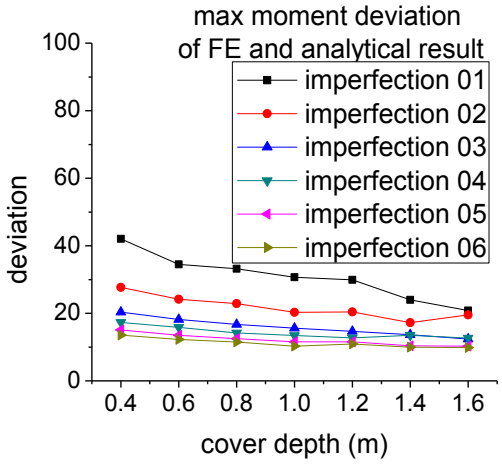

Figure 8-60 Deviation of max bending moment versus cover depth

8.6.4 Investigation on the Effect of Material Type

The elastic-plastic behavior of the pipe is vital important to the upheaval buckling problem. In this section, a study on the effect of material type is conducted.

As it is shown in Figure 8-42 – Figure 8-47, the allowable temperature rise and buckle force from elastic-plastic model will be smaller than elastic model. The maximum bending moment given in the elastic-plastic model is smaller than elastic model as well. It is evident that result from FE model will give conservative results for pipeline design. For example, for$\delta_P = 0.3m$and cover depth of 0.4m, the allowable temperature rise for elastic pipe is 21.23 ℃, the buckle force is 0.7671MN and the maximum bending moment is about 0.0937M.Nm in the elastic model, while in the elastic-plastic model, the allowable temperature rise for elastic pipe is 19.98 ℃, the buckle force is 0.7383MN and the maximum bending moment is about 0.0920M.Nm. For$\delta_P = 0.4m$, $3m$and cover depth of 1.0m the allowable temperature rise for elastic pipe is 55.89 ℃, the buckle force is 1.5664MN and the maximum bending moment is about 0.1201M.Nm in the elastic model, while in the elastic-plastic model, the allowable temperature rise for elastic pipe is 54.46℃, the buckle force is 1.5331MN and the maximum bending moment is about 0.1170M.Nm.

It may be explained by plastic buckling, which generally occurs slightly before the theoretical buckling strength of a structure, due to plasticity of the material. When the compressive load is near buckling, the structure will bow significantly and approach yield. The stress-strain behavior of materials is not strictly linear even below yield, and the modulus of elasticity decreases as stress increases, with more rapid change near yield. This lower rigidity reduces the buckling strength of the structure and causes premature buckling.

Chapter 9 Conclusions and Recommendations for Future Work

9.1 Conclusions

The main purpose of this thesis was to develop a MATLAB program based on Terndrup-Pedersen' analytical method for upheaval buckling analysis and verify the analytical model by comparing with FE analysis using software SIMLA. In addition, an elastic-plastic pipe model was built in SIMLA to investigate the plastic behavior of pipe and its effect on the pipeline design.

The analytical mode provides a design criterion for design against gradual upward movement, i.e. upheaval creep of buried pipelines subjected to time varying temperature and pressure loadings. It is shown that pipelines with an imperfection may move upwards when they experience the operating temperature and pressure. The pipeline will lift the overburden a small amount, not to an extent that it breaks out of the soil. The pipeline may try to trace back to the initial imperfection configuration when it becomes cooler due to temporary shutting down of production line. However, the migration of sand particles will fill the cavity created by the uplift of pipeline, which is below the pipeline gradually. Therefore, it is impossible for the pipeline to go back to the original position as its initial configuration, which causes a gradual upwards movement of pipelines. In addition, a residual compression will be generated at the end of buckle region, which is caused by the axial friction force. After a subsequent of temperature reloading, the pipeline will move up gradually and a larger imperfection will arise, hence a lower temperature load should be applied as the imperfection amplitude increases gradually. The pipeline may be exposed to upheaval buckling when the local imperfection of the pipeline is larger than some critical value.

By comparing the results of analytical and FE model, according to the discussions presented in chapter 8, it is clearly verified the analytical model proposed by Terndrup-Pedersen will always give results that will be consistent with results of FE modeling in SIMLA. The MATLAB program developed is able to implement the analytical method and give very good results for design. However, it should be noted that the analytical model will always give conservative results compared with the results given by FE model.

The simulations of both analytical model and elastic FE model clearly indicate the allowable operating temperature and buckle force will decrease significantly as the imperfection level increases, on the contrary the maximum bending moment will increase as the imperfection level increases. It is also evident to see the allowable operating temperature and buckle force will increase as the burial depth increase, while the maximum bending moment increase a little bit and is nearly a constant for given imperfection level.

The comparison study of the analytical and FE model in section 8.6.1 clearly shows the deviation of the analytical and FE results. The analytical model tends to give results close to FE model for large imperfection levels, say 0.3m or larger in the thesis, while the deviation may be larger for small imperfection level, say 0.2m or smaller. As it has been discussed, it is affected by the difference in the modeling of soil/pipe model in two models. The penetration of pipe into the seabed in the FE model may result a difference. The assumption that the foundation is infinite stiff will always lead to conservative results. Bear in mind that the soil/pipe interaction should be considered in detail design stage for give pipeline design projects. In this thesis, all the comparison is based on fact that the pipe will have a penetration of about 0.013m, which is greatly dependent on the soil conditions or soil

stiffness where the pipeline is to be installed. It would be wise to make some refinements or modifications for the analytical model after considering the soil conditions. It may be achieved by introducing some safety factors, say about 1.5 for small imperfection level and 1.1 for large imperfection level, to refine the results given by the analytical model, according to discussion in section 8.6.2.

Furthermore, it is found that the burial depth will have little effect on the deviation between the analytical and FE model, namely the burial depth will not influence the accuracy of the analytical model, according to discussion in section 8.6.3.

Finally, it is also found the elastic-plastic properties of the pipe will affect the design temperature and buckle force to some extent. The results given by the elastic pipe model will always give conservative results for design. Therefore it is wise to take the elastic-plastic material properties into consideration.

Based on the results and discussions in section 8.5 and 8.6, some actions to avoid upheaval buckling may be identified.

1. Decreasing the operating temperature, the decreasing of operating temperature will significantly decrease the driving axial force caused by temperature different between the internal and external environments, which leads to buckle problem. It can be achieved by using some cooling loop, in fact it has already been used when the oil and gas is transported to the processing facilities.
2. Increasing the pipe weight. The pipe weight will affect the magnitude of the vertical stiffness of the pipeline. A lighter pipeline tends to lift up easier at given operating temperature and pressure. The weight of the pipeline is determined the density of the pipe steel and content and the weight of the coating. Usually the weight of pipe wall and content is a constant, so this method may by applicable by increasing the weight of coating concrete.
3. Increasing the burial depth. The vertical resistance to avoid the uplift of pipeline is largely dependent on the soil cover depth. Usually the increase of uplift resistance resulting from an increase of soil cover will be large compared to increasing the coating weight. It may be achieved by add more soil cover, like sand or rock dump.
4. Limiting the out of straightness. The buckle force is greatly affected by the imperfection level. The decreasing of imperfection level will significantly increase the resistance to uplift buckle of pipeline. It requires a better quality control strategy during the fabrication process and a better control during the laying and trenching of the pipeline.
5. Clamp the pipeline. The clamping of pipeline may significantly reduce the axial feed-in of the pipe to the buckle region, and therefore reduces the amplitude of the resulting buckle to some limits required. It may be achieved by using discrete gravel dumping on critical sections of the pipeline. There are concerns about identifying the critical buckle lengths in pipelines, which may calculated with theoretical methods or FE modeling.
6. Pretension the pipeline. It will help alleviate the operationally induced compressive loads in the pipeline by increasing the lay tension to a maximum possible safe value. The residual lay tension is maintained by friction force from the seabed/pipeline interface. However, it may be difficult to identify the magnitude of the proper lay tension to a critical condition that prevents overstressing of the pipeline. The cycling installation process like lifting up during the

installation process may result in no friction force from the seabed. In general, this method is unpredictable for its uncertainty during the installation process.

7. Snake lay by pre-heat the pipeline. Pre-heating the pipeline before burial process would enable thermal strains to be locked into the pipeline. The pipeline is more likely to deflect laterally instead of moving upwards. And it may enable a pre-tension of the pipeline, which will increase the operating temperature required to cause upheaval of the pipeline. It may be achieved by flushing the pipeline using hot water before operating process.

9.2 Recommendations for Future Work

In order to avoid the gradual movement of the pipeline through the burial during the possible cyclic temperature and pressure loading, Pedersen proposed a limited critical vertical displacement as a criterion to avoid that the elastic response of the soil fails. The suggested method to calculate the critical displacement is presented by Pedersen to be equal to$w_{max} = (0.02 + 0.008H/D_0)D_0$, where D_0 is the overall outside diameter of the pipe and H is the burial depth to the pipeline centerline. It is necessary to verify whether the critical displacement chosen is applicable or not for given project. For the analytical model in this thesis, all simulations are based on an allowable maximum uplift of 2cm. It is shown that the results are more accurate for high imperfection level, for instance, when δ_p is equal to or larger than 0.3m. For small imperfection level, the design parameters, like allowable operating temperature, buckle force given by the analytical model are over conservative. Therefore, it is necessary to investigate the effect from the allowable maximum uplift on the design procedure for given projects. More cases should be studied to investigate the effect from the design critical uplift.

In the FE model in SIMLA, only a small section of the pipeline is modeled, which may not be so similar to the practical situations in industry. There may be several limitations for the model in both analytical model and FE model, which may affect the accuracy of the results. Both the analytical model and the FE model are based on the assumption that the pipeline is fixed at the right end and has 2 degree of freedoms in 3 and 6 directions, i.e. in vertical direction and rotation about z direction, while in fact the pipeline is not fully strained in a long pipeline and the pipeline may have a snake configuration. The snake configuration may lead to energy locking in the lateral direction. It is necessary to model the pipeline with a larger length, with different soil stiffness in buckle region and other regions, to see what will be the difference. In addition, in will be closer to the real situation to allow other degree of freedoms for the pipeline in the soil.

In the FE model, only three load cases are introduced into the process. In the industry, there should be an additional load stage, which is called test stage, where pressure with a magnitude of 1.25 times of operation pressure is applied before the operating stage. It is neglected because it may lead to a difference of the analytical model and FE model. However, it will have an effect on the final buckle temperature and buckle force. It should be included in the future simulations to make the FE model more similar to the reality.

More considerations into soil/pipe and soil/burial interaction should be taken. The accuracy of both the analytical model and FE model is greatly dependent on how the soil/pipe and soil/burial interaction are modeled. Here in the analytical model, the foundation is assumed to be infinite stiff, while in fact the pipeline will penetrate into the soil. In addition, the uplift resistance of the soil cover is assumed to be a constant, which is not so accurate for small cover depth and large vertical displacement. In reality, the soil stiffness is dependent on the soil conditions where the pipeline is

going to be installed, which may not be just simplified as infinite stiff and the uplift resistance of the burial is dependent on the burial conditions, which may not be a constant. In the FE model, all these effects should be considered to obtain better results for design.

There are some assumptions for the analytical model, which may result in an over conservative result for given project. However it is a good method that may be used during the screening design process. It is wise to keep in mind that all the assumptions that are not conforming to reality should be considered when detail design stage starts.

Reference

[1] Palmer A C, Baldry J A S. Lateral buckling of axially-compressed pipelines[J]. Journal of Petroleum Technology, 1974, 26 (11): 1283-1284.

[2] Hobbs R E. Pipeline buckling caused by axial loads[J]. Journal of Constructional Steel Research, 1981, 1(2): 2-10.

[3] Hobbs R E. In-service buckling of heated pipelines[J]. Journal of Transportation Engineering, ASCE, 1984, 110(2): 175- 189.

[4] Guijt J. Upheaval buckling of offshore pipeline: overview and introduction [C]// In proceedings of the 22nd Annual OTC. Houston, Texas, 1990: 573-578.

[5] Nielsen N J R, Lyngberg B, Pedersen P T. Upheaval buckling failures of insulated burial pipelines-a case story[C]// In proceedings of the 22nd Annual OTC. Houston, Texas, 1990: 581-592.

[6] Ballet J P, Hobbs R E. Asymmetric effects of prop imperfections on the upheaval buckling of pipelines[J]. Thin- Walled Structures, 1992, 13: 355-373.

[7] Taylor N, Tran V. Prop-imperfection subsea pipeline buckling[J]. Marine Structures, 1993, 6: 325-358.

[8] Taylor N, Tran V. Experimental and theoretical studies in subsea pipeline buckling [J]. Marine Structures, 1996, 9(2): 211-257.

[9] Maltby T C, Calladine C R. An investigation into upheaval buckling of buried pipelines--i. Experimental apparatus and some observations[J]. International Journal of Mechanical Sciences, 1995, 37(9): 943-963.

[10] Maltby T C, Calladine C R. An investigation into upheaval buckling of buried pipelines--ii. Theory and analysis of experimental observations[J]. International Journal of Mechanical Sciences, 1995, 37(9): 965-983.

[11] Croll J G A. A simplified model of upheaval thermal buckling of subsea pipelines[J]. Thin-Walled Structures, 1997, 29 (1-4): 59-78.

[12] Hunt G W, Blackmore A. Homoclinic and heteroclinic solutions of upheaval buckling[J]. Phil. Trans. R. Soc. Lond., 1997, 355(4): 2185-2195.

[13] Friedmann Y, Debouvry B. Analytical design method helps prevent buried pipe upheaval[J]. Pipeline Industry, 1992, 11: 63-68.

[14] Villarraga J A, Rodriguez J F, Martínez C. Buried pipe modeling with initial imperfections[J]. Journal of Pressure Vessel Technology, 2004, 126(5): 250-257.

[15] Zhou Z J, Murray D W. Behaviour of buried pipelines subjected to imposed deformations[C]// 12th Int. Conference on Offshore and Arctic Engineering. ASCE, 1993, II: 115-122.

[16] Pasqualino I P, Alves J L D, Battista R C. Failure simulation of a buried pipeline under thermal loading[C]// Proceedings of the 20th International Conference on Offshore Mechanics and Arctic Engineering (OMAE), 2001, OMAE2001-4124. Rio De Janeiro, Brazil, 2001.

[17] Einsfeld R A, Murray D W, Yoosef-Ghodsi N. Buckling analysis of high-temperature pressurized pipelines with soilstructure interaction[J]. Journal of the Brazilian Society of Mechanical Sciences and Engineering, 2003, 25(2): 164-169.

[18] Pedersen P T, Jensen J J. Upheaval creep of buried heated pipelines with initial imperfections[J]. Marine Structures, 1988, 1: 11-22.

[19] DNV. Recommended Practice DNV-RP-F110[S], Global buckling of submarine pipelines, 2007.

[20] Yong Bai, Qiang Bai. Subsea pipelines and risers[M]. 2005.

[21] Torgeir Moan. Lecture notes in TMR4190 - Finite Element Modelling and Analysis of Marine Structures. Department of Marine Technology NTNU, 2003.

[22] Torgeir Moan. Lecture notes in TMR4305 – Nonlinear Analysis. Department of Marine Technology NTNU, 2012.

[23] Svein Sævik. Lecture notes in TMR4305 – Advanced Dynamic Analysis. Department of Marine Technology NTNU, 2012.

[24] Svein Sævik. SIMLA - Theory Manual, 2008 edition.

[25] Bernt J. Leira. Kompendium for Marine Structure, Basic Course [M]. NTNU: August, 2011

Appendix

The MATLAB program used to implement Pedersen's model is given in enclosed zip file. All the input files are also included in the zip file.

Appendix I stress/strain relationship of the elastic to plastic material

ε	$\sigma(M.N/m^2)$
0.000E+00	0.000
1.691E-03	350.000
2.000E-03	390.000
2.500E-03	415.000
3.000E-03	427.000
3.500E-03	435.000
4.000E-03	441.000
5.010E-03	450.000
6.000E-03	457.000
7.010E-03	462.000
8.000E-03	466.000
8.970E-03	470.000
9.940E-03	473.000
1.990E-02	492.000

Appendix II Screenshot of SIMLA model

Some of screenshot of the output is presented here as an illustration, all the input files for SIMLA software are enclosed as a zip file.

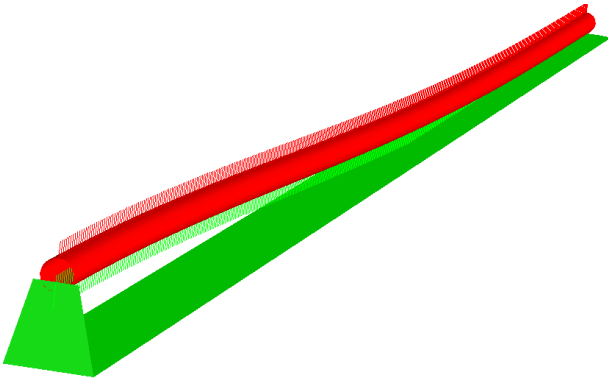

Figure 1 Initial configuration

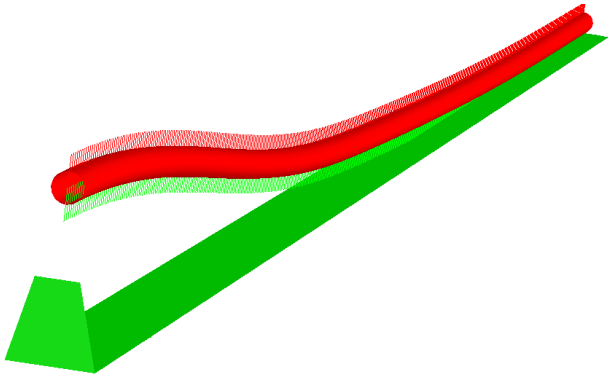

Figure 2 Configuration when lifting up

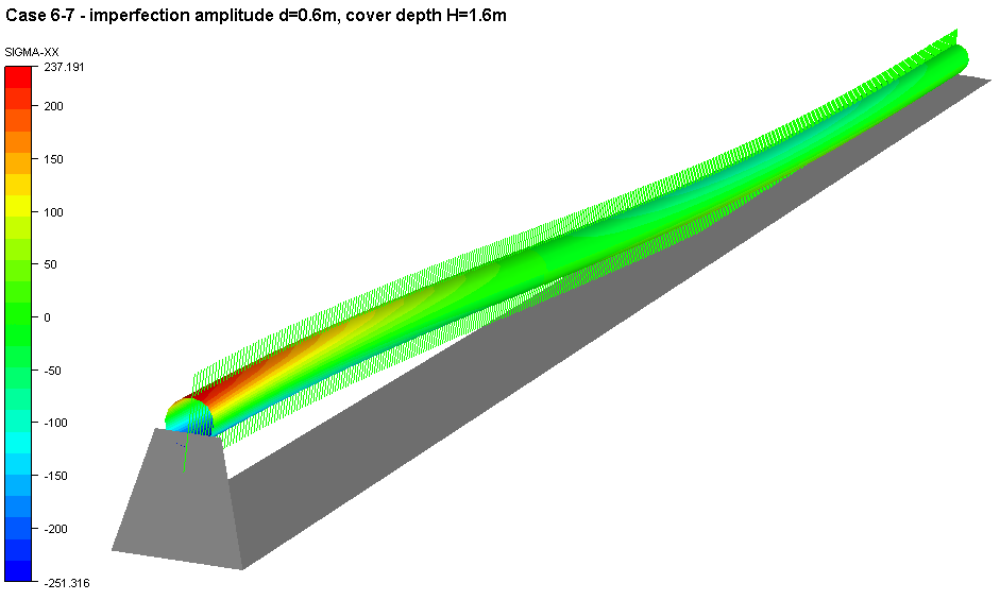

Figure 3 Stress distribution in pipeline section when lift up